EUROPEAN ORGANIZATION FOR NUCLEAR RESEARCH

INELASTIC DIFFRACTIVE SCATTERING AT THE CERN ISR

M.G. Albrow, A. Bagchus, D.P. Barber, P. Benz, A. Bogaerts, B. Bošnjaković, J.R. Brooks, C.Y. Chang[1], A.B. Clegg, F.C. Erné, C.N.P. Gee, P. Kooijman, D.H. Locke, F.K. Loebinger, N.A. McCubbin, P.G. Murphy, D. Radojičić, A. Rudge, J.C. Sens, A.L. Sessoms[2], J. Singh, D. Stork, J. Timmer

CERN, Geneva, Switzerland
Daresbury Laboratory, U.K.
Foundation for Fundamental Research on Matter, (F.O.M.), The Netherlands
University of Lancaster, U.K.
University of Manchester, U.K.
University of Utrecht, The Netherlands
(CHLM Collaboration)

Abstract

The properties of the diffractive peak observed in the mass spectra of systems recoiling against observed high momentum protons emerging from pp collisions at the CERN ISR have been investigated. The cross-sections in this peak have been found to have a steep t-dependence which flattens out as $|t|$ increases. The high mass side of the peak varies approximately as $1/M^2$ (where M is the missing mass of the recoiling system) and scales well in terms of the variable M^2/s. The position of the maximum has been observed to move to lower values of M^2/s as the kinematic boundary of this variable decreases with increasing s. The measured cross-sections, integrated up to $M^2/s = 0.05$, rise by $(15 \pm 5)\%$ over the s range 549 to 1464 GeV^2.

(1) Permanent address: Phys. Dept., University of Maryland, College Park, MD 20742, U.S.A.

(2) Permanent address: Phys. Dept., Harvard University, Cambridge, MA 02138, U.S.A.

Introduction

An earlier experiment at the ISR to study the reaction:

$$p + p \rightarrow p + X$$

has shown the existence of a peak in the mass spectrum of the unobserved system X[1]. This peak has been associated with the diffractive excitation of one of the incident protons; results on its shape and dependence on t and s have been subsequently published by several groups[2].

Several predictions have been made about the s-dependence of the diffractive excitation cross-section; a specific question which has been raised is the extent to which this process might contribute to the rise in the total cross-section measured through the ISR energy range[3)4)]. The aims of the present experiment have been both to extend the s and t ranges of the measurements of the inclusive proton spectrum and to improve their precision so that more accurate conclusions about scaling in the diffractive peak, and its contribution to the total inelastic cross-section, could be reached.

2. Experimental Method

A magnetic spectrometer placed above one of the circulating beams near intersection 2 at the ISR was used to detect emitted protons. The spectrometer, shown in fig. 1, consisted of 2 septum magnets whose apertures could be positioned to within 50 mm of the ISR beam, 3 bending magnets, a system of 21 magnetostrictive wire spark chambers, a series of trigger scintillation counters, and 3 gas Cerenkov counters. The position of the two septum magnets could be varied so that a total angular range from 30 to 180 mrad could be covered in successive settings with an angular width of $\pm$ 5 mrad. The design and operation of the spectrometer have been described previously[5].

In the present experiment two changes were made to the normal spectrometer to improve the momentum resolution. The two ethylene-filled Cerenkov counters, which had previously been used

to distinguish protons from pions and kaons, were lifted out of the spectrometer to reduce the multiple scattering along the 30 m flight path. All positive high momentum particles were then assumed to be protons (the pion and kaon contamination having been measured to be less than 1 in 10^3 for particles having more than 90% of the maximum possible momentum[6]). Hall probes were mounted in all the spectrometer magnets so that the fields could be monitored to an accuracy of better than 1 part in 10^3.

The production angle could be measured by the spectrometer with a precision of about 0.2 mrad, corresponding to an accuracy of $\sim 0.5\%$ in momentum transfer. The accuracy in the measured momentum, $\delta p/p$, varied between 0.6% and 1.1% FWHM from the lowest to the highest production angles (this variation was due to the different magnetic fields used at different angular settings; the resolution was nearly independent of the ISR beam energy, as the bending angles in the magnets depended only on the angular setting). The mean deviations of all spark positions from the calculated track were less than 0.1 mm.
Tracks with spurious spark positions or secondary scatters were rejected by a consistency check on momenta, track angles and positions in different parts of the spectrometer. The production angle, the vertex position in the beam-beam plane and the momentum were fitted to the positions in the 12 chambers which determined the vertical coordinates. One kink in the fitted track was allowed, to take care of the effects of multiple scattering.

The value of M, the missing mass of the system X, is related to the centre of mass energy E_p of the observed proton by

$$M^2 = s + m_p^2 - 2\sqrt{s}\, E_p \qquad (1)$$

For large values of s and for $M^2 \gg m_p^2$ this can be approximated by

$$M^2 = s\,(1 - x), \qquad (2)$$

where x is the Feynman variable $x = 2p_L/\sqrt{s}$. Thus the accuracy of M^2 depends on the accuracy with which the incident momenta and p_L are known. It can readily be shown that

$$(\delta M^2)^2 = (4(p_1 - p_3)\delta p_2)^2 + (4p_2\delta(p_1 - p_3))^2, \qquad (3)$$

where p_1 is the momentum of the incident proton in beam 1 (travelling towards the spectrometer), p_2 is that of the proton in beam 2 and p_3 is that of the proton detected in the spectrometer. In the case of low M^2 ($\ll s$) the first term in the equation is much smaller than the second, even though there is a 2% uncertainty in p_2 because of the energy spread in the ISR. By extrapolation of the fitted track the radial position in beam 1 of the interaction point was determined to $\pm$ 1 mm; using the ISR momentum compaction function the value of p_1 for the intersecting proton could be determined to 0.2% (limited by the amplitude of the radial betatron oscillations). The effect of making this refinement is shown in fig. 2, which shows a measured momentum spectrum (35 mrad production angle, 11.7 to 12.1 GeV in beam 1; 22.2 to 22.8 GeV in beam 2) which is dominated by elastic events. The error in M^2 is then given to a good approximation by

$$\delta M^2 \approx s\delta p_3/p_3 \approx s\delta x. \qquad (4)$$

It should be noted that the missing mass resolution in a colliding beam experiment is inherently worse by a factor s/M^2 than in experiments using a stationary target with measurement of the recoiling target particle. In particular, the mass resolution of the present experiment was not adequate to study the resonance structure seen, for example[8], in the region $M^2 < 4$ GeV^2.

A large fraction of the high momentum protons detected by the spectrometer were p - p elastic scattering events; these had to be identified and removed. A hodoscope of 38 scintillation counters (the 'forward detector' of reference[9]) and a set of 6 spark chambers were arranged around the outgoing beam 2. The counters covered all angles from 8 to 250 mrad with a resolution of 16

mrad, and the chambers covered 10 to 50 mrad vertically and $\pm$ 20 mrad horizontally. Elastic events were identified by a single charged particle detected in this system in a direction colinear in the vertical plane (in the c.m. system) with the spectrometer particle. Multiple scattering and interactions in the ISR beam pipe and in the scintillation counters required the colinearity cut to be 6 - 8 mrad wide in order to include all elastic events. Small corrections were made to allow for the inelastic contribution which satisfied the colinearity condition, and for the inefficiency of the spark chamber system. Fig. 3 illustrates the identification of elastic events in the spark chamber system with 15.4 GeV in each ISR beam and the spectrometer set at 40 mrad. The inelastic events do peak at zero colinearity angle, but much more gently than the elastic events. The shape of the inelastic distribution has been deduced from subsamples of the same data which contained different fractions of elastic events. At small angles the elastic events can
be recognised easily by this method. At large momentum transfers, however, the elastic events become too rare for their contribution to be accurately determined in this way. In these cases elastic events could still be identified by imposing the further constraint that no additional charged particles were produced (in addition to the forward hodoscope a barrel-shaped system of 140 counters[9] covered almost 4π steradians around the intersection region). Another small correction was applied to this selection method to compensate for accidental counts.

The missing mass distributions for all events which satisfied the elastic criteria were used to monitor the momentum resolution and to check the momentum scale of the spectrometer. Where necessary small corrections ($\lesssim$ 0.3%) were made to the measured proton momenta in a run to ensure that the elastic peak centred at the proton mass. This correction was then applied to the inelastic events obtained from the same run. Typical elastic and inelastic missing mass distributions are shown in fig. 4. The differential elastic cross-sections $d\sigma/dt$ were compared with the measurements

of Barbiellini et al.[10] (normalised using the Coulomb scattering data of Amaldi et al.[3]), and good agreement was found. An example of this comparison, at $s = 549$ GeV^2, is shown in fig. 5. The measured differential elastic cross-sections are given in table I.

The inelastic diffractive distribution is known to have a steep t-dependence; in order to detect as large a fraction of this cross-section as possible it was necessary to extend the range of 4-momentum transfer to small values of $|t|$. The smallest $|t|$ (~ 0.2 GeV^2) was achieved by positioning the spectrometer to its minimum angle and using the lowest operational momentum of the ISR (11.8 GeV) in the beam moving towards the spectrometer (beam 1). The selected momentum transfer was then increased when required by raising the spectrometer to larger angles. The t-range of this relatively low t data was kept constant by running with 11.8 GeV in beam 1. The s-dependence was investigated by setting beam 2 successively at 11.8, 15.4, 22.5, 26.6 and 31.4 GeV. The s-range was further increased by running with higher equal energies in the two beams, but this did not cover the smallest values of $|t|$. In all, nine different combinations of beam momenta were used; they are listed in table II, together with the t-ranges covered. Only the six combinations which produced data in the low-t range have been directly used in the analysis of s-dependence.

The luminosity of the interaction region was continuously monitored by two independent systems, each consisting of two telescopes of three scintillation counters. One telescope from each system was positioned immediately below each beam pipe. In this configuration the elastic events were avoided, which would otherwise have caused excessive sensitivity to source position. Each telescope subtended a solid angle of about 8×10^{-4} steradian at the intersection. The scintillation counters were made large (10 cm high by 40 cm wide) compared with the size of the ISR beams ($\sim$ 0.2 cm x 4 cms), so that small vertical and radial shifts between different runs at the same ISR energy had a negligible influence on the counting rates. The counting rates dN_M/dt of these monitors were thus proportional to the luminosity L at the

intersection:

$$\frac{dN_M}{dt} = \sigma_M L. \qquad (5)$$

The luminosity L is related to the beam velocities $\underline{\beta}_1 c$ and $\underline{\beta}_2 c$, the number of particles per unit length, n_1 and n_2, in the beams, the crossing angle $\alpha (= 14.8^o)$ and the effective height h_{eff} at the intersection, by

$$L = \frac{c n_1 n_2}{h_{eff} \sin\alpha} \sqrt{(\underline{\beta}_1 - \underline{\beta}_2)^2 - (\underline{\beta}_1 \times \underline{\beta}_2)^2}$$

$$= \frac{\sqrt{\beta_1 \beta_2}\, c n_1 n_2}{h_{eff}\, tg(\tfrac{1}{2}\alpha)} \left\{ 1 + (1-\beta_1\beta_2) tg^2(\tfrac{1}{2}\alpha) + \frac{(\beta_1 - \beta_2)^2}{\beta_1\beta_2 \cos^2(\tfrac{1}{2}\alpha)} \right\}^{1/2}. \qquad (6)$$

For all combinations of beam momenta between 11.8 and 31.4 GeV this differs less than 0.7% from the usual approximation

$$L \approx \frac{c n_1 n_2}{h_{eff}\, tg(\tfrac{1}{2}\alpha)}. \qquad (7)$$

At each combination of beam momenta the proportionality constant σ_M was determined from repeated measurements using the Van der Meer method[11]. The value of σ_M ranged from 50 μb at 11.8/11.8 GeV to 650 μb at 31.4/31.4 GeV for one of the counter systems, and from 100 to 1300 μb for the other. In general the luminosity constants σ_M obtained over a period of more than one year were found to be consistent to within $\pm$ 3%. The luminosities measured with both the systems in intersection 2 were compared periodically with simultaneous measurements made in the other intersection regions of the ISR. This comparison showed that changes in the I2 spectrometer settings did not severely influence the luminosity monitoring system.

As the relative normalisation of the data at different

s-values is vital to the determination of any s-dependence, all data were passed through the same procedure of Monte Carlo acceptance calculation, cross-section determination and elastic subtraction. Subsets of data in which the track reconstruction efficiency was less than 70% were not included in the final data sample. The uncertainty in the absolute normalisation of the data, from the total analysis procedure, could be as much as 15%, but the relative normalisation of all the data is thought to be accurate to within 5%. The data discussed in this paper have been taken over a period of approximately two years.

3. Results

The data have been analysed as invariant cross-sections $Ed^3\sigma/dp^3$ in terms of (i) the transverse momentum p_T and the Feynman variable x of the detected proton for the range $0.7 < x < 1$, and (ii) the momentum transfer variable t and the missing mass M^2, in finer detail around the peak.

The data are presented in tables III - XX . Fig. 6 (a) shows the dependence on p_T and x ; 6(b)-(d) show the dependence on t and M^2. The errors given in tables and figures are purely statistical. The data show Feynman scaling (dependence on x and p_T but not on s) to a good approximation over the entire range of x and p_T covered.

No attempt has been made to sub-divide the inelastic data into diffractive and non-diffractive components using model-dependent fits. The high-x non-diffractive events come from the tail of the proton fragmentation spectrum; this contribution has been estimated to be small in the region $x > 0.95$ and essentially s-independent when analysed in terms of x and p_T or M^2/s and t.

4. t-dependence

Within any restricted range of t, say 0.5 GeV^2, cross-sections at given values of M^2 and s can be well represented by a simple exponential Ae^{bt}. Over a wider range of t the parameter b depends on t. A parametrisation which is less sensitive to the t-range considered is

$$\frac{s}{\pi}\frac{d^2\sigma}{dM^2dt} = A\exp(bt + ct^2) \qquad (8)$$

Two examples of such fits are shown in fig. 7. The parameters $b(M^2)$ and $c(M^2)$ from fits at $s = 549$ GeV^2 in the range $0.15 \leq |t| \leq 1.45$ GeV^2 are shown in fig. 8. Data at all measured s-values show high values of b at low values of M^2, followed by a constant lower value for $M^2/s > 0.01$. Similar slope-mass correlations have previously been reported from other experiments on inclusive proton production[3,13,14], and from experiments on the exclusive reaction $pp \to p(n\pi^+)$ in the diffractive region[15,16]. In this experiment the effect is most clearly seen at $s = 549$ GeV^2 (possibly because the effect depends on M^2 and not on M^2/s, and the mass resolution is the best at the lowest value of s). There is agreement between these experiments if there is a small increase of b with s and the limited mass resolution of the present experiment is taken into account. The value of b outside the low-M^2 peak is about half the value found in elastic scattering. No significant s-dependence has been observed in the range 549 to 1464 GeV^2 in s.

A b decreasing with increasing M^2 is natural in a triple Regge description of the diffractive peak. The effect is further enhanced in this model by the non-diffractive background being more important at large M^2. An impact parameter description of the slope-mass correlation has been given by Humble[17], for example; the decrease of b with increasing M^2 is caused by an increasing contribution of higher order s-channel helicity flip amplitudes. Several earlier attempts to describe this slope-mass correlation as a kinematical consequence of the Deck effect have been criticised[18]. The present data exclude a parametrisation

$$b = b_o + c/(M^2 - m_p^2), \qquad (9)$$

with $b_o \approx 3$ GeV^{-2}, proposed by Lubatti and Moriyasu[19].

In order to study the overall t-dependence of the diffractive

peak, the invariant cross-sections have been integrated over M^2/s from the largest negative values (to include resolution effects) to $M^2/s = 0.05$. This upper limit is somewhat arbitrary, but over this region $\sim 98\%$ of the inclusive cross-section is estimated to be diffractive, by fitting to a formula of the triple Regge type. Extrapolation of the fits to high M^2, however, indicates that as much as one third of the total diffractive cross-section could be contained in the region $M^2/s > 0.05$. Fig. 9 shows the t-dependence of these integrated data over the entire measured range of the experiment. There is no indication of either the diffraction minimum seen in the t-dependence of the elastic scattering cross-section, nor of the break in the t-distribution of low mass excitation seen in the exclusive channel $pp \to p(n\pi^+)$[15]. After integration over the range of excited masses the t-dependence of $pp \to p(n\pi^+)$, measured at $\sqrt{s} = 53$ GeV[15], and $pp \to p(p\pi^+\pi^-)$, measured at $\sqrt{s} = 45$ GeV [20], are very similar to that of the total diffractive cross-section for $M^2/s < 0.05$. This is illustrated in fig. 9. For $|t| < 0.6$ GeV^2 each of these channels contributes about 10% to the total; at larger $|t|$ the t-dependence of the total inelastic cross-section for $M^2/s < 0.05$ flattens out. Out to the largest momentum transfer ($|t| = 4$ GeV^2) the s-dependence in the data is small; this indicates that large angle diffraction scattering is not a likely source of high-transverse momentum particles at large angles.

At small momentum transfers a triple Pomeron description has been successfully applied in the past[12]. In such a description the t-dependence is mainly determined by the proton form factor squared, and to a lesser extent by a nearly t-independent Pomeron-proton total cross-section and a weak t-dependence from the slope of the Pomeron trajectory. Though such a description can be continued to larger momentum transfers another regularity appears for $|t| > 1$ GeV^2, where the t-distribution starts to behave as

$$d\sigma/dt \propto s^{-m} f(\theta) \qquad (10)$$

Least squares fits in this region gave as best fitted value $m = 3.85$. The fits are shown in fig. 10. A power law

behaviour is expected at large angles on the basis of parton and constituent interchange models[21]. It seems that at ISR energies a similar behaviour is observed at angles below 100 mrad.

5. M^2/s-dependence

The M^2/s-dependence at two values of t is reproduced in fig. 11. The data are seen to scale well in terms of this variable through the high mass ($M^2/s > 0.01$) diffractive region. The function s/M^2 is shown as a dashed line in fig. 11(a) to demonstrate the approximate M^2 dependence of the data. A cross-section which falls as s/M^2 is predicted for triple Pomeron coupling near $t = 0$ and has previously been reported by several groups[12)13)22)]. The non-invariant cross-sections $d^2\sigma/dtdM^2$ would also be independent of s in a region where the invariant cross-section data both scale in terms of the variable M^2/s and also have a s/M^2 dependence. At larger $|t|$ the spectra start to deviate from the s/M^2 dependence, but still show scaling in M^2/s. This is demonstrated in fig. 11(b) for $t = -1.45$ GeV^2. The gradual change with t of the M^2/s dependence of the spectra has been the basis of an estimate of the Pomeron slope parameter, $\alpha_p \simeq 0.2$, in an earlier publication[12].

The behaviour of the cross-sections near the kinematic boundary $(M_p + M_\pi)^2/s$ can be deduced only indirectly in this experiment. Because of the experimental resolution only the mean position of the inelastic cross-section peak on the M^2/s-scale, defined as the weighted mean for $M^2/s < 0.02$, can be determined. It shows a small shift to lower M^2/s with increasing s. The movement relative to the elastic peak position at $t = -0.3$ GeV^2 is shown in fig. 12(a). The statistical errors in the mean values of M^2/s correspond to accuracies of the order of $\frac{\delta p}{p} = \pm 2 \times 10^{-4}$. These accuracies have been achieved by taking mean values in samples of $\sim 10^5$ events per data point , and cannot be obtained from the data tables in which the M^2/s scale is adjusted with an

accuracy $\frac{\delta p}{p} \sim \pm 5 \times 10^{-4}$. Systematic errors resulting from the elastic subtraction procedure are t-dependent, but are also estimated to be of the order of (1 to 2) x 10^{-4}. The effect of the experimental resolution has been taken into account in calculating the mean position of the inelastic peak. The t-dependence of the quantity $\Delta M^2/s = < M^2/s >_{inel} - m_p^2/s$ is shown at a mean value of s = 1000 GeV^2 in fig. 12(b). This figure indicates that a simple M^2/s dependence, which would imply no t-dependence in $\Delta M^2/s$ is inadequate to describe the shape of the inelastic cross-section at very small values of M^2/s. The curves drawn on the figure have been calculated from a parametrisation of the data as

$$E \; d^3\sigma/dp^3 \propto (\nu/s)^{-1-0.2\,t} \qquad (11)$$

with $\nu = M^2 - m_p^2 - t$, and a fixed lower limit in M^2_{min} at 1.4 GeV^2. Such a parametrisation is compatible with the recent high resolution data of Akimov et al.[8] at small $|t|$ and an s-range overlapping that of the present experiment. The s and t dependences of $\Delta M^2/s$ shown in fig. 12 are qualitatively described by this simple parametrisation, though a lower limit of $M^2_{min} = 1.2$ GeV^2 would give better quantitative agreement with the data.

6. s-dependence

The s-dependence of the total diffraction peak can be obtained after successive integrations over M^2/s and t. Figs. 13 (a) and 13 (b) show examples of the s-dependence at fixed t for two different integration ranges in M^2/s. In these figures, a 5% error has been added in quadrature to the statistical errors to take account of possible systematic uncertainties between the data at different s values. The cross-sections integrated over M^2/s from $-\infty$ to 0.01 (fig. 13(a)) show a rise of $\sim$ 35% over the s-range 549 to 1464 GeV^2. When the upper integration limit is increased to $M^2/s = 0.05$ (fig.13(b)), this rise reduces to $\sim$ 15%, demonstrating that the rise in the cross-section is concentrated in the low M^2 region where the kinematic range increases with s.

Table XXI lists cross-sections integrated to $M^2/s = 0.05$ for all s and t values covered in this experiment.

In order to estimate the s-dependence of the total single diffractive cross-section (with $M^2/s < 0.05$), the data have been integrated using the quadratic exponential t-dependence described in eqn. 8. This procedure can be applied in the low-s, low-t range of the experiment where measurements with asymmetric ISR energies have been done. Even at these s-values the procedure implies extrapolation over a factor of 3 in cross-section on the low $|t|$ side. At $s = 549$ GeV^2 and 934 GeV^2 the t-ranges of the measurements have been extended to $0.15 < |t| < 1.45$ GeV^2 and $0.25 < |t| < 2.00$ GeV^2 respectively, so that a value of c could be determined from $|t| < 1.45$ GeV^2. The t-ranges covered at the other s-values were too limited to determine c accurately, so the mean value found from the data with the larger t range ($c = 1.77 \pm 0.15$ GeV^{-4}) was used at all s values. At small $|t|$ the parametrisation can be approximated by a simple exponential with slope b. The values of b obtained in the present experiment show no significant s-dependence, and the mean value obtained, 7.13 ± 0.05 GeV^{-2}, is in good agreement with the average value 7.0 ± 0.4 GeV^{-2} found in the region $0 < |t| < 0.5$ GeV^2 by several experiments at FNAL[14)22)23)]. The parametrisation thus found has been integrated numerically in the range $0 < |t| < 1$ GeV^2. The high $|t|$ data (see fig. 9) can be approximated by a simple exponential function in the range $1.0 < |t| < 3.0$ GeV^2. The contribution of this part is estimated from data at $s = 2783$ GeV^2 to be $\leqslant 1\%$ of the total inelastic diffractive cross-section.

The integrated cross-sections have been doubled, to account for the equal probabilities of the reactions $p_1p_2 \to p_1X$ and $p_1p_2 \to Xp_2$, and are listed in column 2 of table XXII. The variation of the total single diffraction cross-section, σ_{SD} ($M^2/s < 0.05$), is shown in fig. 14 and indicates a rise of $(15 \pm 5)\%$ over the measured s-range. The curves drawn on this figure represent the s-dependence of both a diffraction component which rises by the same amount as the total inelastic cross-section, and a diffractive component which remains a fixed fraction of the inelastic cross-

section. The data favour the second possibility, implying that the single diffractive cross-section (for $M^2/s < 0.05$) cannot account for a large fraction of the rise of the total inelastic cross-section. The result is in agreement with the more speculative conclusion reached in an earlier experiment[12].

Although the relative normalisations of the total inelastic cross-sections obtained above are thought to be accurate to $\sim$ 5%, their absolute normalisations are only known to within $\sim$ 15%. Comparisons of the elastic data obtained in the present experiment with published data[3)10)] indicate that the small angle cross-sections reported here are higher by up to 15%.

The measured cross-sections integrated up to $M^2/s = 0.10$ are given in column 3 of table XXII; they are compared with results from both a hydrogen jet experiment[24)] and several bubble chamber experiments[14)22)23)] in fig. 15. The present cross-sections are $\sim$ 20% higher than those found by Schamberger et al.[24)] by extrapolation from a restricted t-range, $|t| < 0.22$ GeV^2 using a single exponential in t. These authors, however, point out that their cross-sections could rise by as much as 10% if $d\sigma/dt$ were to flatten out at large $|t|$. The flattening t-dependence found in the present experiment indicates that such a 10% rise is expected and the cross-sections deduced from reference 24 by making this increase are shown dotted in fig. 15. With this correction the results from the various experiments are in good agreement within the overlapping s-range.

7. Conclusions

The following properties of the diffractive peak have been determined.

1) t-dependence.

The dependence on t becomes weaker as $|t|$ increases, and a simple exponential in t can only be used to describe the data over a limited t range. No indication of a diffractive dip has been observed in the range $0.2 < |t| < 4$ GeV^2. For $|t| > 1$ GeV^2 the t-dependence of the integrated diffractive peak can be approximated by a power law behaviour in s at fixed angle. The

t-slope decreases with increasing mass and eventually becomes mass independent.

2) M^2-dependence.

For small $|t|$ the long tail of the diffractive peak falls approximately as $1/M^2$ over the range $0.005 < M^2/s < 0.035$. A more complicated M^2 dependence is present at small values of M^2, where a t-dependent effective cut off has been deduced from a shift of the peak of the inelastic cross-section towards the falling M^2_{min}/s limit as s increases.

3) s-dependence.

The data scale well in terms of the variable M^2/s ($\sim$ 1-x) for $M^2/s > 0.01$. For smaller values of M^2/s the integrated cross-sections rise with increasing s. This effect leads to a total single diffraction component which, when integrated up to $M^2/s = 0.05$ increases by $(15 \pm 5)\%$ over the range s = 549 to 1464 GeV^2.

8. Acknowledgment

We are grateful to the ISR Experimental Support, Vacuum, Operations, Power and Survey Groups for their assistance. This experiment has been supported by the Nederlandse Organisatie voor Zuiver Wetenschappelijk Onderzoek through F.O.M., and by the U.K. Science Research Council through the Daresbury Laboratory.

References

1. J.C. Sens, Proceedings of the Fourth International Conference on High Energy Collisions, Oxford, 1972, edited by J.R. Smith (Rutherford High Energy Laboratory, Didcot, Berkshire, England, 1972) p. 177.

2. ACGHT Collaboration:
Nucl. Phys. B79 (1974) 1.
ANL-NAL Collaboration:
Phys. Rev. Lett. 31 (1973) 1080.
Phys. Rev. D 9 (1974) 1171.
Phys. Rev. D 9 (1974) 2689.
CHLM Collaboartion:
Nucl. Phys. B51 (1973) 388.
Nucl. Phys. B54 (1973) 6.
Nucl. Phys. B72 (1974) 376.
Data from present experiment reported to A.P.S. meeting Seattle U.S.A., Aug. 1975: M. Derrick, Argonne Laboratory Report ANL-HEP-CP-75-52.
Columbia-Stony Brook Collaboration:
Phys. Rev. Lett. 32 (1974) 389.
Phys. Rev. Lett. 34 (1975) 1121
Michigan-Rochester Collaboration:
Phys. Rev. Lett. 32 (1974) 257.
NAL-UCLA Collaboration:
Phys. Lett. 45B (1973) 399.
Phys. Lett. 45B (1973) 402.
Rutgers-Imperial College Collaboration:
Phys. Rev. Lett. 30 (1973) 766.
Phys. Rev. Lett. 31 (1973) 1527.
Phys. Rev. Lett. 31 (1973) 1530.
USA-USSR Collaboration:
Phys. Rev. Lett. 35 (1975) 763.
Phys. Rev. Lett. 35 (1975) 766.

3. U. Amaldi, R. Biancastelli, C. Bosio, G. Matthiae, J.V. Allaby, W. Bartel, G. Cocconi, A.N. Diddens, R.W. Dobinson, A.M. Wetherell, Phys. Letters 44B (1973) 112.

4. S.R. Amendolia, G. Bellettini, P.L. Braccini, C. Bradaschia, R. Castaldi, V. Cavasinni, C. Cerri, T. Del Prete, L. Foà, P. Giromini, P. Laurelli, A. Menzione, L. Ristori, G. Sanguinetti, A. Valdata, G. Finocchiaro, P. Grannis, D. Green, R. Mustard, R. Thun, Phys. Letters 44B (1973) 119.

5. M.G. Albrow, D.P. Barber, A. Bogaerts, B. Bošnjaković, J.R. Brooks, A.B. Clegg, F.C. Erné, C.N.P. Gee, A.D. Kanaris, A. Lacourt, D.H. Locke, F.K. Loebinger, P.G. Murphy, A. Rudge, J.C. Sens, K. Terwilliger, F. van der Veen, Phys. Letters 42B (1972) 279.

6. M.G. Albrow, A. Bagchus, D.P. Barber, A. Bogaerts, B. Bošnjaković, J.R. Brooks, A.B. Clegg, F.C. Erné, C.N.P. Gee, D.H. Locke, F.K. Loebinger, P.G. Murphy, A. Rudge, J.C. Sens, Nucl. Phys. B73 (1974) 40.

7. M.G. Albrow, D.P. Barber, P. Benz, B. Bošnjaković, J.R. Brooks, C.Y. Chang, A.B. Clegg, F.C. Erné, P. Kooijman, F.K. Loebinger, N.A. McCubbin, P.G. Murphy, D. Radojičić, A. Rudge, J.C. Sens, A.L. Sessoms, J. Singh, J. Timmer, to be published.

8. Y. Akimov, R. Cool, L. Goulianos, D. Gross, A. Melissinos, E. Malamud, S. Mukhin, D. Nitz, S. Olsen, H. Sticker, G. Takhtamyshev, V. Tsarev, R. Yamada, P. Zimmerman, Phys. Rev. Letters 35 (1975) 763.

9. M.G. Albrow, D.P. Barber, P. Benz, B. Bošnjaković, J.R. Brooks, A.B. Clegg, C.Y. Chang, F.C. Erné, P. Kooijman, F.K. Loebinger, N.A. McCubbin, P.G. Murphy, D. Radojičić, A. Rudge, J.C. Sens, A.L. Sessoms, J. Singh, P. Strolin, J. Timmer, submitted to Nucl. Phys. B.

10. G. Barbiellini, M. Bozzo, P. Darriulat, G. Diambrini Palazzi, G. De Zorzi, A. Fainberg, M.I. Ferrero, M. Holder, A. McFarland, G. Maderni, S. Orito, J. Pilcher, C. Rubbia, A. Santroni, G. Sette, A. Staude, P. Strolin, K. Tittel, Phys. Letters 39B (1972) 663.

11. S. van der Meer, CERN Internal Report, ISR-PO/68-31 (1968).

12. M.G. Albrow, A. Bagchus, D.P. Barber, A. Bogaerts, B. Bošnjaković, J.R. Brooks, A.B. Clegg, F.C. Erné, C.N.P.Gee, D.H. Locke, F.K. Loebinger, P.G. Murphy, A. Rudge, J.C. Sens, F. van der Veen, Nucl. Phys. B72 (1974) 376.

13. Y. Akimov, R. Cool, L. Golovanov, K. Goulianos, D. Gross, A. Melissinos, E. Malamud, S. Mukhin, D. Nitz, S. Olsen, H. Sticker, G. Takhtamyshev, V. Tsarev, R. Yamada, P. Zimmerman, Phys. Rev. Letters 35 (1975) 766.

14. S.J. Barish, D.C. Colley, P.F. Schultz, J. Whitmore, Phys. Rev. Letters 31 (1973) 1080.

15. E. Nagy, M. Regler, W. Schmidt-Parzefall, K. Winter, A. Brandt, G. Flügge, F. Niebergall, K.R. Schubert, P.E. Schumacher, C. Broll, G. Coignet, J. Favier, L. Massonet, M. Vivargent, W. Bartl, H. Dibon, Ch. Gottfried, G. Neuhofer, CHOV Collaboration, Experimental results on inelastic diffraction scattering in proton-proton collision at the ISR, contribution to the London Conference, 1974.

16. K. Böckmann, H.G. Heilmann, U. Idschok, P. Kobe, F. Selonke, V. Blobel, H. Fesefeldt, B. Hellwig, D. Mönkemeyer, H. Franz, P. Freund, W. Schrankel, Bonn University preprint, PIB 3/27.

17. S. Humble, Nucl. Phys. B76 (1974) 137.

18. H.I. Miettinen and P. Pirilä, Phys. Letters 40B (1972) 127.

19. H.J. Lubatti and K. Moriyasu, Nuovo Cimento Letters 12 (1975) 97.

20. R. Webb, G. Trilling, V. Telegdi, P. Strolin, B. Shen, P. Schlein, J.Rander, B. Naroska , T. Meyer, W. Marsh, W. Lockman, J. Layter, A. Kernan, M. Hansroul, S.Y. Fung, H. Foeth, R. Ellis, A. Derevshikov, M. Bozzo, A. Böhm, L. Baksay,Phys. Letters 55B (1975) 331.

21. J.D. Bjorken, Aix-en-Provence Conference report (1973). P.V. Landshoff, London Conference Report (1974),and references therein.

22. J.W. Chapman, J.W. Cooper, N. Green, A.A. Seidl, J.C. J.C. Vander Velde, C.M. Bromberg, D. Cohen, T. Ferbel, P. Slattery, Phys. Rev. Letters 32 (1974) 257.

23. F.T. Dao, D. Gordon, J. Lach, E. Malamud, J. Schirell, T. Meyer, R. Poster, P.E. Schlein, W.E. Slater, Phys. Letters 45B (1973) 399.

24. R.D. Schamberger, Jr., J. Lee-Franzini, R. McCarthy, S. Childress, P. Franzini, Phys. Rev. Letters 34 (1975) 1121.

Table captions

Table I. Elastic cross-sections $d\sigma/dt$ (mb.GeV^{-2}).

Table II. s and t ranges covered in the experiment.

Table III. Inelastic cross-sections $E\, d^3\sigma/dp^3$ (mb.GeV^{-2}) as a function of p_T and x, s = 549 GeV^2.

Table IV. Inelastic cross-sections $E\, d^3\sigma/dp^3$ (mb.GeV^{-2}) as a function of p_T and x, s = 725 GeV^2.

Table V. Inelastic cross-sections $E\, d^3\sigma/dp^3$ (mb.GeV^{-2}) as a function of p_T and x, s = 934 GeV^2.

Table VI. Inelastic cross-sections $E\, d^3\sigma/dp^3$ (mb.GeV^{-2}) as a function of p_T and x, s = 1047 GeV^2.

Table VII. Inelastic cross-sections $E\, d^3\sigma/dp^3$ (mb.GeV^{-2}) as a function of p_T and x, s = 1239 GeV^2.

Table VIII. Inelastic cross-sections $E\, d^3\sigma/dp^3$ (mb.GeV^{-2}) as a function of p_T and x, s = 1464 GeV^2.

Table IX. Inelastic cross-sections $E\, d^3\sigma/dp^3$ (mb.GeV^{-2}) as a function of p_T and x, s = 1995 GeV^2.

Table X. Inelastic cross-sections $E\, d^3\sigma/dp^3$ (mb.GeV^{-2}) as a function of p_T and x, s = 2783 GeV^2.

Table XI. Inelastic cross-sections $E\, d^3\sigma/dp^3$ (mb.GeV^{-2}) as a function of p_T and x, s = 3892 GeV^2.

Table XII. Inelastic cross-sections $\frac{s}{\pi}\, d^2\sigma/dtdM^2$ (mb.GeV^{-2}) as a function of t and M^2, s = 549 GeV^2.

Table XIII. Inelastic cross-sections $\frac{s}{\pi} d^2\sigma/dtdM^2$ (mb.GeV^{-2}) as a function of t and M^2, s = 725 GeV^2.

Table XIV. Inelastic cross-sections $\frac{s}{\pi} d^2\sigma/dtdM^2$ (mb.GeV^{-2}) as a function of t and M^2, s = 934 GeV^2.

Table XV. Inelastic cross-sections $\frac{s}{\pi} d^2\sigma/dtdM^2$ (mb.GeV^{-2}) as a function of t and M^2, s = 1047 GeV^2.

Table XVI. Inelastic cross-sections $\frac{s}{\pi} d^2\sigma/dtdM^2$ (mb.GeV^{-2}) as a function of t and M^2, s = 1239 GeV^2.

Table XVII. Inelastic cross-sections $\frac{s}{\pi} d^2\sigma/dtdM^2$ (mb.GeV^{-2}) as a function of t and M^2, s = 1464 GeV^2.

Table XVIII. Inelastic cross-sections $\frac{s}{\pi} d^2\sigma/dtdM^2$ (mb.GeV^{-2}) as a function of t and M^2, s = 1995 GeV^2.

Table XIX. Inelastic cross-sections $\frac{s}{\pi} d^2\sigma/dtdM^2$ (mb.GeV^{-2}) as a function of t and M^2, s = 2783.

Table XX. Inelastic cross-sections $\frac{s}{\pi} d^2\sigma/dtdM^2$ (mb.GeV^{-2}) as a function of t and M^2, s = 3892 GeV^2.

Table XXI. Inelastic cross-sections $d\sigma/dt$ (mb.GeV^{-2}), integrated over M^2 for $M^2/s < 0.05$.

Table XXII. Inelastic cross-sections integrated over t and M^2, for $M^2/s \leqslant 0.05$ and $M^2/s \leqslant 0.10$.

Figure captions

Fig. 1 Schematic side and plan view of the apparatus.

Fig. 2 Spectrometer-beam momentum before (----) and after (——) correction for radial vertex position. The double peak structure before correction reflects the radial density distribution of beam 1.

Fig. 3 Identification of elastic events; colinearity distribution(in the vertical plane) in the spark chambers opposite to the spectrometer.

Fig. 4 The elastic and inelastic invariant cross-sections at $t = -0.25$ GeV^2 and $s = 934$ GeV^2 after separation. The curves are drawn to guide the eye.

Fig. 5 The elastic differential cross-section at $s = 549$ GeV^2 from the present experiment compared with the data of ref. 10 normalised by the forward scattering measurements of ref. 3.

Fig.6(a) The invariant inelastic cross-section at fixed values of p_T as a function of x and s.

(b)-(d) The invariant inelastic cross-sections at fixed values of t as a function of M^2/s and s.

Fig. 7 The t-dependence of the invariant cross-section for two values of M^2 at $s = 549$ GeV^2. The curves show the quadratic exponential fits described in the text.

Fig. 8 The variation of the exponential slopes b and c with M^2 for $s = 549$ GeV^2. The horizontal bars indicate the M^2 resolution.

Fig. 9 The t-dependence of the inelastic cross-section (integrated up to $M^2/s = 0.05$) over the full t-range of the data. Some data on exclusive channels are also shown.

Fig. 10 The s-dependence of the inelastic cross-section (integrated up to $M^2/s = 0.05$) at fixed angle. The data fit a power law for $|t| > 1$ GeV^2.

Fig. 11 The invariant inelastic cross-section at fixed t as a function of M^2/s and s. The dashed line shows a dependence of the form $(M^2/s)^{-1}$. (a) $t = -0.25$ GeV^2. (b) $t = -1.45$ GeV^2.

Fig.12(a) The separationof the elastic cross-section and the weighted mean of the inelastic cross-section for $M^2/s < 0.02$, $\Delta(M^2/s) = \langle M^2/s \rangle_{inel} - m_p^2/s$, as a function of s at $t = -0.3$ GeV^2.

(b) $\Delta(M^2/s)$ at a mean $s = 1000$ GeV^2 as a function of t. The lines drawn on the figure are from a calculation described in the text.

Fig. 13 The inelastic cross-section integrated up to (a) $M^2/s = 0.01$ and (b) $M^2/s = 0.05$ as a function of s at fixed values of t.

Fig. 14 The single diffractive cross-section (defined as twice the measured inelastic cross-section for $M^2/s < 0.05$) as a function of s. The curves show a diffractive component which rises by the same amount as the total inelastic cross-section (----), and a diffractive component which remains a fixed fraction of this inelastic cross-section (....).

Fig. 15 Comparison of the single diffractive cross-section for

$M^2/s < 0.10$ measured by several experiments. The data of ref. 24 have been increased by 10% (to account for the decreasing t-dependence at higher t observed by the present experiment) and are shown dotted.

ELASTIC CROSS-SECTIONS $\frac{d\sigma}{dt}$ (mb. GeV^{-2})

$-t$ (GeV^2)	s = 549 GeV^2	s = 725 GeV^2	s = 934 GeV^2	s = 1047 GeV^2	s = 1239 GeV^2	s = 1464 GeV^2
0.15	16.77 ± 0.12	12.32 ± 0.17				
0.20	9.55 ± 0.06	8.84 ± 0.09		9.39 ± 0.22	9.74 ± 0.12	10.16 ± 0.08
0.25	5.40 ± 0.04	4.63 ± 0.04	5.27 ± 0.19	6.04 ± 0.15	4.64 ± 0.06	5.99 ± 0.05
0.30	3.15 ± 0.03	2.91 ± 0.03	3.02 ± 0.11	3.39 ± 0.09	2.80 ± 0.05	3.22 ± 0.04
0.35	2.04 ± 0.03	1.66 ± 0.02	1.98 ± 0.07	1.96 ± 0.08	1.64 ± 0.02	2.00 ± 0.03
0.40	1.20 ± 0.03		1.24 ± 0.04			
0.45	0.720 ± 0.023	0.67 ± 0.01	0.76 ± 0.03		0.644 ± 0.014	0.638 ± 0.016
0.50	0.425 ± 0.014	0.40 ± 0.01	0.44 ± 0.02		0.404 ± 0.009	0.387 ± 0.012
0.55	0.258 ± 0.010	0.20 ± 0.01	0.251 ± 0.010		0.243 ± 0.005	0.209 ± 0.009
0.60	0.175 ± 0.003		0.179 ± 0.009			0.135 ± 0.008
0.65	0.100 ± 0.006		0.106 ± 0.008		0.087 ± 0.003	
0.70	0.068 ± 0.005		0.069 ± 0.003			0.047 ± 0.006
0.75	0.047 ± 0.004		0.044 ± 0.004		0.033 ± 0.003	
0.80	0.025 ± 0.004		0.031 ± 0.003			
0.85	0.019 ± 0.002		0.021 ± 0.003			
0.90	0.011 ± 0.002		0.015 ± 0.002			
0.95	0.009 ± 0.002		0.007 ± 0.002			
1.00	0.006 ± 0.002					
1.05	0.005 ± 0.002					

Table I

TABLE II

BEAM 1 MOMENTUM (GeV)	BEAM 2 MOMENTUM (GeV)	c.m. ENERGY s (GeV^2)	t RANGE COVERED $(GeV)^2$
11.8	11.8	549	0.15 - 1.45
11.8	15.4	725	0.15 - 0.55
15.4	15.4	934	0.25 - 2.00
11.8	22.5	1047	0.20 - 0.35
11.8	26.6	1239	0.20 - 0.75
11.8	31.4	1464	0.20 - 0.70
22.5	22.5	1995	0.45 - 3.55
26.6	26.6	2783	0.65 - 4.15
31.4	31.4	3892	1.15 - 2.65

INELASTIC CROSS-SECTION $E\,d^3\sigma/dp^3$ $(mb.GeV^{-2})$; $s = 549\ GeV^2$

x	p_T = 0.3 GeV/c	p_T = 0.4 GeV/c	p_T = 0.5 GeV/c	p_T = 0.6 GeV/c	p_T = 0.7 GeV/c	p_T = 0.8 GeV/c	p_T = 0.9 GeV/c	p_T = 1.0 GeV/c	p_T = 1.1 GeV/c
.702	12.95 ± 0.25	8.66 ± 0.22	4.51 ± 0.13	2.99 ± 0.08	2.13 ± 0.06				
.715	12.00 ± 0.28	8.80 ± 0.25	4.33 ± 0.14	2.95 ± 0.08	1.91 ± 0.05				
.728	12.87 ± 0.25	9.01 ± 0.23	4.64 ± 0.15	3.03 ± 0.08	1.83 ± 0.05				
.740	11.73 ± 0.25	8.40 ± 0.21	4.73 ± 0.15	2.96 ± 0.08	1.87 ± 0.05				
.753	11.62 ± 0.24	8.91 ± 0.20	4.51 ± 0.13	2.90 ± 0.08	1.77 ± 0.05				
.766	11.26 ± 0.24	9.09 ± 0.21	4.38 ± 0.15	2.66 ± 0.08	1.57 ± 0.05				
.779	11.05 ± 0.24	8.74 ± 0.18	4.48 ± 0.13	2.68 ± 0.08	1.62 ± 0.05				
.792	11.05 ± 0.24	8.45 ± 0.18	4.38 ± 0.14	2.60 ± 0.07	1.52 ± 0.04	0.99 ± 0.04	0.47 ± 0.03		
.804	11.06 ± 0.27	9.42 ± 0.19	5.17 ± 0.15	2.56 ± 0.08	1.59 ± 0.05	0.99 ± 0.04	0.51 ± 0.03		
.817	10.50 ± 0.28	9.02 ± 0.18	5.26 ± 0.15	2.60 ± 0.08	1.60 ± 0.05	0.97 ± 0.04	0.44 ± 0.03	0.28 ± 0.02	
.830	10.03 ± 0.28	9.18 ± 0.17	4.94 ± 0.14	2.45 ± 0.08	1.44 ± 0.05	0.90 ± 0.03	0.43 ± 0.03	0.29 ± 0.02	
.843	10.10 ± 0.31	8.74 ± 0.17	4.94 ± 0.14	2.47 ± 0.09	1.46 ± 0.05	0.87 ± 0.03	0.40 ± 0.03	0.27 ± 0.02	
.856		9.45 ± 0.17	4.99 ± 0.13	2.62 ± 0.09	1.38 ± 0.05	0.83 ± 0.03	0.44 ± 0.03	0.25 ± 0.02	
.869		9.28 ± 0.18	5.46 ± 0.14	2.48 ± 0.09	1.47 ± 0.05	0.81 ± 0.03	0.61 ± 0.04	0.23 ± 0.02	
.881		9.02 ± 0.17	5.39 ± 0.13	2.59 ± 0.09	1.46 ± 0.05	0.80 ± 0.03	0.52 ± 0.03	0.21 ± 0.02	
.894		9.18 ± 0.17	5.58 ± 0.14	2.51 ± 0.09	1.34 ± 0.05	0.82 ± 0.02	0.48 ± 0.03	0.20 ± 0.02	
.907		9.24 ± 0.19	5.62 ± 0.13	2.89 ± 0.10	1.47 ± 0.05	0.81 ± 0.03	0.48 ± 0.03	0.20 ± 0.02	
.920		9.71 ± 0.19	6.31 ± 0.14	3.37 ± 0.11	1.54 ± 0.06	0.83 ± 0.03	0.53 ± 0.02	0.18 ± 0.02	
.933		10.71 ± 0.21	6.57 ± 0.14	3.74 ± 0.12	1.71 ± 0.06	0.86 ± 0.03	0.54 ± 0.02	0.21 ± 0.02	0.12 ± 0.01
.945		12.89 ± 0.25	8.40 ± 0.16	4.32 ± 0.13	1.97 ± 0.07	1.04 ± 0.04	0.59 ± 0.03	0.17 ± 0.02	0.17 ± 0.02
.958		14.12 ± 0.28	9.65 ± 0.18	4.97 ± 0.13	2.37 ± 0.08	1.25 ± 0.04	0.75 ± 0.03	0.29 ± 0.02	0.22 ± 0.02
.971		20.30 ± 0.39	13.74 ± 0.21	7.84 ± 0.17	3.44 ± 0.10	1.81 ± 0.05	0.91 ± 0.03	0.42 ± 0.03	0.26 ± 0.02
.984		41.52 ± 0.57	33.42 ± 0.32	18.32 ± 0.25	7.48 ± 0.14	3.58 ± 0.07	1.80 ± 0.04	1.01 ± 0.05	0.35 ± 0.02
.997		74.94 ± 1.03	41.57 ± 0.36	16.42 ± 0.22	6.98 ± 0.15	3.00 ± 0.07	1.28 ± 0.04	0.52 ± 0.03	0.09 ± 0.01
1.009		0.64 ± 0.10	0.31 ± 0.04	0.17 ± 0.02	0.14 ± 0.02	0.08 ± 0.01	0.05 ± 0.01	0.02 ± 0.01	

Table III

INELASTIC CROSS-SECTION $E\,d^3\sigma/dp^3$ $(mb.GeV^{-2})$; $s = 725\ GeV^2$						
x	$p_T = 0.3$ GeV	$p_T = 0.4$ GeV	$p_T = 0.5$ GeV	$p_T = 0.6$ GeV	$p_T = 0.7$ GeV	$p_T = 0.8$ GeV
0.616	10.3 ± 0.6	7.5 ± 0.4	5.1 ± 0.3			
0.646	10.2 ± 0.6	7.0 ± 0.4	4.4 ± 0.3			
0.676	10.2 ± 0.6	7.1 ± 0.4	4.5 ± 0.2			
0.705	10.2 ± 0.6	7.0 ± 0.4	4.5 ± 0.2	2.8 ± 0.2		
0.735	10.2 ± 0.6	6.8 ± 0.4	4.5 ± 0.2	2.9 ± 0.2		
0.765	10.7 ± 0.6	7.0 ± 0.4	4.5 ± 0.2	2.5 ± 0.1		
0.794	10.8 ± 0.6	6.8 ± 0.4	4.3 ± 0.2	2.4 ± 0.1	1.6 ± 0.2	
0.824	11.5 ± 0.7	7.0 ± 0.4	4.0 ± 0.2	2.6 ± 0.1	1.5 ± 0.1	
0.854	10.9 ± 0.8	7.1 ± 0.4	3.9 ± 0.2	2.4 ± 0.1	1.5 ± 0.1	
0.883	12.1 ± 1.1	7.3 ± 0.4	4.4 ± 0.2	2.5 ± 0.1	1.4 ± 0.1	0.9 ± 0.2
0.913	12.3 ± 1.2	7.8 ± 0.5	4.6 ± 0.3	2.6 ± 0.1	1.6 ± 0.1	1.0 ± 0.1
0.943	14.9 ± 1.5	10.6 ± 0.6	5.8 ± 0.3	3.5 ± 0.2	2.0 ± 0.1	1.0 ± 0.1
0.975	34.3 ± 3.1	22.8 ± 1.3	12.2 ± 0.6	7.3 ± 0.4	4.2 ± 0.2	2.1 ± 0.1
0.995	169.2 ± 14.1	66.0 ± 3.6	29.2 ± 1.5	12.2 ± 0.6	5.7 ± 0.3	2.7 ± 0.2

TABLE IV

INELASTIC CROSS-SECTION $E\,d^3\sigma/d\bar{p}^3$ $(mb.GeV^{-2})$; $s = 934\ GeV^2$							
x	$p_T = 0.4$ GeV	$p_T = 0.5$ GeV	$p_T = 0.6$ GeV	$p_T = 0.7$ GeV	$p_T = 0.8$ GeV	$p_T = 0.9$ GeV	$p_T = 1.0$ GeV
0.676	8.1 ± 0.4	4.97 ± 0.27	3.00 ± 0.16	1.90 ± 0.16			
0.701	8.0 ± 0.3	5.02 ± 0.21	3.26 ± 0.14	1.86 ± 0.12			
0.726	8.5 ± 0.4	5.01 ± 0.19	2.78 ± 0.11	1.87 ± 0.09			
0.753	7.5 ± 0.4	4.52 ± 0.17	2.84 ± 0.11	1.73 ± 0.08			
0.779	8.4 ± 0.5	4.79 ± 0.18	2.63 ± 0.10	1.62 ± 0.07	1.01 ± 0.08		
0.805	9.3 ± 0.5	4.78 ± 0.18	2.53 ± 0.10	1.58 ± 0.07	0.82 ± 0.05		
0.831	8.7 ± 0.5	4.87 ± 0.19	2.60 ± 0.10	1.52 ± 0.06	0.79 ± 0.05		
0.857	9.2 ± 0.6	4.87 ± 0.19	2.73 ± 0.11	1.34 ± 0.06	0.72 ± 0.04	0.42 ± 0.05	
0.884	8.7 ± 0.7	5.05 ± 0.20	2.62 ± 0.10	1.39 ± 0.06	0.75 ± 0.04	0.40 ± 0.04	
0.910	9.9 ± 1.0	5.75 ± 0.23	2.87 ± 0.11	1.52 ± 0.06	0.82 ± 0.04	0.44 ± 0.03	0.17 ± 0.04
0.936	12.3 ± 1.6	6.25 ± 0.26	3.41 ± 0.13	1.84 ± 0.07	0.95 ± 0.04	0.49 ± 0.03	0.23 ± 0.04
0.963		10.21 ± 0.45	5.05 ± 0.19	2.57 ± 0.10	1.34 ± 0.06	0.70 ± 0.04	0.37 ± 0.03
0.992		29.96 ± 1.53	17.73 ± 0.77	8.09 ± 0.31	4.11 ± 0.16	1.88 ± 0.07	0.80 ± 0.05
1.008		4.01 ± 0.38	1.47 ± 0.05	0.56 ± 0.05	0.26 ± 0.02	0.09 ± 0.01	0.03 ± 0.01

TABLE V

INELASTIC CROSS-SECTION $E\,d^3\sigma/dp^{-3}$ (mb.GeV^{-2}); s = 1047 GeV^2			
x	p_T = 0.4 GeV	p_T = 0.5 GeV	p_T = 0.6 GeV
0.810	7.5 ± 0.4		
0.835	7.7 ± 0.4		
0.860	7.8 ± 0.4	4.7 ± 0.3	
0.885	8.4 ± 0.4	4.5 ± 0.3	
0.909	9.0 ± 0.4	5.7 ± 0.3	2.7 ± 0.4
0.934	10.7 ± 0.5	6.7 ± 0.3	3.1 ± 0.3
0.959	14.6 ± 0.7	8.7 ± 0.4	4.8 ± 0.3
0.987	46.1 ± 2.1	28.1 ± 1.1	16.0 ± 0.7
1.002	37.0 ± 2.8	17.6 ± 1.2	7.0 ± 0.5
1.028	0.02 ± 0.03	0.01 ± 0.01	0.01 ± 0.01

TABLE VI

INELASTIC CROSS-SECTION $E\,d^3\sigma/d\bar{p}^3$ (mb.GeV^{-2}); s = 1239 GeV^2							
x	p_T = 0.3 GeV	p_T = 0.4 GeV	p_T = 0.5 GeV	p_T = 0.6 GeV	p_T = 0.7 GeV	p_T = 0.8 GeV	p_T = 0.9 GeV
0.702	11.88 ± 0.37	7.38 ± 0.22	4.34 ± 0.15	2.88 ± 0.11	2.05 ± 0.20		
0.725	11.09 ± 0.35	7.18 ± 0.21	4.49 ± 0.16	2.80 ± 0.11	1.74 ± 0.14		
0.747	12.98 ± 0.41	6.78 ± 0.20	4.29 ± 0.14	2.70 ± 0.10	1.72 ± 0.10		
0.770	12.42 ± 0.41	7.52 ± 0.22	4.20 ± 0.14	2.62 ± 0.10	1.78 ± 0.09		
0.792	12.84 ± 0.44	7.57 ± 0.22	4.33 ± 0.14	2.53 ± 0.09	1.55 ± 0.07	1.25 ± 0.21	
0.815		7.98 ± 0.24	4.22 ± 0.13	2.66 ± 0.10	1.48 ± 0.06	0.69 ± 0.09	
0.838		7.39 ± 0.22	4.41 ± 0.13	2.41 ± 0.09	1.51 ± 0.06	1.02 ± 0.09	
0.860		7.70 ± 0.23	4.54 ± 0.14	2.56 ± 0.10	1.29 ± 0.05	0.78 ± 0.06	
0.883		8.42 ± 0.26	4.68 ± 0.15	2.72 ± 0.09	1.43 ± 0.06	0.77 ± 0.05	
0.906		8.97 ± 0.28	5.09 ± 0.16	2.76 ± 0.10	1.38 ± 0.06	0.73 ± 0.04	0.44 ± 0.14
0.928		10.36 ± 0.35	5.71 ± 0.19	3.08 ± 0.10	1.57 ± 0.06	0.86 ± 0.04	0.41 ± 0.07
0.951		13.33 ± 0.48	7.01 ± 0.23	4.07 ± 0.13	1.99 ± 0.08	0.96 ± 0.05	0.53 ± 0.07
0.975		29.35 ± 1.05	12.36 ± 0.43	7.34 ± 0.23	3.63 ± 0.13	1.68 ± 0.07	0.83 ± 0.06
0.996		67.12 ± 1.54	33.44 ± 0.65	18.36 ± 0.36	8.49 ± 0.28	3.88 ± 0.14	1.72 ± 0.09

TABLE VII

INELASTIC CROSS-SECTION $E\,d^3\sigma/d\bar{p}^3$ $(mb.GeV^{-2})$; $s = 1464\ GeV^2$						
x	$p_T = 0.3$ GeV	$p_T = 0.4$ GeV	$p_T = 0.5$ GeV	$p_T = 0.6$ GeV	$p_T = 0.7$ GeV	$p_T = 0.8$ GeV
0.703	11.5 ± 0.5	8.78 ± 0.34	5.35 ± 0.23	3.20 ± 0.16	2.01 ± 0.26	
0.729	12.2 ± 0.5	8.89 ± 0.33	5.21 ± 0.21	3.01 ± 0.15	1.72 ± 0.16	
0.755	11.8 ± 0.5	8.66 ± 0.32	4.69 ± 0.19	2.97 ± 0.14	1.66 ± 0.12	
0.781	10.6 ± 0.5	9.09 ± 0.33	5.00 ± 0.20	3.14 ± 0.15	1.33 ± 0.09	
0.807	10.5 ± 0.5	8.95 ± 0.32	5.01 ± 0.19	3.05 ± 0.14	1.31 ± 0.09	
0.833	10.3 ± 0.6	9.36 ± 0.34	4.96 ± 0.20	2.88 ± 0.13	1.68 ± 0.10	0.72 ± 0.09
0.859		8.77 ± 0.33	5.35 ± 0.21	2.99 ± 0.14	1.58 ± 0.09	0.50 ± 0.06
0.885		9.09 ± 0.35	5.28 ± 0.21	2.91 ± 0.13	1.54 ± 0.09	0.63 ± 0.06
0.911		10.05 ± 0.40	5.76 ± 0.22	3.19 ± 0.14	1.68 ± 0.09	0.55 ± 0.05
0.937		11.08 ± 0.46	6.74 ± 0.25	3.66 ± 0.16	2.06 ± 0.11	0.84 ± 0.06
0.964		14.55 ± 0.62	9.73 ± 0.35	5.62 ± 0.22	3.08 ± 0.14	1.14 ± 0.07
0.992		49.39 ± 1.88	32.67 ± 1.05	18.80 ± 0.62	10.00 ± 0.36	3.61 ± 0.16
1.009		8.64 ± 0.73	3.25 ± 0.16	1.16 ± 0.07	0.69 ± 0.06	0.33 ± 0.04

TABLE VIII

INELASTIC CROSS-SECTION E $d^3\sigma/dp^3$ (mb.GeV^{-2}); s = 1995 GeV^2							
x	p_T = 0.6 GeV	p_T = 0.7 GeV	p_T = 0.8 GeV	p_T = 0.9 GeV	p_T = 1.0 GeV $\times 10^{-3}$	p_T = 1.1 GeV $\times 10^{-3}$	p_T = 1.2 GeV $\times 10^{-3}$
0.645			1.20 ± 0.07	0.83 ± 0.05	454 ± 31	295 ± 22	135 ± 11
0.663			1.27 ± 0.07	0.81 ± 0.05	469 ± 28	273 ± 21	136 ± 9
0.681	2.78 ± 0.22	1.90 ± 0.12	1.12 ± 0.07	0.70 ± 0.05	432 ± 31	228 ± 19	134 ± 10
0.699	3.09 ± 0.24	2.03 ± 0.11	1.05 ± 0.06	0.74 ± 0.05	384 ± 26	264 ± 19	131 ± 10
0.716	3.07 ± 0.17	1.62 ± 0.10	1.06 ± 0.06	0.61 ± 0.04	377 ± 24	219 ± 16	120 ± 9
0.734	3.14 ± 0.19	1.62 ± 0.10	0.90 ± 0.06	0.55 ± 0.04	307 ± 23	154 ± 14	91 ± 9
0.752	2.55 ± 0.17	1.45 ± 0.09	0.98 ± 0.06	0.55 ± 0.04	320 ± 23	177 ± 14	107 ± 9
0.770	2.57 ± 0.14	1.76 ± 0.12	0.92 ± 0.06	0.48 ± 0.03	274 ± 21	144 ± 12	108 ± 10
0.788	2.61 ± 0.14	1.77 ± 0.10	0.92 ± 0.06	0.48 ± 0.04	257 ± 21	148 ± 13	76 ± 8
0.806	2.55 ± 0.13	1.42 ± 0.08	0.78 ± 0.05	0.47 ± 0.03	242 ± 19	119 ± 11	88 ± 8
0.824	2.35 ± 0.14	1.48 ± 0.09	0.86 ± 0.06	0.45 ± 0.03	250 ± 22	140 ± 12	70 ± 8
0.842	2.33 ± 0.16	1.30 ± 0.08	0.76 ± 0.05	0.46 ± 0.04	216 ± 20	154 ± 14	67 ± 8
0.860	2.52 ± 0.17	1.36 ± 0.09	0.84 ± 0.06	0.38 ± 0.03	216 ± 20	105 ± 11	68 ± 8
0.878	2.60 ± 0.18	1.29 ± 0.09	0.74 ± 0.06	0.41 ± 0.04	195 ± 21	92 ± 11	47 ± 6
0.896	2.86 ± 0.34	1.48 ± 0.10	0.80 ± 0.06	0.40 ± 0.04	193 ± 22	101 ± 13	61 ± 8
0.913	2.52 ± 0.33	1.42 ± 0.10	0.84 ± 0.06	0.36 ± 0.03	198 ± 23	104 ± 13	42 ± 6
0.931	3.04 ± 0.37	1.65 ± 0.13	0.82 ± 0.06	0.39 ± 0.04	233 ± 25	103 ± 15	60 ± 9
0.949		1.89 ± 0.14	1.01 ± 0.07	0.52 ± 0.04	243 ± 25	112 ± 16	86 ± 11
0.967		2.90 ± 0.23	1.28 ± 0.09	0.75 ± 0.06	359 ± 34	168 ± 21	79 ± 11
0.985		7.34 ± 0.43	4.36 ± 0.25	1.60 ± 0.09	858 ± 63	448 ± 35	208 ± 19
1.003		9.70 ± 0.61	4.40 ± 0.22	1.52 ± 0.09	560 ± 44	188 ± 22	80 ± 12
1.021			0.02 ± 0.01				

TABLE IX

INELASTIC CROSS-SECTION $E\,d^3\sigma/d\bar{p}^3$ (mb.GeV^{-2}) ; s = 1995 GeV^2 (continued)							
x	p_T = 1.3 GeV $\times 10^{-3}$	p_T = 1.4 GeV $\times 10^{-3}$	p_T = 1.5 GeV $\times 10^{-3}$	p_T = 1.6 GeV $\times 10^{-3}$	p_T = 1.7 GeV $\times 10^{-3}$	p_T = 1.8 GeV $\times 10^{-3}$	p_T = 1.9 GeV $\times 10^{-3}$
0.645	62 ± 5						
0.663	83 ± 6						
0.681	79 ± 5	27.3 ± 3.8					
0.699	79 ± 6	31.3 ± 3.3					
0.716	61 ± 5	32.1 ± 2.9					
0.734	68 ± 6	27.7 ± 2.6	12.1 ± 2.6				
0.752	62 ± 5	32.1 ± 2.7	13.4 ± 2.1				
0.770	60 ± 5	31.3 ± 2.8	11.5 ± 1.7				
0.788	57 ± 6	22.5 ± 2.6	15.5 ± 2.0	4.4 ± 1.5			
0.806	43 ± 5	26.5 ± 2.7	13.4 ± 1.7	6.7 ± 1.5			
0.824	43 ± 5	22.0 ± 2.5	12.6 ± 1.6	5.2 ± 1.1	3.5 ± 1.6		
0.842	37 ± 5	18.5 ± 2.6	12.3 ± 1.6	6.1 ± 1.2	3.6 ± 1.4		
0.860	31 ± 5	17.0 ± 2.8	11.0 ± 1.5	7.1 ± 1.2	3.2 ± 1.0		
0.878	26 ± 4	19.2 ± 3.0	11.7 ± 1.7	5.1 ± 1.0	3.0 ± 0.9		
0.896	26 ± 5	10.3 ± 2.5	10.8 ± 1.7	4.5 ± 0.9	3.6 ± 0.9	3.7 ± 1.4	
0.913	27 ± 5	10.1 ± 2.3	7.6 ± 1.6	6.8 ± 1.1	2.7 ± 0.8	1.3 ± 0.8	
0.931	33 ± 6	13.1 ± 3.0	11.2 ± 2.3	7.8 ± 1.4	3.4 ± 0.8	1.9 ± 1.0	
0.949	35 ± 5	21.6 ± 3.8	13.0 ± 2.4	6.2 ± 1.3	5.6 ± 1.0	3.5 ± 0.9	
0.967	51 ± 8	18.7 ± 3.8	15.1 ± 3.0	9.8 ± 1.9	4.6 ± 0.9	4.8 ± 1.1	
0.985	82 ± 10	49.3 ± 6.3	23.8 ± 4.4	19.3 ± 2.9	8.2 ± 1.2	4.7 ± 1.1	2.1 ± 1.1
1.003	37 ± 7	16.8 ± 3.7	8.1 ± 2.4	5.8 ± 1.6	2.6 ± 0.7	0.5 ± 0.3	1.0 ± 0.7
1.021		0.8 ± 0.8					

TABLE IX

INELASTIC CROSS-SECTION $E\,d^3\sigma/dp^3$ $(mb.GeV^{-2})$; $s = 2783\ GeV^2$									
x	$p_T = 0.6$ GeV	$p_T = 0.7$ GeV	$p_T = 0.8$ GeV	$p_T = 0.9$ GeV	$p_T = 1.0$ GeV $\times 10^{-3}$	$p_T = 1.1$ GeV $\times 10^{-3}$	$p_T = 1.2$ GeV $\times 10^{-3}$	$p_T = 1.3$ GeV $\times 10^{-3}$	$p_T = 1.4$ GeV $\times 10^{-3}$
0.688	3.43 ± 0.17	2.34 ± 0.17							
0.705	2.76 ± 0.15	2.11 ± 0.10			463 ± 38			90 ± 9	
0.722	2.63 ± 0.15	2.05 ± 0.09		0.56 ± 0.05	379 ± 35	282 ± 25	128 ± 13	85 ± 7	37.2 ± 5.4
0.739	3.10 ± 0.32	1.95 ± 0.10	1.05 ± 0.06	0.70 ± 0.04	401 ± 40	251 ± 19	125 ± 10	92 ± 11	37.9 ± 4.3
0.756	2.58 ± 0.28	1.75 ± 0.08	0.93 ± 0.05	0.63 ± 0.05	297 ± 25	197 ± 16	125 ± 12	67 ± 7	42.5 ± 6.3
0.773		1.62 ± 0.10	0.99 ± 0.05	0.58 ± 0.03	326 ± 27	183 ± 17	115 ± 11	62 ± 7	35.4 ± 4.2
0.791		1.56 ± 0.15	0.94 ± 0.05	0.51 ± 0.03	261 ± 19	186 ± 17	81 ± 8	51 ± 6	34.4 ± 4.2
0.808		2.18 ± 0.27	0.89 ± 0.04	0.53 ± 0.03	278 ± 20	182 ± 20	94 ± 11	49 ± 5	31.2 ± 4.6
0.825		1.69 ± 0.23	0.92 ± 0.05	0.46 ± 0.03	265 ± 18	132 ± 17	100 ± 10	46 ± 5	29.2 ± 3.7
0.842		1.46 ± 0.24	0.76 ± 0.04	0.44 ± 0.03	266 ± 18	145 ± 14	71 ± 8	43 ± 6	21.4 ± 4.0
0.859		1.33 ± 0.22	0.84 ± 0.06	0.42 ± 0.03	217 ± 15	115 ± 11	77 ± 10	35 ± 5	22.1 ± 3.4
0.876		1.49 ± 0.25	0.98 ± 0.08	0.43 ± 0.03	244 ± 19	101 ± 10	69 ± 12	32 ± 5	22.1 ± 3.4
0.893		1.82 ± 0.40	0.86 ± 0.08	0.41 ± 0.03	199 ± 16	111 ± 11	71 ± 9	35 ± 5	18.2 ± 3.6
0.910		1.65 ± 0.38	0.74 ± 0.08	0.40 ± 0.03	229 ± 18	120 ± 11	60 ± 7	28 ± 6	21.7 ± 4.0
0.927		1.49 ± 0.39	0.92 ± 0.19	0.48 ± 0.04	236 ± 18	124 ± 11	69 ± 8	36 ± 6	19.1 ± 3.7
0.944			1.19 ± 0.20	0.59 ± 0.06	273 ± 23	121 ± 12	66 ± 8	38 ± 6	16.9 ± 3.6
0.961			1.13 ± 0.20	0.72 ± 0.08	349 ± 29	169 ± 16	86 ± 9	47 ± 7	20.4 ± 4.1
0.978			2.42 ± 0.47	0.97 ± 0.09	523 ± 41	231 ± 18	145 ± 12	78 ± 9	46.9 ± 6.7
0.995			4.53 ± 0.77	2.95 ± 0.34	1378 ± 77	613 ± 35	258 ± 18	151 ± 12	76.9 ± 8.7
1.012					5 ± 4	14 ± 5	8 ± 3	2 ± 1	0.7 ± 0.7
1.029					3 ± 3		1 ± 1		

TABLE X

INELASTIC CROSS-SECTION $E\,d^3\sigma/dp^3$ (mb.GeV^{-2}); s = 2783 GeV^2 (continued)									
x	p_T = 1.5 GeV $\times 10^{-3}$	p_T = 1.6 GeV $\times 10^{-3}$	p_T = 1.7 GeV $\times 10^{-3}$	p_T = 1.8 GeV $\times 10^{-3}$	p_T = 1.9 GeV $\times 10^{-3}$	p_T = 2.0 GeV $\times 10^{-3}$	p_T = 2.1 GeV $\times 10^{-3}$	p_T = 2.2 GeV $\times 10^{-3}$	p_T = 2.3 GeV $\times 10^{-3}$
0.688									
0.705	22.4 ± 4.0								
0.722	17.2 ± 3.9	11.0 ± 2.6							
0.739	25.5 ± 3.7	11.1 ± 2.5							
0.756	15.7 ± 2.2	7.1 ± 1.6	6.1 ± 2.2						
0.773	20.0 ± 2.5	12.1 ± 2.0	6.2 ± 1.5	3.2 ± 1.3					
0.791	16.6 ± 2.6	5.8 ± 1.3	3.9 ± 1.1	3.5 ± 1.1					
0.808	13.7 ± 2.1	10.3 ± 1.7	3.7 ± 1.1	4.1 ± 1.0	2.5 ± 1.2				
0.825	13.1 ± 2.1	7.9 ± 1.4	3.1 ± 0.8	5.1 ± 1.3	3.8 ± 1.1				
0.842	18.1 ± 3.1	8.5 ± 1.4	3.6 ± 1.1	3.0 ± 0.8	2.0 ± 0.8	1.3 ± 0.9			
0.859	12.5 ± 1.9	6.7 ± 1.2	3.4 ± 0.9	3.1 ± 0.8	1.5 ± 0.6	2.6 ± 1.0			
0.876	14.6 ± 2.7	8.3 ± 1.6	3.9 ± 0.9	1.6 ± 0.6	1.2 ± 0.4	1.7 ± 0.8			
0.893	11.8 ± 2.1	5.1 ± 1.3	4.0 ± 0.9	1.7 ± 0.5	1.1 ± 0.5	2.7 ± 0.8	1.7 ± 1.0		
0.910	12.6 ± 2.7	7.4 ± 1.5	6.1 ± 1.4	3.4 ± 0.9	2.0 ± 0.6	1.7 ± 0.6	1.4 ± 0.4		
0.927	10.8 ± 2.2	10.4 ± 2.3	4.6 ± 1.1	1.9 ± 0.6	2.1 ± 0.6	1.5 ± 0.5	1.4 ± 0.7		
0.944	12.4 ± 2.3	8.3 ± 1.8	4.3 ± 1.1	2.5 ± 0.7	1.8 ± 0.5	2.1 ± 0.7	0.4 ± 0.3		
0.961	16.2 ± 3.2	8.8 ± 2.2	7.7 ± 1.5	1.6 ± 0.7	1.5 ± 0.5	1.2 ± 0.4	1.5 ± 0.6	1.5 ± 0.8	
0.978	16.9 ± 3.6	14.4 ± 2.6	7.2 ± 1.5	6.1 ± 1.2	2.1 ± 0.6	0.9 ± 0.4	1.0 ± 0.4	1.0 ± 0.6	1.2 ± 0.9
0.995	30.9 ± 4.4	19.6 ± 3.5	7.2 ± 1.7	5.5 ± 1.3	2.3 ± 0.6	0.9 ± 0.3	1.2 ± 0.4	1.3 ± 0.5	
1.012	2.6 ± 1.2	0.9 ± 0.7	1.7 ± 0.9	1.2 ± 0.5	0.5 ± 0.3	0.3 ± 0.2	0.3 ± 0.2		
1.029					0.2 ± 0.2				

TABLE X

INELASTIC CROSS-SECTION $E\,d^3\sigma/dp^{-3}$ $(mb.GeV^{-2})$; $s = 3892\ GeV^2$								
x	$p_T = 0.8$ GeV/c	$p_T = 0.9$ GeV $\times 10^{-3}$	$p_T = 1.0$ GeV $\times 10^{-3}$	$p_T = 1.1$ GeV $\times 10^{-3}$	$p_T = 1.2$ GeV $\times 10^{-3}$	$p_T = 1.3$ GeV $\times 10^{-3}$	$p_T = 1.4$ GeV $\times 10^{-3}$	$p_T = 1.5$ GeV $\times 10^{-3}$
0.625	1.09 ± 0.09							
0.641	1.11 ± 0.07							
0.657	1.18 ± 0.07							
0.673	1.18 ± 0.05							
0.689	1.02 ± 0.04	675 ± 42						
0.705	1.06 ± 0.05	673 ± 37	342 ± 47					
0.721	1.05 ± 0.04	625 ± 31	438 ± 33					
0.737	0.91 ± 0.04	588 ± 27	339 ± 25					
0.753	0.91 ± 0.04	568 ± 25	335 ± 21					
0.769	0.86 ± 0.04	541 ± 23	302 ± 17	152 ± 18				
0.785	0.86 ± 0.04	469 ± 21	263 ± 15	154 ± 15				
0.801	0.73 ± 0.04	463 ± 21	267 ± 14	142 ± 13	86 ± 13			
0.818	0.79 ± 0.05	459 ± 21	256 ± 13	144 ± 11	50 ± 9			
0.834	0.71 ± 0.05	454 ± 23	239 ± 13	134 ± 9	49 ± 8	34 ± 8		
0.850		403 ± 22	229 ± 13	111 ± 8	66 ± 7	33 ± 7		
0.866		340 ± 21	224 ± 13	104 ± 8	68 ± 7	29 ± 6	17 ± 7	
0.882		355 ± 23	190 ± 13	105 ± 8	60 ± 6	38 ± 6	17 ± 5	
0.898		361 ± 30	216 ± 15	106 ± 8	54 ± 5	26 ± 4	14 ± 5	
0.914			216 ± 17	109 ± 8	62 ± 6	27 ± 4	10 ± 3	
0.930			180 ± 16	100 ± 9	69 ± 6	37 ± 4	15 ± 3	
0.946			265 ± 26	110 ± 11	59 ± 6	30 ± 4	20 ± 3	14 ± 4
0.962			321 ± 54	141 ± 13	85 ± 8	42 ± 5	29 ± 4	15 ± 4
0.978			533 ± 115	212 ± 17	116 ± 10	54 ± 6	27 ± 3	24 ± 4
0.994			1506 ± 200	628 ± 42	296 ± 19	145 ± 10	68 ± 6	34 ± 5
1.010				18 ± 13	18 ± 4	13 ± 2	6 ± 1	4 ± 1

TABLE XI

INELASTIC CROSS-SECTION $\frac{s}{\pi}\frac{d^2\sigma}{dtdM^2}$ (mb.GeV^{-2}); s = 549 GeV^2								
M^2 (GeV^2)	M^2/s	-t = 0.15 GeV^2	-t = 0.20 GeV^2	-t = 0.25 GeV^2	-t = 0.30 GeV^2	-t = 0.35 GeV^2	-t = 0.40 GeV^2	-t = 0.45 GeV^2
-7.5	-.0137	0.07 ± 0.04	0.20 ± 0.05	0.11 ± 0.02	0.07 ± 0.02	0.03 ± 0.02		0.01 ± 0.01
-5.0	-.0091	1.14 ± 0.15	0.91 ± 0.12	0.6 ± 0.1	0.55 ± 0.10	0.4 ± 0.2	0.4 ± 0.3	0.10 ± 0.05
-2.5	-.0046	17.4 ± 0.5	9.1 ± 0.5	7.5 ± 0.3	5.7 ± 0.3	3.2 ± 0.3	1.5 ± 0.4	1.6 ± 0.3
0.0	0	86.7 ± 2.0	51.3 ± 0.9	34.2 ± 0.8	21.1 ± 0.6	14.0 ± 0.6	9.0 ± 0.6	7.1 ± 0.6
2.5	.0046	131.2 ± 2.2	79.4 ± 1.0	52.1 ± 0.9	38.1 ± 0.7	25.8 ± 0.7	19.6 ± 0.7	14.6 ± 0.6
5.0	.0091	87.8 ± 1.9	60.7 ± 0.8	42.7 ± 0.7	29.3 ± 0.6	23.7 ± 0.7	17.8 ± 0.7	14.2 ± 0.6
7.5	.0137	50.1 ± 1.3	38.0 ± 0.8	26.9 ± 0.6	18.8 ± 0.4	15.5 ± 0.6	12.5 ± 0.6	8.8 ± 0.4
10.0	.0182	38.9 ± 1.0	26.7 ± 0.6	18.5 ± 0.4	13.1 ± 0.4	11.0 ± 0.4	8.2 ± 0.5	6.1 ± 0.4
12.5	.0226	30.5 ± 0.9	20.9 ± 0.5	16.3 ± 0.4	11.3 ± 0.4	8.9 ± 0.4	6.6 ± 0.4	5.1 ± 0.3
15.0	.0273	25.9 ± 0.8	18.2 ± 0.5	13.3 ± 0.4	9.5 ± 0.3	7.7 ± 0.4	5.7 ± 0.4	4.5 ± 0.3
17.5	.0319	22.2 ± 0.6	15.4 ± 0.4	10.9 ± 0.4	7.8 ± 0.3	7.7 ± 0.4	5.5 ± 0.4	4.1 ± 0.2
20.0	.0364	18.3 ± 0.6	14.7 ± 0.4	11.1 ± 0.4	7.4 ± 0.3	6.7 ± 0.4	4.6 ± 0.4	3.8 ± 0.2
22.5	.0410	17.4 ± 0.6	13.0 ± 0.4	9.3 ± 0.4	6.5 ± 0.3	5.6 ± 0.3	4.1 ± 0.3	3.1 ± 0.2
25.0	.0456	16.3 ± 0.6	12.1 ± 0.4	8.6 ± 0.3	6.3 ± 0.3	5.0 ± 0.3	4.0 ± 0.3	3.3 ± 0.2
27.5	.0501	15.9 ± 0.5	11.7 ± 0.4	8.9 ± 0.3	6.8 ± 0.3	4.9 ± 0.3	3.6 ± 0.3	3.1 ± 0.2
30.0	.0547	14.1 ± 0.5	11.3 ± 0.4	8.6 ± 0.3	6.2 ± 0.3	4.6 ± 0.2	3.6 ± 0.4	2.7 ± 0.2
32.5	.0592	13.5 ± 0.5	10.3 ± 0.3	7.8 ± 0.3	6.0 ± 0.3	4.5 ± 0.2	4.0 ± 0.4	2.6 ± 0.2
35.0	.0638	12.9 ± 0.5	9.8 ± 0.3	7.4 ± 0.3	5.8 ± 0.3	4.1 ± 0.2	3.5 ± 0.3	2.7 ± 0.2
37.5	.0683	13.0 ± 0.5	9.4 ± 0.3	7.2 ± 0.3	5.4 ± 0.2	4.1 ± 0.3	3.3 ± 0.3	2.5 ± 0.2
40.0	.0729	13.1 ± 0.5	9.5 ± 0.3	7.3 ± 0.3	5.3 ± 0.2	3.7 ± 0.3	3.1 ± 0.3	2.4 ± 0.2
42.5	.0775	11.6 ± 0.5	9.6 ± 0.3	6.9 ± 0.3	5.5 ± 0.2	4.1 ± 0.3	3.7 ± 0.3	2.5 ± 0.2
45.0	.0820	12.4 ± 0.4	9.9 ± 0.3	7.0 ± 0.3	5.2 ± 0.3	3.7 ± 0.3	4.0 ± 0.3	2.7 ± 0.2
47.5	.0867	12.2 ± 0.4	8.8 ± 0.3	6.9 ± 0.3	4.8 ± 0.2	3.5 ± 0.3	2.8 ± 0.3	2.5 ± 0.1
50.0	.0912	11.6 ± 0.4	9.5 ± 0.4	7.1 ± 0.3	4.9 ± 0.3	3.9 ± 0.3	2.7 ± 0.3	2.5 ± 0.2
52.5	.0956	13.2 ± 0.5	9.4 ± 0.4	6.5 ± 0.4	4.9 ± 0.4	4.0 ± 0.4	2.8 ± 0.4	2.3 ± 0.2
55.0	.1002	13.3 ± 0.5	8.7 ± 0.4	6.5 ± 0.4	4.9 ± 0.4	4.1 ± 0.4	2.6 ± 0.4	2.3 ± 0.3

TABLE XII.

INELASTIC CROSS-SECTION $\frac{s}{\pi}\frac{d^2\sigma}{dtdM^2}$ $(mb.GeV^{-2})$; $s = 549\ GeV^2$ (continued)

M^2 (GeV^2)	M^2/s	$-t = 0.50$ GeV^2	$-t = 0.55$ GeV^2	$-t = 0.60$ GeV^2	$-t = 0.65$ GeV^2	$-t = 0.70$ GeV^2	$-t = 0.75$ GeV^2	$-t = 0.85$ GeV^2
-7.5	-.0137	0.10 ± 0.10	0.03 ± 0.02		0.08 ± 0.06		0.08 ± 0.03	
-5.0	-.0091	0.2 ± 0.2	0.5 ± 0.1	0.1 ± 0.1	0.3 ± 0.1	0.1 ± 0.1	0.23 ± 0.06	0.07 ± 0.05
-2.5	-.0046	1.7 ± 0.2	1.6 ± 0.2	0.8 ± 0.1	1.1 ± 0.2	0.6 ± 0.1	0.79 ± 0.06	0.48 ± 0.07
0.0	0	6.5 ± 0.4	5.5 ± 0.4	3.6 ± 0.2	3.6 ± 0.3	2.3 ± 0.2	2.06 ± 0.14	1.27 ± 0.08
2.5	.0046	11.3 ± 0.4	8.2 ± 0.3	6.9 ± 0.4	4.7 ± 0.2	4.0 ± 0.2	2.82 ± 0.14	1.73 ± 0.09
5.0	.0091	10.8 ± 0.4	7.0 ± 0.3	6.1 ± 0.3	4.0 ± 0.2	3.6 ± 0.2	2.75 ± 0.15	1.72 ± 0.08
7.5	.0137	7.4 ± 0.4	5.5 ± 0.3	3.9 ± 0.3	3.1 ± 0.2	2.4 ± 0.2	2.19 ± 0.15	1.46 ± 0.08
10.0	.0182	5.0 ± 0.3	3.9 ± 0.2	3.0 ± 0.2	2.6 ± 0.2	2.0 ± 0.2	1.63 ± 0.08	1.06 ± 0.07
12.5	.0226	4.0 ± 0.3	3.1 ± 0.2	2.6 ± 0.2	2.0 ± 0.1	1.8 ± 0.1	1.32 ± 0.08	0.92 ± 0.05
15.0	.0273	3.6 ± 0.3	2.5 ± 0.2	2.4 ± 0.2	1.6 ± 0.1	1.4 ± 0.1	1.20 ± 0.08	0.81 ± 0.05
17.5	.0319	2.8 ± 0.2	2.4 ± 0.2	1.7 ± 0.2	1.5 ± 0.1	1.2 ± 0.1	1.00 ± 0.08	0.83 ± 0.05
20.0	.0364	3.0 ± 0.3	2.3 ± 0.2	1.8 ± 0.2	1.3 ± 0.1	1.1 ± 0.1	1.01 ± 0.08	0.69 ± 0.04
22.5	.0410	2.7 ± 0.3	2.0 ± 0.1	1.6 ± 0.2	1.3 ± 0.1	1.2 ± 0.1	1.02 ± 0.08	0.69 ± 0.05
25.0	.0456	2.3 ± 0.2	1.9 ± 0.1	1.3 ± 0.2	1.2 ± 0.1	1.0 ± 0.1	0.98 ± 0.08	0.62 ± 0.05
27.5	.0501	2.3 ± 0.2	2.0 ± 0.1	1.6 ± 0.2	1.3 ± 0.1	0.9 ± 0.1	0.80 ± 0.08	0.62 ± 0.04
30.0	.0547	2.1 ± 0.2	1.7 ± 0.1	1.6 ± 0.2	1.0 ± 0.1	1.1 ± 0.1	0.74 ± 0.06	0.59 ± 0.05
32.5	.0592	2.0 ± 0.2	1.6 ± 0.1	1.4 ± 0.2	1.0 ± 0.1	1.1 ± 0.1	0.80 ± 0.06	0.58 ± 0.05
35.0	.0638	2.0 ± 0.2	1.8 ± 0.1	1.4 ± 0.1	1.2 ± 0.1	0.9 ± 0.1	0.88 ± 0.07	0.57 ± 0.05
37.5	.0683	1.7 ± 0.2	1.8 ± 0.1	1.1 ± 0.1	1.0 ± 0.1	0.8 ± 0.1	0.82 ± 0.07	0.49 ± 0.04
40.0	.0729	1.8 ± 0.2	1.8 ± 0.1	1.1 ± 0.1	1.0 ± 0.1	0.9 ± 0.1	0.77 ± 0.07	0.57 ± 0.04
42.5	.0775	2.3 ± 0.2	1.6 ± 0.1	1.3 ± 0.1	1.0 ± 0.1	1.0 ± 0.1	0.77 ± 0.07	0.61 ± 0.04
45.0	.0820	1.9 ± 0.2	1.6 ± 0.1	1.3 ± 0.1	1.0 ± 0.1	0.9 ± 0.1	0.69 ± 0.07	0.49 ± 0.04
47.5	.0867	2.2 ± 0.2	1.5 ± 0.1	1.3 ± 0.2	1.2 ± 0.1	0.9 ± 0.1	0.70 ± 0.07	0.54 ± 0.04
50.0	.0912	1.7 ± 0.2	1.5 ± 0.1	1.4 ± 0.2	1.1 ± 0.1	1.0 ± 0.1	0.75 ± 0.07	0.55 ± 0.04
52.5	.0956	1.8 ± 0.2	1.7 ± 0.2	1.4 ± 0.2	1.0 ± 0.1	0.9 ± 0.1	0.80 ± 0.10	0.60 ± 0.06
55.0	.1002	1.6 ± 0.2	1.5 ± 0.2	1.3 ± 0.2	1.2 ± 0.1	0.8 ± 0.1	0.80 ± 0.10	0.59 ± 0.06

TABLE XII

INELASTIC CROSS-SECTION $\frac{s}{\pi}\frac{d^2\sigma}{dtdM^2}$ $(mb.GeV^{-2})$; $s = 549\ GeV^2$ (continued)

M^2 (GeV^2)	M^2/s	$-t = 0.95$ GeV^2	$-t = 1.05$ GeV^2	$-t = 1.15$ GeV^2	$-t = 1.25$ GeV^2	$-t = 1.45$ GeV^2	$-t = 1.75$ GeV^2
-7.5	-.0137	0.03 ± 0.03	0.02 ± 0.04				
-5.0	-.0091	0.04 ± 0.03	0.05 ± 0.02	0.08 ± 0.03	0.03 ± 0.03		
-2.5	-.0046	0.45 ± 0.06	0.13 ± 0.04	0.16 ± 0.03	0.08 ± 0.03		
0.0	0	0.85 ± 0.09	0.45 ± 0.06	0.23 ± 0.07	0.10 ± 0.04	0.25 ± 0.07	
2.5	.0046	1.16 ± 0.07	0.73 ± 0.06	0.39 ± 0.07	0.19 ± 0.03	0.10 ± 0.05	
5.0	.0091	1.17 ± 0.07	0.71 ± 0.06	0.41 ± 0.04	0.37 ± 0.04	0.20 ± 0.07	
7.5	.0137	0.93 ± 0.08	0.59 ± 0.05	0.32 ± 0.04	0.43 ± 0.04	0.19 ± 0.07	0.14 ± 0.13
10.0	.0182	0.78 ± 0.06	0.45 ± 0.04	0.33 ± 0.04	0.25 ± 0.04	0.25 ± 0.09	0.03 ± 0.04
12.5	.0226	0.68 ± 0.06	0.37 ± 0.04	0.23 ± 0.04	0.23 ± 0.04	0.12 ± 0.05	
15.0	.0273	0.50 ± 0.05	0.38 ± 0.03	0.23 ± 0.04	0.21 ± 0.04	0.06 ± 0.03	
17.5	.0319	0.51 ± 0.05	0.33 ± 0.03	0.26 ± 0.04	0.26 ± 0.04	0.12 ± 0.07	
20.0	.0364	0.52 ± 0.04	0.29 ± 0.03	0.21 ± 0.04	0.17 ± 0.03	0.13 ± 0.05	0.06 ± 0.09
22.5	.0410	0.38 ± 0.05	0.26 ± 0.03	0.27 ± 0.04	0.19 ± 0.03	0.23 ± 0.09	0.12 ± 0.18
25.0	.0456	0.44 ± 0.05	0.22 ± 0.03	0.19 ± 0.04	0.19 ± 0.03	0.10 ± 0.04	0.03 ± 0.05
27.5	.0501	0.46 ± 0.05	0.23 ± 0.03	0.21 ± 0.03	0.19 ± 0.03	0.12 ± 0.07	
30.0	.0547	0.30 ± 0.05	0.27 ± 0.03	0.18 ± 0.03	0.20 ± 0.03	0.28 ± 0.10	0.15 ± 0.10
32.5	.0592	0.51 ± 0.06	0.29 ± 0.03	0.21 ± 0.03	0.17 ± 0.03	0.06 ± 0.03	0.05 ± 0.07
35.0	.0638	0.46 ± 0.05	0.25 ± 0.03	0.20 ± 0.03	0.14 ± 0.03	0.11 ± 0.05	0.06 ± 0.08
37.5	.0683	0.41 ± 0.06	0.21 ± 0.03	0.21 ± 0.03	0.14 ± 0.03	0.06 ± 0.03	
40.0	.0729	0.42 ± 0.06	0.23 ± 0.03	0.22 ± 0.03	0.14 ± 0.03	0.11 ± 0.05	0.07 ± 0.09
42.5	.0775	0.37 ± 0.06	0.20 ± 0.03	0.22 ± 0.03	0.15 ± 0.03	0.12 ± 0.06	
45.0	.0820	0.37 ± 0.06	0.21 ± 0.03	0.18 ± 0.03	0.16 ± 0.03	0.19 ± 0.07	
47.5	.0867	0.35 ± 0.06	0.30 ± 0.03	0.20 ± 0.03	0.15 ± 0.03	0.12 ± 0.05	0.17 ± 0.11
50.0	.0912	0.37 ± 0.06	0.23 ± 0.03	0.27 ± 0.03	0.17 ± 0.03	0.07 ± 0.04	0.07 ± 0.06
52.5	.0956	0.42 ± 0.06	0.13 ± 0.03	0.26 ± 0.05	0.14 ± 0.04		
55.0	.1002	0.40 ± 0.06	0.13 ± 0.03	0.21 ± 0.05	0.15 ± 0.04		

TABLE XII

INELASTIC CROSS-SECTION $\frac{s}{\pi}\frac{d^2\sigma}{dtdM^2}$ $(mb.GeV^{-2})$; $s = 725\ GeV^2$

M^2 (GeV^2)	M^2/s	$-t = 0.15$ GeV^2	$-t = 0.20$ GeV^2	$-t = 0.25$ GeV^2	$-t = 0.30$ GeV^2	$-t = 0.35$ GeV^2	$-t = 0.45$ GeV^2	$-t = 0.50$ GeV^2	$-t = 0.55$ GeV^2
-9.0	-.0124	.05 ± .04	.28 ± .12	.08 ± .13	.06 ± .03	.05 ± .04	.06 ± .04	.06 ± .04	.04 ± .03
-6.5	-.0090	.49 ± .13	1.4 ± 0.3	.53 ± .07	.30 ± .11	.27 ± .09	.18 ± .05	.13 ± .06	.22 ± .03
-4.0	-.0055	5.0 ± 0.5	7.6 ± 0.6	3.7 ± 0.3	2.3 ± 0.3	1.3 ± 0.2	1.0 ± 0.2	.40 ± .13	.83 ± .08
-1.5	-.0021	50.3 ± 1.8	47.8 ± 1.5	17.8 ± 0.6	9.1 ± 0.7	7.0 ± 0.5	4.5 ± 0.3	3.2 ± 0.3	3.0 ± 0.2
1.0	+.0014	148.3 ± 3.3	118.2 ± 2.6	48.8 ± 1.0	27.4 ± 1.1	18.9 ± 0.8	9.7 ± 0.6	9.4 ± 0.5	7.1 ± 0.3
3.5	.0048	136.3 ± 4.0	104.9 ± 2.6	57.4 ± 1.3	34.0 ± 1.3	29.7 ± 1.0	14.7 ± 0.6	11.7 ± 0.6	9.3 ± 0.4
6.0	.0083	82.8 ± 4.5	74.2 ± 2.2	43.6 ± 1.2	31.9 ± 1.3	25.0 ± 1.0	15.4 ± 0.7	10.2 ± 0.5	8.6 ± 0.5
8.5	.0117	46.4 ± 3.7	46.0 ± 1.6	28.8 ± 1.1	24.0 ± 1.1	19.3 ± 0.9	10.6 ± 0.5	8.2 ± 0.5	7.3 ± 0.5
11.0	.0152	36.1 ± 3.5	34.5 ± 1.4	21.0 ± 1.1	16.7 ± 0.9	12.4 ± 0.7	8.1 ± 0.5	6.0 ± 0.4	4.8 ± 0.4
13.5	.0186	26.1 ± 2.8	24.2 ± 1.1	15.3 ± 0.9	13.0 ± 0.8	10.1 ± 0.6	6.6 ± 0.4	4.6 ± 0.3	3.5 ± 0.3
16.0	.0221	23.7 ± 2.9	20.7 ± 1.0	12.9 ± 0.9	11.0 ± 0.7	8.7 ± 0.6	5.8 ± 0.4	4.5 ± 0.4	3.4 ± 0.3
18.5	.0255	19.7 ± 2.8	19.2 ± 1.0	11.2 ± 0.9	9.4 ± 0.6	7.5 ± 0.5	4.0 ± 0.3	4.1 ± 0.3	2.7 ± 0.3
21.0	.0290	14.8 ± 2.4	18.3 ± 1.0	9.5 ± 0.7	8.0 ± 0.6	6.1 ± 0.4	3.6 ± 0.3	2.5 ± 0.2	2.4 ± 0.3
23.5	.0324	15.3 ± 2.5	15.5 ± 0.9	9.6 ± 0.8	6.7 ± 0.6	5.9 ± 0.4	4.0 ± 0.3	3.2 ± 0.3	2.4 ± 0.2
26.0	.0359	13.5 ± 2.2	13.2 ± 0.9	8.2 ± 0.7	7.5 ± 0.5	5.8 ± 0.4	3.3 ± 0.3	2.8 ± 0.2	2.1 ± 0.2
28.5	.0393	12.3 ± 2.2	14.1 ± 0.8	8.8 ± 0.7	6.6 ± 0.6	4.2 ± 0.4	2.7 ± 0.2	2.7 ± 0.3	2.2 ± 0.2
31.0	.0428	12.6 ± 2.4	14.2 ± 0.8	7.7 ± 0.6	6.4 ± 0.5	4.3 ± 0.4	3.7 ± 0.3	2.2 ± 0.2	2.1 ± 0.2
33.5	.0462	14.6 ± 2.4	11.6 ± 0.8	8.1 ± 0.7	5.9 ± 0.5	4.3 ± 0.4	3.0 ± 0.3	2.6 ± 0.2	2.1 ± 0.2
36.0	.0497	9.5 ± 2.0	11.2 ± 0.7	7.9 ± 0.7	5.1 ± 0.5	4.2 ± 0.3	2.9 ± 0.2	2.2 ± 0.2	1.9 ± 0.2
38.5	.0531	10.4 ± 2.1	12.6 ± 0.7	7.6 ± 0.6	4.8 ± 0.4	4.1 ± 0.4	2.4 ± 0.2	2.5 ± 0.2	1.6 ± 0.2
41.0	.0566	10.8 ± 2.2	9.6 ± 0.7	5.8 ± 0.5	5.2 ± 0.5	3.8 ± 0.4	2.4 ± 0.2	2.6 ± 0.2	1.7 ± 0.2
43.5	.0600	11.9 ± 2.4	10.2 ± 0.7	5.9 ± 0.5	4.5 ± 0.4	3.5 ± 0.3	2.4 ± 0.2	1.9 ± 0.2	1.2 ± 0.2
46.0	.0634	11.8 ± 2.4	11.9 ± 0.7	6.5 ± 0.6	5.3 ± 0.5	3.7 ± 0.3	2.7 ± 0.3	2.4 ± 0.2	1.4 ± 0.2
48.5	.0669	9.8 ± 2.4	9.8 ± 0.7	6.0 ± 0.6	5.0 ± 0.5	3.4 ± 0.3	2.7 ± 0.3	1.6 ± 0.2	1.3 ± 0.2
51.0	.0703	9.9 ± 2.4	10.3 ± 0.7	6.0 ± 0.6	5.0 ± 0.5	3.9 ± 0.4	2.2 ± 0.3	1.8 ± 0.2	1.7 ± 0.2

TABLE XIII

INELASTIC CROSS-SECTION $\frac{s}{\pi}\frac{d^2\sigma}{dtdM^2}$ $(mb.GeV^{-2})$; $s = 934\ GeV^2$									
M^2 (GeV^2)	M^2/s	$-t = 0.25$ GeV^2	$-t = 0.30$ GeV^2	$-t = 0.35$ GeV^2	$-t = 0.40$ GeV^2	$-t = 0.45$ GeV^2	$-t = 0.50$ GeV^2	$-t = 0.55$ GeV^2	$-t = 0.60$ GeV^2
-18	-.0193		.005 ± .002	.002 ± .002					
-14	-.0150	.04 ± .06	.05 ± .03	.03 ± .02	.03 ± .03	.01 ± .01	.02 ± .02	.01 ± .01	.01 ± .01
-10	-.0107	.25 ± .17	.19 ± .11	.17 ± .04	.12 ± .05	.07 ± .04	.09 ± .05	.03 ± .02	.09 ± .04
-6	-.0064	2.1 ± 1.4	2.1 ± 0.4	3.3 ± .2	1.5 ± .2	.84 ± .16	.91 ± .15	.41 ± .12	.72 ± .12
-2	-.0021	25.7 ± 2.2	20.5 ± .8	15.5 ± .6	9.0 ± .6	8.0 ± .5	4.8 ± .4	2.54 ± .40	2.52 ± .29
2	.0021	64.7 ± 2.7	50.0 ± .8	32.5 ± .8	25.5 ± .8	22.0 ± .7	12.7 ± .5	9.10 ± .55	6.30 ± .36
6	.0064	65.0 ± 2.7	38.3 ± .8	30.8 ± .8	26.0 ± .8	18.0 ± .6	13.1 ± .6	9.66 ± .44	8.17 ± .38
10	.0107	33.0 ± 2.1	21.5 ± .6	19.2 ± .7	13.5 ± .7	11.2 ± .6	8.0 ± .4	6.18 ± .36	6.14 ± .33
14	.0150	19.5 ± 1.6	13.1 ± .6	12.2 ± .6	9.2 ± .5	6.9 ± .4	5.6 ± .4	4.13 ± .30	3.76 ± .27
18	.0193	18.8 ± 1.6	12.8 ± .5	9.5 ± .5	7.2 ± .5	5.0 ± .3	4.3 ± .3	3.34 ± .26	3.21 ± .24
22	.0236	16.4 ± 1.4	10.1 ± .5	8.1 ± .5	5.5 ± .4	4.9 ± .3	3.8 ± .3	2.68 ± .23	2.96 ± .22
26	.0279	13.4 ± 1.3	8.1 ± .4	6.7 ± .5	5.0 ± .4	4.7 ± .3	3.7 ± .3	2.49 ± .20	2.22 ± .21
30	.0321	12.0 ± 1.3	7.7 ± .4	6.1 ± .4	4.9 ± .4	3.9 ± .3	2.6 ± .3	2.37 ± .20	1.79 ± .19
34	.0364	11.6 ± 1.2	7.3 ± .4	6.0 ± .4	4.2 ± .4	3.6 ± .2	2.5 ± .3	2.18 ± .20	1.74 ± .19
38	.0407	10.2 ± 1.2	6.9 ± .4	5.8 ± .4	4.5 ± .4	3.3 ± .2	3.0 ± .3	1.80 ± .16	1.81 ± .18
42	.0450	9.4 ± 1.1	6.8 ± .4	4.6 ± .4	4.6 ± .4	3.2 ± .2	2.6 ± .3	1.76 ± .17	1.71 ± .18
46	.0493	9.1 ± 1.1	6.6 ± .4	4.8 ± .3	3.5 ± .4	3.1 ± .2	2.3 ± .3	1.80 ± .17	1.47 ± .18
50	.0536	7.2 ± 1.0	5.4 ± .3	4.9 ± .3	3.2 ± .3	2.6 ± .2	2.4 ± .3	1.76 ± .16	1.36 ± .19
54	.0578	7.4 ± 1.0	6.4 ± .4	4.4 ± .3	3.2 ± .3	2.8 ± .2	1.9 ± .3	1.73 ± .16	1.34 ± .19
58	.0621	7.5 ± 1.0	5.7 ± .3	4.4 ± .3	3.7 ± .2	2.8 ± .3	2.0 ± .2	1.73 ± .16	1.39 ± .19
62	.0664	7.8 ± 1.0	5.0 ± .3	4.1 ± .3	3.1 ± .2	2.7 ± .3	2.2 ± .2	1.60 ± .17	1.40 ± .19
66	.0707	6.9 ± 1.0	4.5 ± .3	4.1 ± .3	3.0 ± .2	2.6 ± .3	2.1 ± .2	1.56 ± .16	1.45 ± .19
70	.0750	5.3 ± .9	4.9 ± .3	4.0 ± .3	3.1 ± .2	2.3 ± .2	1.9 ± .2	1.35 ± .16	1.53 ± .18
74	.0793	6.6 ± .9	5.1 ± .3	4.2 ± .3	3.2 ± .2	2.5 ± .2	1.9 ± .2	1.44 ± .16	1.22 ± .18
78	.0836	6.5 ± 1.0	4.5 ± .3	4.2 ± .3	3.1 ± .2	2.3 ± .3	2.3 ± .2	1.57 ± .17	1.03 ± .16
82	.0878	7.3 ± 1.0	4.5 ± .3	4.0 ± .3	3.0 ± .2	2.3 ± .2	2.1 ± .2	1.42 ± .18	1.20 ± .15
86	.0921	7.8 ± 1.0	5.1 ± .3	4.2 ± .3	3.2 ± .2	2.4 ± .3	1.9 ± .2	1.40 ± .18	1.30 ± .14
90	.0964	5.8 ± 0.9	4.7 ± .3	4.3 ± .3	3.4 ± .2	2.1 ± .3	2.0 ± .2	1.52 ± .19	1.06 ± .14
94	.1007	6.5 ± 1.4	4.7 ± .4	3.7 ± .6	2.9 ± .3	2.1 ± .4	1.9 ± .3	1.21 ± .28	.94 ± .20

TABLE XIV

INELASTIC CROSS-SECTION $\frac{s}{\pi}\frac{d^2\sigma}{dtdM^2}$ ($mb.GeV^{-2}$); $s = 934\ GeV^2$ (continued)

M^2 (GeV^2)	M^2/s	$-t = 0.65\ GeV^2$	$-t = 0.70\ GeV^2$	$-t = 0.75\ GeV^2$	$-t = 0.80\ GeV^2$	$-t = 0.85\ GeV^2$	$-t = 0.90\ GeV^2$
-18	-.0193		.003 ± .003				.004 ± .002
-14	-.0150	.00 ± .01	.01 ± .01	.01 ± .01	.00 ± .01	.04 ± .03	.012 ± .005
-10	-.0107	.04 ± .03	.06 ± .02	.05 ± .03	.07 ± .03	.10 ± .05	.05 ± .01
-6	-.0064	.44 ± .11	.42 ± .05	.32 ± .08	.42 ± .10	.27 ± .10	.18 ± .03
-2	-.0021	2.14 ± .30	1.63 ± .08	1.41 ± .19	1.11 ± .18	.25 ± .16	.63 ± .05
2	.0021	5.60 ± .39	3.85 ± .13	3.58 ± .24	2.45 ± .21	2.14 ± .18	1.76 ± .08
6	.0064	6.58 ± .41	4.69 ± .13	4.00 ± .25	3.17 ± .23	2.59 ± .20	1.75 ± .09
10	.0107	4.62 ± .35	3.41 ± .11	2.86 ± .22	2.65 ± .20	1.58 ± .16	1.34 ± .08
14	.0150	2.95 ± .29	2.49 ± .10	2.23 ± .19	1.82 ± .18	1.20 ± .15	1.17 ± .07
18	.0193	2.61 ± .26	1.74 ± .08	1.79 ± .17	1.25 ± .14	1.09 ± .14	.86 ± .06
22	.0236	2.09 ± .24	1.44 ± .08	1.22 ± .15	1.12 ± .14	.99 ± .13	.60 ± .05
26	.0279	1.76 ± .22	1.29 ± .08	1.01 ± .14	.92 ± .13	.84 ± .13	.68 ± .06
30	.0321	1.55 ± .21	1.17 ± .07	1.04 ± .15	1.03 ± .13	.70 ± .11	.61 ± .05
34	.0364	1.40 ± .19	1.14 ± .08	.85 ± .15	.88 ± .12	.70 ± .11	.53 ± .05
38	.0407	1.25 ± .17	1.05 ± .07	.86 ± .15	.52 ± .10	.68 ± .12	.53 ± .05
42	.0450	1.17 ± .16	.95 ± .07	1.04 ± .15	.60 ± .11	.61 ± .12	.51 ± .05
46	.0493	1.11 ± .14	.92 ± .07	.90 ± .15	.74 ± .12	.50 ± .14	.48 ± .05
50	.0536	1.10 ± .06	.85 ± .13	.90 ± .14	.80 ± .13	.59 ± .14	.42 ± .05
54	.0578	1.16 ± .07	.99 ± .12	1.01 ± .15	.77 ± .13	.76 ± .15	.40 ± .05
58	.0621	1.08 ± .07	.84 ± .13	.82 ± .14	.70 ± .12	.60 ± .12	.48 ± .05
62	.0664	1.00 ± .07	.70 ± .13	.71 ± .13	.61 ± .11	.45 ± .12	.45 ± .04
66	.0707	1.01 ± .07	.97 ± .15	.66 ± .12	.51 ± .10	.56 ± .12	.44 ± .05
70	.0750	.93 ± .07	1.19 ± .16	.80 ± .12	.57 ± .11	.60 ± .12	.36 ± .04
74	.0793	1.04 ± .07	1.02 ± .16	.75 ± .12	.74 ± .12	.43 ± .11	.33 ± .04
78	.0836	.90 ± .07	.87 ± .14	.73 ± .11	.87 ± .14	.51 ± .12	.45 ± .05
82	.0878	.93 ± .07	.85 ± .14	.73 ± .11	.75 ± .13	.59 ± .12	.44 ± .05
86	.0921	.97 ± .07	.84 ± .14	.59 ± .10	.71 ± .14	.62 ± .12	.45 ± .05
90	.0964	1.05 ± .08	.86 ± .15	.55 ± .11	.77 ± .14	.48 ± .12	.49 ± .05
94	.1007	.99 ± .08	.92 ± .24	.73 ± .18	.70 ± .21	.50 ± .18	.47 ± .06

TABLE XIV

INELASTIC CROSS-SECTION $\frac{s}{\pi}\frac{d^2\sigma}{dtdM^2}$ ($mb.GeV^{-2}$); $s = 934\ GeV^2$ (continued)

M^2 (GeV^2)	M^2/s	$-t = 0.95$ GeV^2	$-t = 1.25$ GeV^2	$-t = 1.45$ GeV^2	$-t = 1.60$ GeV^2	$-t = 2.00$ GeV^2
-18	-.0193					
-14	-.0150	.00 ± .01	.003 ± .003	.004 ± .004	.006 ± .002	
-10	-.0107	.03 ± .02	.015 ± .006	.011 ± .005	.005 ± .002	.001 ± .001
-6	-.0064	.10 ± .05	.065 ± .012	.043 ± .008	.027 ± .004	.006 ± .006
-2	-.0021	.42 ± .13	.249 ± .037	.128 ± .018	.079 ± .007	.025 ± .008
2	.0021	1.00 ± .17	.450 ± .039	.225 ± .020	.154 ± .010	.039 ± .008
6	.0064	1.38 ± .18	.396 ± .036	.236 ± .019	.169 ± .010	.038 ± .008
10	.0107	1.33 ± .17	.328 ± .033	.191 ± .017	.126 ± .009	.042 ± .007
14	.0150	.77 ± .15	.272 ± .030	.147 ± .016	.096 ± .008	.036 ± .007
18	.0193	.74 ± .13	.222 ± .026	.132 ± .015	.111 ± .008	.031 ± .006
22	.0236	.63 ± .14	.166 ± .024	.132 ± .014	.090 ± .007	.026 ± .006
26	.0279	.42 ± .11	.168 ± .023	.120 ± .013	.076 ± .007	.023 ± .006
30	.0321	.62 ± .13	.157 ± .023	.106 ± .012	.070 ± .006	.026 ± .006
34	.0364	.56 ± .12	.150 ± .022	.093 ± .012	.069 ± .006	.020 ± .006
38	.0407	.50 ± .11	.154 ± .023	.087 ± .012	.071 ± .006	.025 ± .006
42	.0450	.29 ± .10	.159 ± .022	.099 ± .011	.062 ± .006	.032 ± .006
46	.0493	.20 ± .08	.154 ± .021	.092 ± .011	.055 ± .005	.027 ± .006
50	.0536	.32 ± .10	.135 ± .021	.080 ± .011	.053 ± .005	.024 ± .005
54	.0578	.25 ± .09	.136 ± .020	.073 ± .011	.060 ± .006	.020 ± .005
58	.0621	.30 ± .10	.131 ± .021	.089 ± .011	.054 ± .005	.021 ± .004
62	.0664	.40 ± .10	.158 ± .021	.097 ± .011	.053 ± .005	.015 ± .004
66	.0707	.41 ± .10	.137 ± .019	.089 ± .011	.068 ± .006	.012 ± .004
70	.0750	.27 ± .10	.113 ± .019	.096 ± .011	.064 ± .006	.017 ± .005
74	.0793	.33 ± .10	.120 ± .021	.092 ± .010	.053 ± .005	.015 ± .005
78	.0836	.42 ± .12	.133 ± .022	.080 ± .010	.054 ± .005	.018 ± .005
82	.0878	.41 ± .14	.159 ± .020	.085 ± .010	.053 ± .005	.031 ± .005
86	.0921	.33 ± .15	.133 ± .018	.088 ± .010	.068 ± .006	.030 ± .005
90	.0964	.22 ± .16	.112 ± .018	.079 ± .010	.058 ± .005	.022 ± .005
94	.1007	.22 ± .26	.134 ± .020	.083 ± .013	.067 ± .008	.019 ± .004

TABLE XIV

INELASTIC CROSS-SECTION $\frac{s}{\pi}\frac{d^2\sigma}{dtdM^2}$ $(mb.GeV^{-2})$; $s = 1047\ GeV^2$

M^2 $(GeV)^2$	M^2/s	$-t = 0.20$ GeV^2	$-t = 0.25$ GeV^2	$-t = 0.30$ GeV^2	$-t = 0.35$ GeV^2
-18.2	-.0173	.08 ± .03	.06 ± .06	.04 ± .06	.03 ± .06
-13.2	-.0126	.28 ± .15	.30 ± .14	.38 ± .18	.09 ± .10
-8.2	-.0078	3.9 ± .7	3.6 ± 0.6	2.8 ± 0.5	1.6 ± 0.5
-3.2	-.0030	39.0 ± 3.6	30.2 ± 2.6	23.2 ± 2.0	13.5 ± 1.5
1.8	.0018	87.3 ± 5.9	67.8 ± 4.4	51.6 ± 3.3	44.4 ± 3.5
6.8	.0065	69.9 ± 3.7	50.5 ± 2.7	36.7 ± 2.2	29.0 ± 2.2
11.8	.0113	37.8 ± 2.2	34.6 ± 1.9	20.8 ± 1.4	19.4 ± 1.8
16.8	.0161	21.7 ± 1.5	18.3 ± 1.2	15.0 ± 1.3	12.0 ± 1.3
21.8	.0209	21.5 ± 1.5	16.4 ± 1.2	11.6 ± 1.1	8.9 ± 1.1
26.8	.0256	16.4 ± 1.1	11.2 ± 0.9	9.4 ± 0.9	5.3 ± 0.8
31.8	.0304	12.6 ± 1.0	10.9 ± 0.9	9.7 ± 1.0	8.6 ± 1.3
36.8	.0352	13.1 ± 1.0	12.4 ± 1.0	8.7 ± 0.9	4.8 ± 0.9
41.8	.0400	11.2 ± 0.9	8.9 ± 0.8	6.7 ± 0.8	5.9 ± 1.0
46.8	.0447	14.2 ± 1.1	7.0 ± 0.8	7.3 ± 0.9	4.1 ± 0.8
51.8	.0495	9.5 ± 0.9	7.9 ± 0.8	7.4 ± 1.0	5.3 ± 0.9
56.8	.0543	7.6 ± 0.7	8.2 ± 0.8	6.6 ± 0.8	3.2 ± 0.7
61.8	.0591	8.8 ± 0.7	9.2 ± 0.9	4.3 ± 0.7	5.3 ± 0.9
66.8	.0639	8.3 ± 0.7	8.3 ± 0.8	4.7 ± 0.7	3.5 ± 0.9
71.8	.0686	7.9 ± 0.7	7.5 ± 0.8	5.1 ± 0.8	4.0 ± 0.8
76.8	.0734	9.7 ± 0.8	6.5 ± 0.7	5.0 ± 0.7	3.6 ± 0.8
81.8	.0782	8.0 ± 0.7	7.2 ± 0.8	5.0 ± 0.8	5.1 ± 1.1
86.8	.0830	8.7 ± 0.9	8.1 ± 0.9	4.9 ± 0.8	5.1 ± 1.1
91.8	.0877	6.7 ± 0.8	6.6 ± 0.8	5.1 ± 0.8	3.4 ± 0.9
96.8	.0925	7.6 ± 0.9	6.3 ± 0.8	5.6 ± 0.8	2.3 ± 0.7
101.8	.0973	7.3 ± 0.9	5.5 ± 0.7	4.7 ± 0.7	3.5 ± 0.7
106.8	.1021	6.7 ± 0.8	7.0 ± 0.8	4.3 ± 0.7	5.2 ± 1.0
111.8	.1068	6.0 ± 0.8	6.1 ± 0.7	4.0 ± 0.7	3.1 ± 0.9
116.8	.1116	6.6 ± 0.8	5.5 ± 0.7	3.6 ± 0.6	2.9 ± 0.8

TABLE XV

INELASTIC CROSS-SECTION $\frac{s}{\pi}\frac{d\sigma}{dtdM^2}$ $(mb.GeV^{-2})$; $s = 1239\ GeV^2$

M^2 (GeV^2)	M^2/s	$-t = 0.20$ GeV^2	$-t = 0.25$ GeV^2	$-t = 0.30$ GeV^2	$-t = 0.35$ GeV^2
-17	-.0137	.23 ± .18	.36 ± .15	.20 ± .12	.12 ± .03
-13	-.0105	.58 ± .33	.91 ± .22	.36 ± .16	.29 ± .10
-9	-.0073	2.9 ± 0.7	3.6 ± 0.5	2.5 ± 0.5	1.6 ± 0.3
-5	-.0040	15.4 ± 1.8	15.2 ± 0.9	13.5 ± 1.0	8.0 ± 0.5
-1	-.0008	64.7 ± 3.3	55.1 ± 1.8	37.3 ± 1.9	25.5 ± 1.1
3	+.0024	93.3 ± 4.0	76.5 ± 2.2	51.5 ± 2.1	33.7 ± 1.0
7	.0057	97.5 ± 3.7	59.8 ± 1.9	42.9 ± 2.1	33.7 ± 1.0
11	.0089	57.7 ± 2.8	39.4 ± 1.4	29.6 ± 1.6	23.5 ± 0.9
15	.0121	41.4 ± 2.3	27.3 ± 1.0	20.4 ± 1.2	16.9 ± 0.9
19	.0153	36.6 ± 2.3	22.3 ± 1.3	14.9 ± 1.2	12.0 ± 0.6
23	.0186	29.8 ± 2.0	17.2 ± 0.8	13.3 ± 1.0	10.4 ± 0.5
27	.0218	23.1 ± 1.8	13.9 ± 0.8	11.2 ± 0.9	7.4 ± 0.6
31	.0250	16.6 ± 1.5	12.9 ± 0.8	8.0 ± 0.9	7.9 ± 0.5
35	.0283	17.8 ± 1.6	12.1 ± 0.8	8.6 ± 0.8	6.7 ± 0.4
39	.0315	16.0 ± 1.6	9.5 ± 0.7	8.8 ± 0.8	6.0 ± 0.5
43	.0348	14.9 ± 1.5	10.4 ± 0.8	7.0 ± 0.8	5.6 ± 0.4
47	.0379	16.8 ± 1.6	10.0 ± 0.7	6.7 ± 0.7	5.3 ± 0.4
51	.0412	11.5 ± 1.3	8.4 ± 0.7	5.1 ± 0.7	5.9 ± 0.4
55	.0444	14.9 ± 1.5	8.3 ± 0.7	6.3 ± 0.7	4.7 ± 0.4
59	.0476	11.9 ± 1.4	7.8 ± 0.7	6.8 ± 0.7	4.7 ± 0.4
63	.0509	15.1 ± 1.5	8.3 ± 0.7	5.2 ± 0.7	4.0 ± 0.3
67	.0541	12.6 ± 1.5	6.7 ± 0.7	6.0 ± 0.7	4.2 ± 0.4
71	.0573	11.8 ± 1.4	6.6 ± 0.7	6.0 ± 0.6	4.2 ± 0.4
75	.0605	12.9 ± 1.5	7.2 ± 0.6	5.3 ± 0.6	4.4 ± 0.4
79	.0638	12.3 ± 1.4	7.2 ± 0.6	5.6 ± 0.8	3.1 ± 0.3
83	.0670	12.6 ± 1.6	6.4 ± 0.6	6.4 ± 0.8	3.8 ± 0.3
87	.0702	10.6 ± 1.3	6.5 ± 0.5	5.6 ± 0.6	3.6 ± 0.4
91	.0735	11.9 ± 1.5	6.5 ± 0.5	4.8 ± 0.6	4.3 ± 0.4

TABLE XVI

INELASTIC CROSS-SECTION $\frac{s}{\pi}\frac{d^2\sigma}{dtdM^2}$ $(mb.GeV^{-2})$; $s = 1239\ GeV^2$ (continued)

M^2 (GeV^2)	M^2/s	$-t = 0.45$ GeV^2	$-t = 0.50$ GeV^2	$-t = 0.55$ GeV^2	$-t = 0.65$ GeV^2	$-t = 0.75$ GeV^2
-17	-.0137	.07 ± .05	.10 ± .05	.05 ± .05	.07 ± .07	.15 ± .08
-13	-.0105	.32 ± .05	.19 ± .06	.17 ± .05	.14 ± .07	.07 ± .03
-9	-.0073	1.3 ± 0.2	.75 ± .05	.74 ± .12	.44 ± .05	.22 ± .07
-5	-.0040	5.1 ± 0.4	2.9 ± 0.1	2.4 ± 0.2	1.4 ± 0.2	.77 ± .13
-1	-.0008	12.9 ± 0.5	8.9 ± 0.3	6.8 ± 0.3	3.2 ± 0.2	2.1 ± 0.2
3	+.0024	18.4 ± 0.6	14.3 ± 0.5	9.4 ± 0.3	6.2 ± 0.2	3.1 ± 0.3
7	.0057	17.1 ± 0.7	14.0 ± 0.5	11.3 ± 0.3	6.6 ± 0.2	3.5 ± 0.3
11	.0089	13.6 ± 0.6	10.2 ± 0.4	8.4 ± 0.3	4.5 ± 0.2	3.1 ± 0.3
15	.0121	9.5 ± 0.4	8.9 ± 0.4	6.1 ± 0.2	3.1 ± 0.1	2.6 ± 0.2
19	.0153	7.6 ± 0.4	6.2 ± 0.4	3.7 ± 0.2	2.9 ± 0.1	1.2 ± 0.2
23	.0186	5.4 ± 0.4	4.6 ± 0.3	3.4 ± 0.2	2.3 ± 0.1	1.5 ± 0.2
27	.0218	4.9 ± 0.4	3.8 ± 0.3	3.4 ± 0.2	1.7 ± 0.1	1.2 ± 0.2
31	.0250	4.9 ± 0.3	3.7 ± 0.3	3.1 ± 0.2	1.7 ± 0.1	1.0 ± 0.2
35	.0283	4.2 ± 0.3	3.3 ± 0.2	2.6 ± 0.2	1.6 ± 0.1	0.9 ± 0.1
39	.0315	3.6 ± 0.3	3.0 ± 0.2	2.4 ± 0.1	1.2 ± 0.1	0.8 ± 0.2
43	.0348	2.9 ± 0.2	2.7 ± 0.2	1.8 ± 0.1	1.3 ± 0.1	0.8 ± 0.1
47	.0379	3.1 ± 0.2	2.6 ± 0.2	1.9 ± 0.1	1.3 ± 0.1	0.8 ± 0.1
51	.0412	2.9 ± 0.2	2.3 ± 0.2	1.7 ± 0.1	1.1 ± 0.1	0.6 ± 0.1
55	.0444	3.0 ± 0.2	2.5 ± 0.2	1.6 ± 0.1	0.8 ± 0.1	0.7 ± 0.1
59	.0476	2.4 ± 0.2	2.1 ± 0.2	1.7 ± 0.1	1.0 ± 0.1	0.8 ± 0.1
63	.0509	2.8 ± 0.2	2.2 ± 0.2	1.6 ± 0.1	1.1 ± 0.1	0.7 ± 0.1
67	.0541	2.4 ± 0.2	2.2 ± 0.2	1.6 ± 0.1	1.0 ± 0.1	0.6 ± 0.1
71	.0573	2.6 ± 0.2	2.2 ± 0.2	1.6 ± 0.1	0.9 ± 0.1	0.5 ± 0.1
75	.0605	2.6 ± 0.2	1.7 ± 0.2	1.3 ± 0.1	1.0 ± 0.1	0.7 ± 0.1
79	.0638	2.3 ± 0.2	2.0 ± 0.2	1.3 ± 0.1	0.9 ± 0.1	0.9 ± 0.1
83	.0670	2.2 ± 0.2	1.8 ± 0.2	1.6 ± 0.1	0.9 ± 0.1	0.7 ± 0.1
87	.0702	2.4 ± 0.2	1.8 ± 0.2	1.4 ± 0.1	0.9 ± 0.1	0.6 ± 0.1
91	.0735	2.1 ± 0.2	1.5 ± 0.1	1.4 ± 0.1	1.0 ± 0.1	0.5 ± 0.1

TABLE XVI

INELASTIC CROSS-SECTION $\frac{s}{\pi}\frac{d^2\sigma}{dtdM^2}$ $(mb.GeV^{-2})$; $s = 1464$ (GeV^2)

M^2 (GeV^2)	M^2/s	$-t = 0.20$ GeV^2	$-t = 0.25$ GeV^2	$-t = 0.30$ GeV^2	$-t = 0.35$ GeV^2	$-t = 0.45$ GeV^2
-16.5	-.0113	.90 ± .29	.60 ± .20	.32 ± .18	.22 ± .17	.19 ± .04
-11.5	-.0079	2.7 ± 0.2	3.2 ± 0.5	2.0 ± 0.4	1.3 ± 0.1	.94 ± .09
-6.5	-.0044	15.2 ± 0.6	13.3 ± 0.4	8.7 ± 1.0	6.2 ± 0.4	4.4 ± 0.6
-1.5	-.0010	56.4 ± 1.0	45.6 ± 0.9	29.1 ± 1.2	20.8 ± 0.9	12.0 ± 0.8
3.5	+.0024	93.4 ± 1.6	72.1 ± 1.4	47.4 ± 1.5	38.6 ± 1.6	18.9 ± 0.8
8.5	.0058	80.7 ± 1.9	60.0 ± 1.6	42.6 ± 1.2	35.4 ± 1.5	20.1 ± 0.7
13.5	.0092	52.5 ± 1.7	41.2 ± 1.4	40.0 ± 1.5	25.1 ± 1.3	12.9 ± 0.8
18.5	.0126	32.3 ± 1.7	23.9 ± 1.1	21.5 ± 1.0	16.3 ± 1.2	9.4 ± 0.7
23.5	.0160	27.8 ± 1.4	19.9 ± 1.1	18.1 ± 0.9	12.1 ± 0.8	7.6 ± 0.6
28.5	.0195	22.5 ± 1.1	16.0 ± 0.8	11.2 ± 0.7	9.8 ± 0.8	6.1 ± 0.6
33.5	.0229	18.2 ± 1.1	15.0 ± 0.8	13.0 ± 0.7	10.1 ± 0.7	5.1 ± 0.4
38.5	.0263	16.0 ± 1.1	12.7 ± 0.7	7.9 ± 0.5	6.8 ± 0.7	4.5 ± 0.3
43.5	.0297	15.0 ± 0.9	10.7 ± 0.7	8.1 ± 0.6	7.4 ± 0.7	4.6 ± 0.4
48.5	.0331	14.6 ± 0.9	10.7 ± 0.7	6.2 ± 0.5	6.9 ± 0.7	4.2 ± 0.3
53.5	.0365	13.2 ± 0.8	10.2 ± 0.7	8.1 ± 0.6	5.5 ± 0.6	2.7 ± 0.3
58.5	.0400	13.2 ± 0.9	9.8 ± 0.7	9.2 ± 0.6	4.7 ± 0.5	3.2 ± 0.3
63.5	.0434	12.3 ± 0.8	9.5 ± 0.6	6.6 ± 0.5	5.4 ± 0.6	2.9 ± 0.3
68.5	.0468	13.8 ± 0.7	8.3 ± 0.7	6.8 ± 0.4	4.7 ± 0.5	2.9 ± 0.3
73.5	.0502	10.9 ± 0.7	8.3 ± 0.5	6.4 ± 0.5	5.1 ± 0.5	2.6 ± 0.3
78.5	.0536	12.5 ± 1.0	7.8 ± 0.5	5.8 ± 0.4	4.0 ± 0.5	2.7 ± 0.4
83.5	.0570	9.5 ± 0.6	7.7 ± 0.5	4.9 ± 0.4	4.3 ± 0.5	2.8 ± 0.4
88.5	.0604	11.3 ± 0.7	8.0 ± 0.5	4.0 ± 0.5	4.1 ± 0.6	2.5 ± 0.3
93.5	.0639	8.9 ± 0.7	7.4 ± 0.5	6.3 ± 0.5	4.4 ± 0.5	3.3 ± 0.4
98.5	.0673	10.6 ± 0.6	7.1 ± 0.5	6.0 ± 0.4	3.8 ± 0.4	2.6 ± 0.3
103.5	.0707	8.7 ± 0.9	7.1 ± 0.6	5.5 ± 0.4	3.9 ± 0.4	2.1 ± 0.3
108.5	.0741	9.4 ± 0.8	6.6 ± 0.6	4.6 ± 0.4	4.4 ± 0.4	2.3 ± 0.3
113.5	.0775	9.9 ± 0.7	6.5 ± 0.5	4.3 ± 0.4	4.5 ± 0.5	1.8 ± 0.3

TABLE XVII

INELASTIC CROSS-SECTION $\frac{s}{\pi}\frac{d^2\sigma}{dtdM^2}$ $(mb.GeV^{-2})$; $s = 1464(GeV^2)$

(continued)

M^2 (GeV^2)	M^2/s	$-t = 0.50$ GeV^2	$-t = 0.55$ GeV^2	$-t = 0.60$ GeV^2	$-t = 0.70$ GeV^2
-16.5	-.0113	.34 ± .13	.26 ± .03	.13 ± .03	.19 ± .10
-11.5	-.0079	1.1 ± 0.2	.92 ± .11	.74 ± .11	.71 ± .19
-6.5	-.0044	4.4 ± 0.4	3.4 ± 0.3	2.4 ± 0.2	1.4 ± 0.3
-1.5	-.0010	8.8 ± 0.7	8.2 ± 0.6	5.3 ± 0.3	3.5 ± 0.4
3.5	+.0024	13.7 ± 0.6	12.3 ± 0.7	7.1 ± 0.5	5.2 ± 0.6
8.5	.0058	13.7 ± 0.6	10.1 ± 0.6	7.2 ± 0.4	3.7 ± 0.5
13.5	.0092	9.6 ± 0.5	6.1 ± 0.4	5.3 ± 0.4	2.7 ± 0.4
18.5	.0126	7.5 ± 0.5	4.1 ± 0.4	4.2 ± 0.4	2.5 ± 0.4
23.5	.0160	5.1 ± 0.5	2.8 ± 0.3	2.5 ± 0.3	1.3 ± 0.3
28.5	.0195	3.7 ± 0.3	2.9 ± 0.4	2.7 ± 0.3	1.5 ± 0.3
33.5	.0229	3.3 ± 0.3	3.2 ± 0.3	2.4 ± 0.3	2.1 ± 0.4
38.5	.0263	3.7 ± 0.4	2.5 ± 0.3	2.0 ± 0.2	1.4 ± 0.2
43.5	.0297	3.3 ± 0.4	2.7 ± 0.3	1.6 ± 0.2	0.7 ± 0.2
48.5	.0331	2.3 ± 0.3	2.0 ± 0.3	1.2 ± 0.2	1.0 ± 0.3
53.5	.0365	3.0 ± 0.3	1.7 ± 0.3	1.0 ± 0.2	0.9 ± 0.2
58.5	.0400	2.5 ± 0.3	2.3 ± 0.3	1.3 ± 0.2	0.7 ± 0.2
63.5	.0434	1.7 ± 0.3	1.8 ± 0.3	1.6 ± 0.2	0.7 ± 0.2
68.5	.0468	2.4 ± 0.3	1.5 ± 0.2	1.1 ± 0.2	0.9 ± 0.2
73.5	.0502	2.2 ± 0.2	1.5 ± 0.2	1.4 ± 0.2	0.7 ± 0.2
78.5	.0536	1.9 ± 0.2	1.7 ± 0.3	1.4 ± 0.2	0.5 ± 0.2
83.5	.0570	2.4 ± 0.3	1.5 ± 0.2	1.1 ± 0.2	0.9 ± 0.2
88.5	.0604	1.9 ± 0.3	1.4 ± 0.2	1.3 ± 0.2	0.6 ± 0.2
93.5	.0639	1.9 ± 0.3	1.5 ± 0.2	1.2 ± 0.2	1.0 ± 0.2
98.5	.0673	2.2 ± 0.3	1.4 ± 0.2	0.9 ± 0.2	0.9 ± 0.2
103.5	.0707	2.2 ± 0.3	1.3 ± 0.3	1.2 ± 0.2	1.1 ± 0.2
108.5	.0741	2.0 ± 0.3	1.4 ± 0.2	1.1 ± 0.2	1.0 ± 0.3
113.5	.0775	2.1 ± 0.3	1.2 ± 0.2	1.4 ± 0.2	1.0 ± 0.2

TABLE XVII

INELASTIC CROSS-SECTION $\frac{s}{\pi} d^2\sigma/dtdM^2$ (mb.GeV^{-2}); s = 1995 GeV^2							
M^2 (GeV^2)	M^2/s	$-t$ = 0.45 GeV^2	$-t$ = 0.55 GeV^2	$-t$ = 0.65 GeV^2	$-t$ = 0.75 GeV^2	$-t$ = 0.85 GeV^2	$-t$ = 0.95 GeV^2
-27.3	-.0137				0.02 ± 0.02		0.01 ± 0.02
-17.3	-.0087			0.1 ± 0.1	0.07 ± 0.04		0
- 7.3	-.0037			2.0 ± 0.4	1.60 ± 0.25	0.79 ± 0.17	0.46 ± 0.10
2.7	.0014			12.3 ± 1.1	7.06 ± 0.56	4.08 ± 0.39	2.46 ± 0.23
12.7	.0064		8.3 ± 0.8	6.6 ± 0.7	3.42 ± 0.34	3.31 ± 0.36	1.69 ± 0.22
22.7	.0114		5.2 ± 0.6	3.6 ± 0.6	3.03 ± 0.34	1.32 ± 0.18	1.10 ± 0.15
32.7	.0164		4.4 ± 0.6	3.2 ± 0.6	1.61 ± 0.23	0.78 ± 0.12	0.59 ± 0.11
42.7	.0214		4.3 ± 0.6	1.7 ± 0.4	1.28 ± 0.20	0.69 ± 0.12	0.71 ± 0.14
52.7	.0264		2.2 ± 0.4	1.2 ± 0.3	0.92 ± 0.17	0.61 ± 0.11	0.77 ± 0.15
62.7	.0314		3.1 ± 0.5	1.4 ± 0.2	0.72 ± 0.14	0.79 ± 0.14	0.31 ± 0.09
72.7	.0364		2.8 ± 0.5	1.1 ± 0.2	0.91 ± 0.17	0.62 ± 0.11	0.47 ± 0.11
82.7	.0415		1.5 ± 0.3	1.4 ± 0.2	0.75 ± 0.16	0.71 ± 0.13	0.32 ± 0.08
92.7	.0465		1.4 ± 0.3	1.1 ± 0.2	0.87 ± 0.17	0.46 ± 0.10	0.51 ± 0.10
102.7	.0515	1.7 ± 0.4	1.7 ± 0.4	1.3 ± 0.2	0.93 ± 0.18	0.53 ± 0.10	0.44 ± 0.09
112.7	.0565	2.5 ± 0.5	1.5 ± 0.4	1.1 ± 0.2	0.55 ± 0.11	0.59 ± 0.12	0.20 ± 0.06
122.7	.0615	3.1 ± 0.6	2.5 ± 0.5	0.8 ± 0.2	0.56 ± 0.11	0.49 ± 0.11	0.32 ± 0.07
132.7	.0665	1.9 ± 0.4	2.1 ± 0.4	1.2 ± 0.2	0.75 ± 0.12	0.35 ± 0.10	0.32 ± 0.08
142.7	.0715	2.2 ± 0.4	1.9 ± 0.4	1.3 ± 0.2	0.60 ± 0.11	0.44 ± 0.12	0.30 ± 0.07
152.7	.0765	2.1 ± 0.4	1.3 ± 0.2	1.0 ± 0.2	0.49 ± 0.10	0.60 ± 0.12	0.28 ± 0.07
162.7	.0815	2.1 ± 0.5	1.9 ± 0.3	1.0 ± 0.2	0.66 ± 0.11	0.42 ± 0.11	0.30 ± 0.07
172.7	.0866	1.9 ± 0.4	1.0 ± 0.2	1.3 ± 0.2	0.81 ± 0.13	0.50 ± 0.12	0.22 ± 0.06
182.7	.0916	2.7 ± 0.5	2.1 ± 0.3	1.0 ± 0.2	0.73 ± 0.13	0.44 ± 0.11	0.35 ± 0.08
192.7	.0966	1.6 ± 0.3	1.4 ± 0.2	1.0 ± 0.2	0.70 ± 0.12	0.51 ± 0.12	0.48 ± 0.10
202.7	.1016	2.2 ± 0.5	1.8 ± 0.2	0.8 ± 0.2	0.79 ± 0.13	0.57 ± 0.10	0.24 ± 0.06
212.7	.1066	2.5 ± 0.4	1.5 ± 0.2	1.0 ± 0.2	0.79 ± 0.13	0.56 ± 0.11	0.33 ± 0.08
222.7	.1116	2.7 ± 0.5	1.6 ± 0.2	0.9 ± 0.2	0.75 ± 0.13	0.39 ± 0.08	0.35 ± 0.08
232.7	.1166	2.3 ± 0.4	1.7 ± 0.2	1.0 ± 0.2	0.62 ± 0.12	0.40 ± 0.08	0.41 ± 0.09

TABLE XVIII

INELASTIC CROSS-SECTION $\frac{s}{\pi} d^2\sigma/dtdM^2$ (mb.GeV^2); s = 1995 GeV^2 (continued)

M^2 (GeV^2)	M^2/s	-t = 1.05 GeV^2	-t = 1.15 GeV^2	-t = 1.25 GeV^2	-t = 1.45 GeV^2 x10^{-3}	-t = 1.75 GeV^2 x10^{-3}	-t = 2.05 GeV^2 x10^{-3}
-27.3	-.0137						
-17.3	-.0087	0.02 ± 0.02	0.02 ± 0.02			4 ± 4	
- 7.3	-.0037	0.48 ± 0.10	0.13 ± 0.04	0.25 ± 0.06	87 ± 21	61 ± 15	30 ± 10
2.7	.0014	1.24 ± 0.15	1.09 ± 0.14	0.74 ± 0.14	328 ± 41	138 ± 22	47 ± 11
12.7	.0064	1.12 ± 0.16	1.03 ± 0.14	0.74 ± 0.15	351 ± 44	96 ± 18	41 ± 11
22.7	.0114	0.62 ± 0.11	0.74 ± 0.13	0.32 ± 0.07	224 ± 33	65 ± 14	53 ± 14
32.7	.0164	0.41 ± 0.08	0.23 ± 0.07	0.36 ± 0.08	150 ± 30	66 ± 15	17 ± 7
42.7	.0214	0.27 ± 0.07	0.31 ± 0.08	0.26 ± 0.06	84 ± 21	56 ± 13	36 ± 10
52.7	.0264	0.41 ± 0.09	0.26 ± 0.07	0.16 ± 0.05	118 ± 27	83 ± 21	8 ± 5
62.7	.0314	0.29 ± 0.07	0.29 ± 0.09	0.29 ± 0.07	75 ± 20	31 ± 10	14 ± 6
72.7	.0364	0.31 ± 0.08	0.23 ± 0.08	0.19 ± 0.07	79 ± 22	57 ± 14	19 ± 7
82.7	.0415	0.35 ± 0.08	0.13 ± 0.05	0.05 ± 0.03	75 ± 20	40 ± 12	24 ± 8
92.7	.0465	0.26 ± 0.07	0.31 ± 0.10	0.16 ± 0.06	91 ± 25	30 ± 10	19 ± 7
102.7	.0515	0.28 ± 0.07	0.26 ± 0.09	0.09 ± 0.04	145 ± 31	41 ± 11	23 ± 7
112.7	.0565	0.23 ± 0.07	0.17 ± 0.05	0.02 ± 0.02	118 ± 28	44 ± 11	20 ± 6
122.7	.0615	0.38 ± 0.09	0.22 ± 0.06	0.18 ± 0.06	111 ± 26	49 ± 11	18 ± 6
132.7	.0665	0.15 ± 0.05	0.18 ± 0.05	0.12 ± 0.05	55 ± 19	52 ± 14	21 ± 7
142.7	.0715	0.26 ± 0.07	0.16 ± 0.05	0.15 ± 0.07	58 ± 19	30 ± 9	10 ± 4
152.7	.0765	0.37 ± 0.09	0.22 ± 0.06	0.13 ± 0.05	70 ± 19	30 ± 9	3 ± 3
162.7	.0815	0.17 ± 0.07	0.17 ± 0.05	0.06 ± 0.04	69 ± 19	44 ± 11	9 ± 5
172.7	.0866	0.13 ± 0.05	0.16 ± 0.06	0.20 ± 0.06	96 ± 25	26 ± 8	18 ± 6
182.7	.0916	0.34 ± 0.10	0.14 ± 0.05	0.09 ± 0.04	77 ± 18	35 ± 10	18 ± 6
192.7	.0966	0.13 ± 0.06	0.11 ± 0.04	0.10 ± 0.05	88 ± 21	58 ± 12	11 ± 5
202.7	.1016	0.46 ± 0.10	0.17 ± 0.05	0.02 ± 0.02	75 ± 19	44 ± 12	24 ± 8
212.7	.1066	0.34 ± 0.07	0.18 ± 0.05	0.13 ± 0.05	134 ± 29	33 ± 9	19 ± 7
222.7	.1116	0.29 ± 0.07	0.31 ± 0.07	0.15 ± 0.06	112 ± 25	44 ± 12	10 ± 5
232.7	.1166	0.12 ± 0.04	0.21 ± 0.06	0.17 ± 0.06	97 ± 21	29 ± 9	26 ± 7

TABLE XVIII

INELASTIC CROSS-SECTION $\frac{s}{\pi} d^2\sigma/dtdM^2$ (mb.GeV^2); s = 1995 GeV^2 (continued)						
M^2 (GeV^2)	M^2/s	-t = 2.35 GeV^2 x10^{-3}	-t = 2.65 GeV^2 x10^{-3}	-t = 2.95 GeV^2 x10^{-3}	-t = 3.25 GeV^2 x10^{-3}	-t = 3.55 GeV^2 x10^{-3}
-27.3	-.0137					
-17.3	-.0087		1.6 ± 1.6	1.2 ± 1.2	0.7 ± 0.7	
- 7.3	-.0037	18 ± 6	6.1 ± 3.1	3.6 ± 2.1	1.3 ± 0.9	
2.7	.0014	47 ± 13	25.2 ± 6.5	10.3 ± 2.9	4.3 ± 1.6	4.6 ± 2.1
12.7	.0064	25 ± 8	18.5 ± 5.2	12.8 ± 3.2	7.0 ± 2.0	1.2 ± 1.2
22.7	.0114	13 ± 5	6.1 ± 3.5	4.8 ± 2.0	1.6 ± 1.1	2.7 ± 1.9
32.7	.0164	11 ± 4	14.2 ± 4.5	6.3 ± 2.8	2.0 ± 1.1	1.0 ± 1.0
42.7	.0214	21 ± 6	18.4 ± 5.1	4.4 ± 2.0	2.4 ± 1.4	3.2 ± 1.9
52.7	.0264	14 ± 6	5.2 ± 3.0	6.2 ± 2.3	2.4 ± 1.4	4.9 ± 2.2
62.7	.0314	10 ± 5	4.3 ± 2.5	4.0 ± 1.6	1.7 ± 1.0	1.3 ± 1.3
72.7	.0364	10 ± 4	15.0 ± 4.8	3.8 ± 1.7	2.5 ± 1.2	2.2 ± 1.3
82.7	.0415	12 ± 5	4.2 ± 2.1	6.2 ± 2.4	7.6 ± 2.5	1.2 ± 1.2
92.7	.0465	11 ± 5	6.1 ± 2.5	5.4 ± 2.0	4.4 ± 1.7	1.4 ± 1.4
102.7	.0515	10 ± 4	4.3 ± 2.1	3.5 ± 1.4	5.6 ± 2.1	5.1 ± 2.3
112.7	.0565	7 ± 4	13.2 ± 4.0	5.5 ± 2.0	3.5 ± 1.7	1.4 ± 1.4
122.7	.0615	8 ± 4	7.1 ± 3.2	3.2 ± 1.3	2.9 ± 1.4	0 ± 1.4
132.7	.0665	5 ± 3	4.7 ± 2.4	5.3 ± 1.8	0.7 ± 0.7	3.9 ± 1.9
142.7	.0715	10 ± 4	7.9 ± 3.0	9.7 ± 2.7	3.9 ± 1.8	0 ± 1.5
152.7	.0765	8 ± 4	5.5 ± 2.5	6.2 ± 2.1	1.4 ± 1.0	1.1 ± 1.1
162.7	.0815	10 ± 4	2.0 ± 1.4	7.3 ± 2.1	1.8 ± 1.2	1.1 ± 1.1
172.7	.0866	8 ± 3	5.7 ± 2.6	2.5 ± 1.2	4.3 ± 1.9	1.2 ± 1.2
182.7	.0916	4 ± 2	1.1 ± 1.1	5.0 ± 1.8	3.5 ± 1.6	0 ± 1.2
192.7	.0966	8 ± 4	10.3 ± 3.3	3.1 ± 1.5	2.5 ± 1.4	3.7 ± 2.1
202.7	.1016	18 ± 6	9.2 ± 2.9	2.8 ± 1.2	7.3 ± 2.6	3.3 ± 1.9
212.7	.1066	8 ± 4	4.8 ± 2.4	4.3 ± 1.6	2.3 ± 1.3	5.3 ± 3.1
222.7	.1116	15 ± 5	7.5 ± 2.9	2.9 ± 1.4	5.9 ± 3.0	4.1 ± 2.4
232.7	.1166	22 ± 7	6.0 ± 2.4	3.9 ± 1.6	1.5 ± 1.1	0 ± 1.2

TABLE XVIII

INELASTIC CROSS-SECTION $\frac{s}{\pi} d^2\sigma/dtdM^2$ (mb.GeV^{-2}) ; s = 2783 GeV^2								
M^2 (GeV^2)	M^2/s	-t = 0.65 GeV^2	-t = 0.75 GeV^2	-t = 0.85 GeV^2	-t = 0.95 GeV^2	-t = 1.05 GeV^2	-t = 1.15 GeV^2	-t = 1.25 GeV^2
-37.5	-.0135						0.01 ± 0.01	0.01 ± 0.01
-22.5	-.0086		0.15 ± 0.18		0.02 ± 0.02	0.02 ± 0.02	0.02 ± 0.02	0.04 ± 0.02
-7.5	-.0027		2.03 ± 0.59	2.29 ± 0.67	0.68 ± 0.11	0.84 ± 0.13	0.32 ± 0.07	0.42 ± 0.08
7.5	.0027		4.42 ± 0.92	2.25 ± 0.64	2.98 ± 0.27	1.97 ± 0.21	1.35 ± 0.15	0.75 ± 0.09
22.5	.0086		2.70 ± 0.66	2.21 ± 0.64	1.84 ± 0.20	0.93 ± 0.13	0.82 ± 0.12	0.46 ± 0.07
37.5	.0135		1.90 ± 0.57	2.01 ± 0.64	0.95 ± 0.15	0.68 ± 0.12	0.51 ± 0.09	0.32 ± 0.05
52.5	.0189		1.34 ± 0.47	0.51 ± 0.29	0.58 ± 0.10	0.50 ± 0.08	0.25 ± 0.06	0.21 ± 0.04
67.5	.0243		2.00 ± 0.58	1.18 ± 0.45	0.43 ± 0.09	0.41 ± 0.08	0.45 ± 0.08	0.19 ± 0.04
82.5	.0296		0.96 ± 0.43	0.96 ± 0.43	0.47 ± 0.09	0.44 ± 0.09	0.23 ± 0.06	0.13 ± 0.03
97.5	.0350	1.2 ± 0.5	1.17 ± 0.44	0.23 ± 0.23	0.48 ± 0.09	0.55 ± 0.09	0.20 ± 0.04	0.12 ± 0.03
112.5	.0404	1.5 ± 0.5	0.33 ± 0.23	1.03 ± 0.42	0.53 ± 0.10	0.23 ± 0.06	0.27 ± 0.05	0.15 ± 0.04
127.5	.0458	1.4 ± 0.5	0.98 ± 0.40	0.51 ± 0.10	0.48 ± 0.10	0.28 ± 0.07	0.16 ± 0.04	0.15 ± 0.04
142.5	.0512	1.2 ± 0.4	1.26 ± 0.45	0.39 ± 0.09	0.37 ± 0.08	0.39 ± 0.08	0.17 ± 0.04	0.13 ± 0.04
157.5	.0566	0.8 ± 0.4	1.06 ± 0.40	0.39 ± 0.08	0.54 ± 0.10	0.20 ± 0.05	0.21 ± 0.04	0.19 ± 0.05
172.5	.0620	0.6 ± 0.3	0.59 ± 0.30	0.40 ± 0.09	0.33 ± 0.07	0.37 ± 0.07	0.19 ± 0.04	0.13 ± 0.04
187.5	.0674	1.2 ± 0.4	0.71 ± 0.36	0.55 ± 0.10	0.32 ± 0.07	0.27 ± 0.06	0.21 ± 0.04	0.09 ± 0.03
202.5	.0728	0.6 ± 0.3	0.48 ± 0.10	0.46 ± 0.09	0.29 ± 0.07	0.31 ± 0.06	0.18 ± 0.04	0.09 ± 0.03
217.5	.0782	0.5 ± 0.3	0.70 ± 0.13	0.39 ± 0.08	0.41 ± 0.08	0.25 ± 0.05	0.28 ± 0.05	0.16 ± 0.04
232.5	.0836	1.3 ± 0.5	0.58 ± 0.12	0.56 ± 0.10	0.36 ± 0.07	0.30 ± 0.05	0.20 ± 0.04	0.15 ± 0.04
247.5	.0889	1.0 ± 0.4	0.74 ± 0.13	0.48 ± 0.09	0.31 ± 0.07	0.30 ± 0.05	0.18 ± 0.04	0.11 ± 0.03
262.5	.0943	1.1 ± 0.4	0.35 ± 0.25	0.53 ± 0.10	0.29 ± 0.07	0.28 ± 0.05	0.24 ± 0.05	0.11 ± 0.02
277.5	.0997	1.1 ± 0.4	0.79 ± 0.13	0.38 ± 0.08	0.41 ± 0.08	0.27 ± 0.05	0.28 ± 0.05	0.13 ± 0.03
292.5	.1051	0.8 ± 0.3	0.56 ± 0.11	0.54 ± 0.10	0.26 ± 0.06	0.27 ± 0.05	0.13 ± 0.04	0.16 ± 0.04
307.5	.1105	1.9 ± 0.6	0.92 ± 0.15	0.42 ± 0.08	0.39 ± 0.07	0.38 ± 0.06	0.22 ± 0.04	0.11 ± 0.03
322.5	.1159	0.3 ± 0.2	0.74 ± 0.12	0.67 ± 0.10	0.31 ± 0.06	0.39 ± 0.06	0.23 ± 0.05	0.20 ± 0.04
337.5	.1213	1.7 ± 0.6	0.54 ± 0.11	0.73 ± 0.11	0.44 ± 0.07	0.37 ± 0.06	0.13 ± 0.05	0.24 ± 0.04
352.5	.1267	1.2 ± 0.5	0.56 ± 0.12	0.76 ± 0.11	0.34 ± 0.06	0.33 ± 0.05	0.19 ± 0.04	0.21 ± 0.04

TABLE XIX

INELASTIC CROSS-SECTION $\frac{s}{\pi} d^2\sigma/dtdM^2$ (mb.GeV^{-2}); s = 2783 GeV^2								
M^2 (GeV^2)	M^2/s	-t = 1.45 GeV^2 x10^{-3}	-t = 1.75 GeV^2 x10^{-3}	-t = 2.05 GeV^2 x10^{-3}	-t = 2.35 GeV^2 x10^{-3}	-t = 2.65 GeV^2 x10^{-3}	-t = 3.10 GeV^2 x10^{-4}	-t = 4.15 GeV^2 x10^{-4}
-37.5	-.0135	8 ± 5			3 ± 2	2 ± 2	10 ± 10	7 ± 4
-22.5	-.0086	21 ± 8		2 ± 2	3 ± 2	2 ± 2	73 ± 53	5 ± 3
- 7.5	-.0027	184 ± 23	107 ± 16	62 ± 12	18 ± 5	11 ± 3	27 ± 16	27 ± 7
7.5	.0027	369 ± 33	171 ± 20	70 ± 12	28 ± 7	15 ± 4	23 ± 17	8 ± 4
22.5	.0086	261 ± 28	92 ± 14	57 ± 11	30 ± 7	18 ± 5	82 ± 26	13 ± 5
37.5	.0135	152 ± 22	92 ± 16	47 ± 9	12 ± 5	10 ± 3	75 ± 25	10 ± 4
52.2	.0189	148 ± 21	55 ± 12	47 ± 11	15 ± 5	23 ± 5	68 ± 28	21 ± 6
67.5	.0243	148 ± 19	57 ± 12	24 ± 7	18 ± 6	7 ± 3	5 ± 5	11 ± 4
82.5	.0296	96 ± 16	40 ± 10	28 ± 8	11 ± 4	11 ± 4	64 ± 26	7 ± 3
97.5	.0350	116 ± 16	72 ± 13	24 ± 7	14 ± 5	9 ± 3	26 ± 15	15 ± 5
112.5	.0404	78 ± 14	31 ± 8	26 ± 7	13 ± 5	7 ± 3	67 ± 24	9 ± 4
127.5	.0458	90 ± 16	50 ± 11	16 ± 6	17 ± 6	12 ± 4	37 ± 19	8 ± 4
142.5	.0512	70 ± 12	43 ± 10	15 ± 5	4 ± 3	5 ± 3	53 ± 21	11 ± 4
157.5	.0566	75 ± 12	54 ± 11	13 ± 5	9 ± 4	12 ± 4	30 ± 15	9 ± 3
172.5	.0620	65 ± 12	30 ± 8	24 ± 7	7 ± 3	13 ± 4	41 ± 23	11 ± 4
187.5	.0674	103 ± 15	47 ± 10	13 ± 5	10 ± 4	4 ± 2	8 ± 8	18 ± 5
202.5	.0728	116 ± 16	28 ± 8	23 ± 6	15 ± 4	11 ± 4	70 ± 24	13 ± 5
217.5	.0782	91 ± 14	53 ± 11	22 ± 6	15 ± 5	4 ± 2	43 ± 21	13 ± 5
232.5	.0836	70 ± 13	36 ± 9	25 ± 8	14 ± 5	11 ± 4	53 ± 24	29 ± 8
247.5	.0889	73 ± 13	42 ± 10	21 ± 7	11 ± 4	7 ± 3	38 ± 17	22 ± 6
262.5	.0943	72 ± 12	51 ± 11	16 ± 6	10 ± 3	8 ± 3	43 ± 22	15 ± 5
277.5	.0997	92 ± 14	45 ± 10	19 ± 6	6 ± 3	12 ± 4	11 ± 11	17 ± 5
292.5	.1051	107 ± 16	60 ± 11	20 ± 6	12 ± 4	11 ± 4	56 ± 26	23 ± 6
307.5	.1105	88 ± 15	56 ± 11	28 ± 8	21 ± 5	6 ± 3	54 ± 24	10 ± 4
322.5	.1159	69 ± 12	57 ± 12	38 ± 8	14 ± 4	17 ± 5	128 ± 33	12 ± 5
337.5	.1213	99 ± 15	48 ± 11	19 ± 6	13 ± 4	9 ± 4	70 ± 28	14 ± 5
352.5	.1267	100 ± 15	59 ± 11	24 ± 6	24 ± 6	12 ± 5	41 ± 20	10 ± 4

(continued)

TABLE XIX

INELASTIC CROSS-SECTION $\frac{s}{\pi} d^2\sigma/dtdM^2$ $(mb.GeV^{-2})$; $s = 3892\ GeV^2$

M^2 (GeV^2)	M^2/s	$-t = 1.15$ GeV^2	$-t = 1.25$ GeV^2	$-t = 1.45$ GeV^2 $\times 10^{-3}$	$-t = 1.75$ GeV^2 $\times 10^{-3}$	$-t = 2.05$ GeV^2 $\times 10^{-3}$	$-t = 2.35$ GeV^2 $\times 10^{-3}$	$-t = 2.65$ GeV^2 $\times 10^{-3}$
- 50	-.0128	0.01 ± 0.01		5 ± 3	1 ± 1	2 ± 2		2 ± 2
- 30	-.0077	0.02 ± 0.02		25 ± 7	5 ± 3	6 ± 3	3 ± 2	11 ± 5
- 10	-.0026	0.59 ± 0.08	0.25 ± 0.05	278 ± 27	125 ± 14	49 ± 8	24 ± 6	11 ± 5
10	.0026	0.99 ± 0.10	0.85 ± 0.09	433 ± 34	160 ± 16	72 ± 9	24 ± 6	18 ± 6
30	.0077	0.61 ± 0.08	0.36 ± 0.05	246 ± 25	105 ± 12	39 ± 7	30 ± 7	8 ± 5
50	.0128	0.31 ± 0.05	0.30 ± 0.04	164 ± 19	73 ± 10	25 ± 5	23 ± 6	13 ± 6
70	.0180	0.37 ± 0.06	0.20 ± 0.04	114 ± 17	60 ± 9	29 ± 6	12 ± 4	0
90	.0231	0.24 ± 0.05	0.16 ± 0.03	117 ± 16	49 ± 8	13 ± 4	24 ± 6	10 ± 7
110	.0283	0.22 ± 0.04	0.18 ± 0.03	74 ± 13	51 ± 8	20 ± 5	15 ± 5	0
130	.0334	0.16 ± 0.04	0.20 ± 0.04	82 ± 13	48 ± 8	27 ± 6	14 ± 5	0
150	.0385	0.21 ± 0.03	0.12 ± 0.03	83 ± 12	52 ± 9	23 ± 6	12 ± 6	12 ± 7
170	.0437	0.16 ± 0.03	0.14 ± 0.03	71 ± 11	46 ± 7	19 ± 5	13 ± 5	0
190	.0488	0.19 ± 0.04	0.10 ± 0.02	74 ± 12	39 ± 7	20 ± 5	9 ± 4	8 ± 6
210	.0540	0.20 ± 0.04	0.10 ± 0.02	72 ± 11	36 ± 7	13 ± 4	11 ± 5	4 ± 4
230	.0591	0.16 ± 0.03	0.14 ± 0.03	81 ± 11	28 ± 6	16 ± 5	22 ± 7	14 ± 8
250	.0642	0.14 ± 0.03	0.08 ± 0.02	76 ± 11	52 ± 8	12 ± 4	15 ± 7	9 ± 6
270	.0694	0.10 ± 0.02	0.12 ± 0.03	79 ± 10	42 ± 7	18 ± 5	13 ± 7	19 ± 11
290	.0745	0.15 ± 0.03	0.10 ± 0.03	63 ± 8	43 ± 7	17 ± 5	13 ± 8	0
310	.0797	0.21 ± 0.04	0.18 ± 0.03	62 ± 8	43 ± 7	18 ± 5	6 ± 4	8 ± 8
330	.0848	0.10 ± 0.02	0.14 ± 0.03	80 ± 10	32 ± 6	19 ± 6	2.5 ± 2.5	
350	.0899	0.18 ± 0.04	0.15 ± 0.03	75 ± 10	40 ± 6	2 ± 2		
370	.0951	0.22 ± 0.04	0.15 ± 0.02	78 ± 10	31 ± 6	8 ± 4	7 ± 4	
390	.1002	0.20 ± 0.03	0.14 ± 0.02	74 ± 10	39 ± 6	28 ± 7		
410	.1053	0.15 ± 0.03	0.12 ± 0.02	74 ± 11	43 ± 7	13 ± 5	5.5 ± 4	
430	.1105	0.18 ± 0.03	0.15 ± 0.02	96 ± 10	33 ± 6	27 ± 7		
450	.1156	0.19 ± 0.03	0.14 ± 0.02	90 ± 10	54 ± 8	24 ± 8	16.5 ± 6.5	
470	.1206	0.18 ± 0.02	0.14 ± 0.02	82 ± 10	41 ± 7	33 ± 11		

TABLE XX

Table XXI

INELASTIC CROSS-SECTIONS $d\sigma/dt$ (mb.GeV^{-2}); $M^2/s \leqslant 0.05$ (5% error added in quadrature)

$-t$ (GeV^2) \ s (GeV^2)	549	725	934	1047	1239	1464	1995	2783	3892
0.15	8.0 ± 0.5	7.1 ± 0.5							
0.20	5.2 ± 0.3	6.3 ± 0.4		5.4 ± 0.3	6.1 ± 0.4	5.5 ± 0.3			
0.25	3.7 ± 0.2	3.4 ± 0.2	4.2 ± 0.3	4.2 ± 0.3	4.3 ± 0.3	4.1 ± 0.2			
0.30	2.58 ± 0.15	2.38 ± 0.14	2.78 ± 0.17	3.16 ± 0.20	3.07 ± 0.18	3.09 ± 0.18			
0.35	1.99 ± 0.12	1.85 ± 0.11	2.17 ± 0.13	2.44 ± 0.16	2.29 ± 0.14	2.35 ± 0.14			
0.40	1.46 ± 0.09		1.65 ± 0.10						
0.45	1.12 ± 0.07	1.10 ± 0.07	1.29 ± 0.08		1.24 ± 0.07	1.32 ± 0.08			
0.50	0.91 ± 0.06	0.85 ± 0.05	0.91 ± 0.06		1.00 ± 0.06	0.97 ± 0.06			
0.55	0.69 ± 0.04	0.70 ± 0.04	0.68 ± 0.04		0.74 ± 0.04	0.68 ± 0.04			
0.60	0.49 ± 0.03		0.60 ± 0.04			0.54 ± 0.04			
0.65	0.42 ± 0.03		0.47 ± 0.03		0.43 ± 0.03		0.57 ± 0.04		
0.70	0.33 ± 0.02		0.35 ± 0.02			0.34 ± 0.03			
0.75	0.28 ± 0.02		0.31 ± 0.02		0.26 ± 0.02		0.35 ± 0.03	0.31 ± 0.04	
0.80			0.251 ± 0.015						
0.85	0.182 ± 0.011		0.192 ± 0.013				0.225 ± 0.016	0.225 ± 0.029	
0.90			0.157 ± 0.012						
0.95	0.126 ± 0.009		0.119 ± 0.008				0.149 ± 0.012	0.162 ± 0.012	
1.05	0.072 ± 0.005						0.092 ± 0.008	0.118 ± 0.009	
1.15	0.050 ± 0.004						0.076 ± 0.007	0.079 ± 0.006	0.065 ± 0.005
1.25	0.041 ± 0.004		0.041 ± 0.003				0.056 ± 0.006	0.051 ± 0.004	0.046 ± 0.004
1.45	0.025 ± 0.003		0.0245 ± 0.0015				0.027 ± 0.002	0.029 ± 0.002	0.028 ± 0.002
1.60			0.0170 ± 0.0010						
1.75							0.0116 ± 0.0011	0.0132 ± 0.0010	0.0130 ± 0.0010
2.00			0.0053 ± 0.0004						
2.05							0.0049 ± 0.0006	0.0069 ± 0.0006	0.0055 ± 0.0005
2.35							0.0031 ± 0.0004	0.0031 ± 0.0003	0.0032 ± 0.0003
2.65							0.0020 ± 0.0002	0.0022 ± 0.0002	0.0015 ± 0.0003
2.95							0.00110 ± 0.00014		
3.10								0.00097 ± 0.00016	
3.25							0.00061 ± 0.00009		
3.55							0.00039 ± 0.00008		
4.15								0.00024 ± 0.00008	

TABLE XXII

s (GeV^2)	σ_{SD} $M^2/s < 0.05$	σ_{SD} $M^2/s < 0.10$
549	6.07 ± 0.17	7.61 ± 0.23
725	6.05 ± 0.22	7.24 ± 0.53
934	6.37 ± 0.15	7.78 ± 0.25
1047	6.32 ± 0.22	7.84 ± 0.30
1239	7.01 ± 0.28	8.28 ± 0.31
1464	6.80 ± 0.29	8.23 ± 0.19

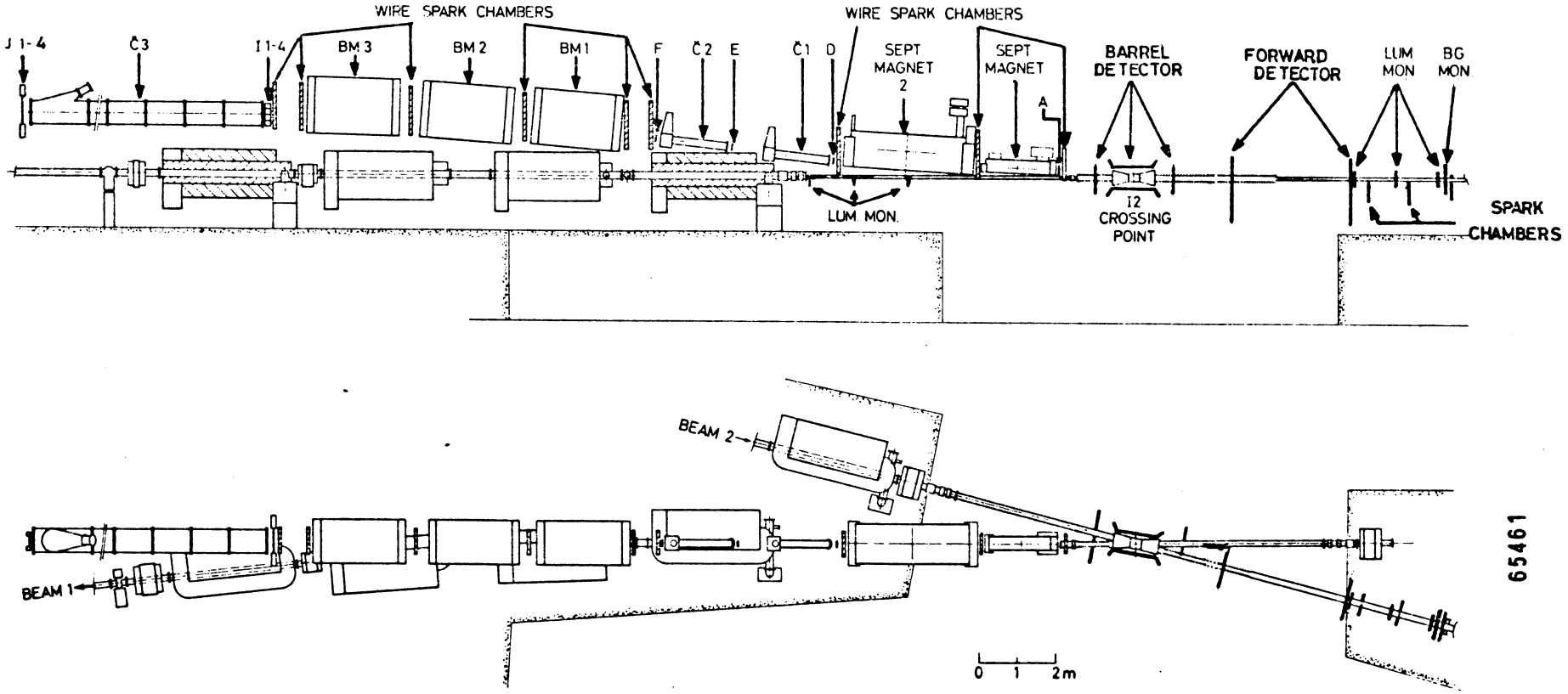
WIRE SPARK CHAMBERS
WIRE SPARK CHAMBERS
J 1-4
Č3
I 1-4
BM 3
BM 2
BM 1
F
Č2
E
Č1
D
SEPT MAGNET 2
SEPT MAGNET
A
BARREL DETECTOR
FORWARD DETECTOR
LUM MON
BG MON
LUM MON.
I2 CROSSING POINT
SPARK CHAMBERS
BEAM 2
BEAM 1
0 1 2m
65461

Fig. 1

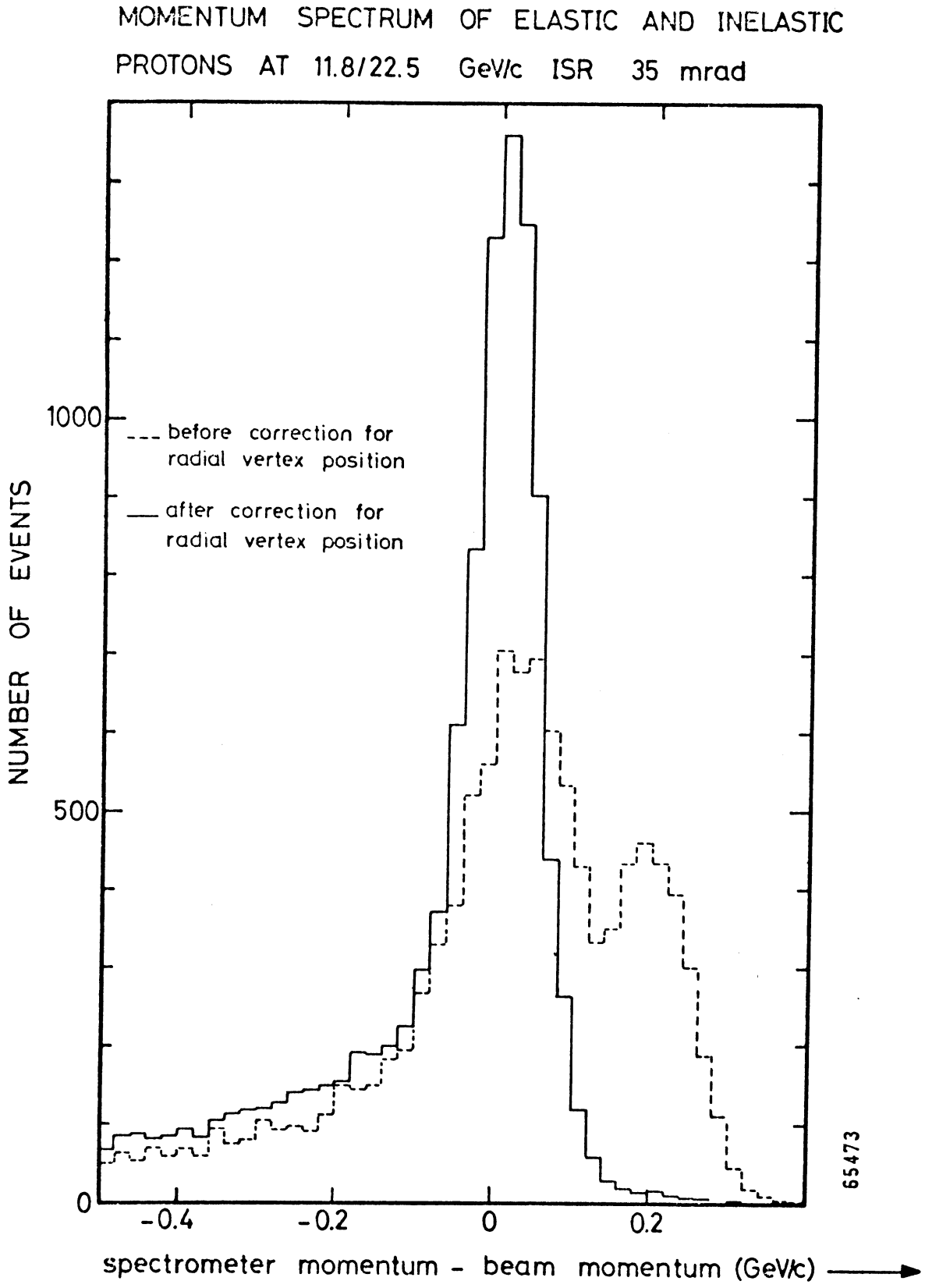
MOMENTUM SPECTRUM OF ELASTIC AND INELASTIC
PROTONS AT 11.8/22.5 GeV/c ISR 35 mrad
NUMBER OF EVENTS
1000
500
0
--- before correction for radial vertex position
— after correction for radial vertex position
-0.4
-0.2
0
0.2
spectrometer momentum - beam momentum (GeV/c)
65473

Fig. 2

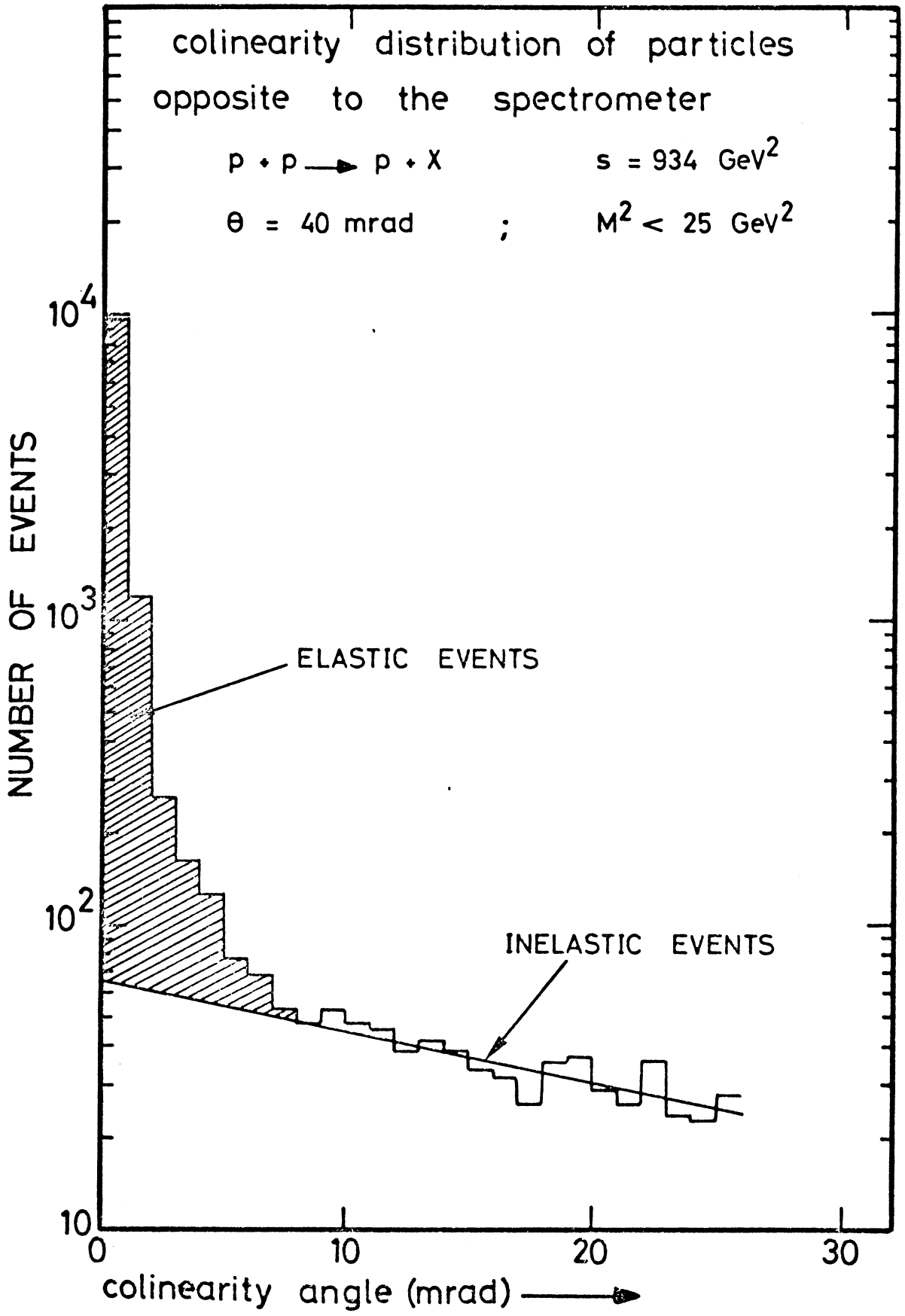
colinearity distribution of particles
opposite to the spectrometer
p + p → p + X
s = 934 GeV²
θ = 40 mrad ; M² < 25 GeV²
NUMBER OF EVENTS
10⁴
10³
10²
10
ELASTIC EVENTS
INELASTIC EVENTS
0
10
20
30
colinearity angle (mrad)
65471

Fig. 3

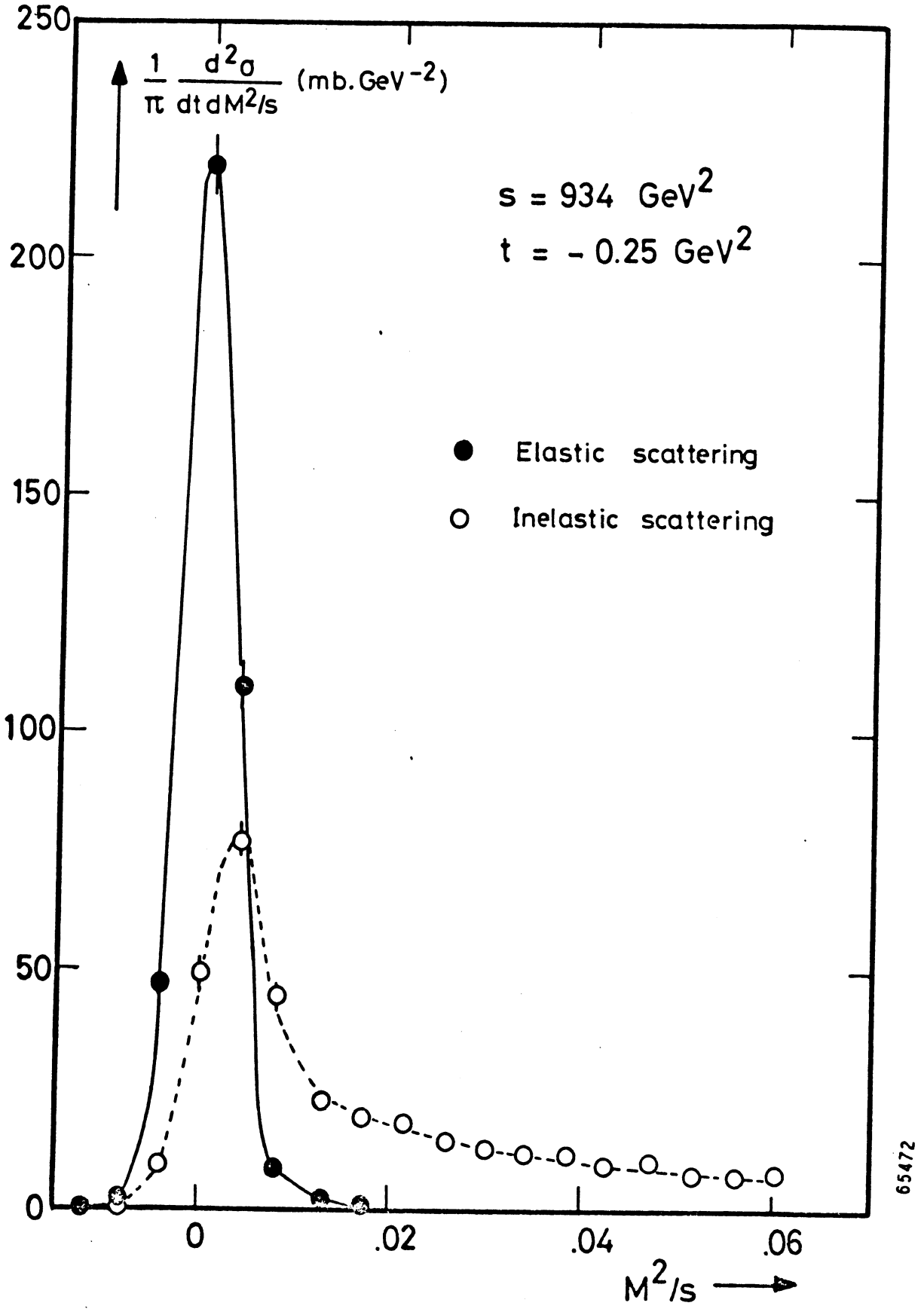
250
200
150
100
50
0
$\frac{1}{\pi}\frac{d^2\sigma}{dt\,dM^2/s}$ (mb.GeV^{-2})
s = 934 GeV^2
t = - 0.25 GeV^2
Elastic scattering
Inelastic scattering
0
.02
.04
.06
M^2/s
65472

Fig. 4

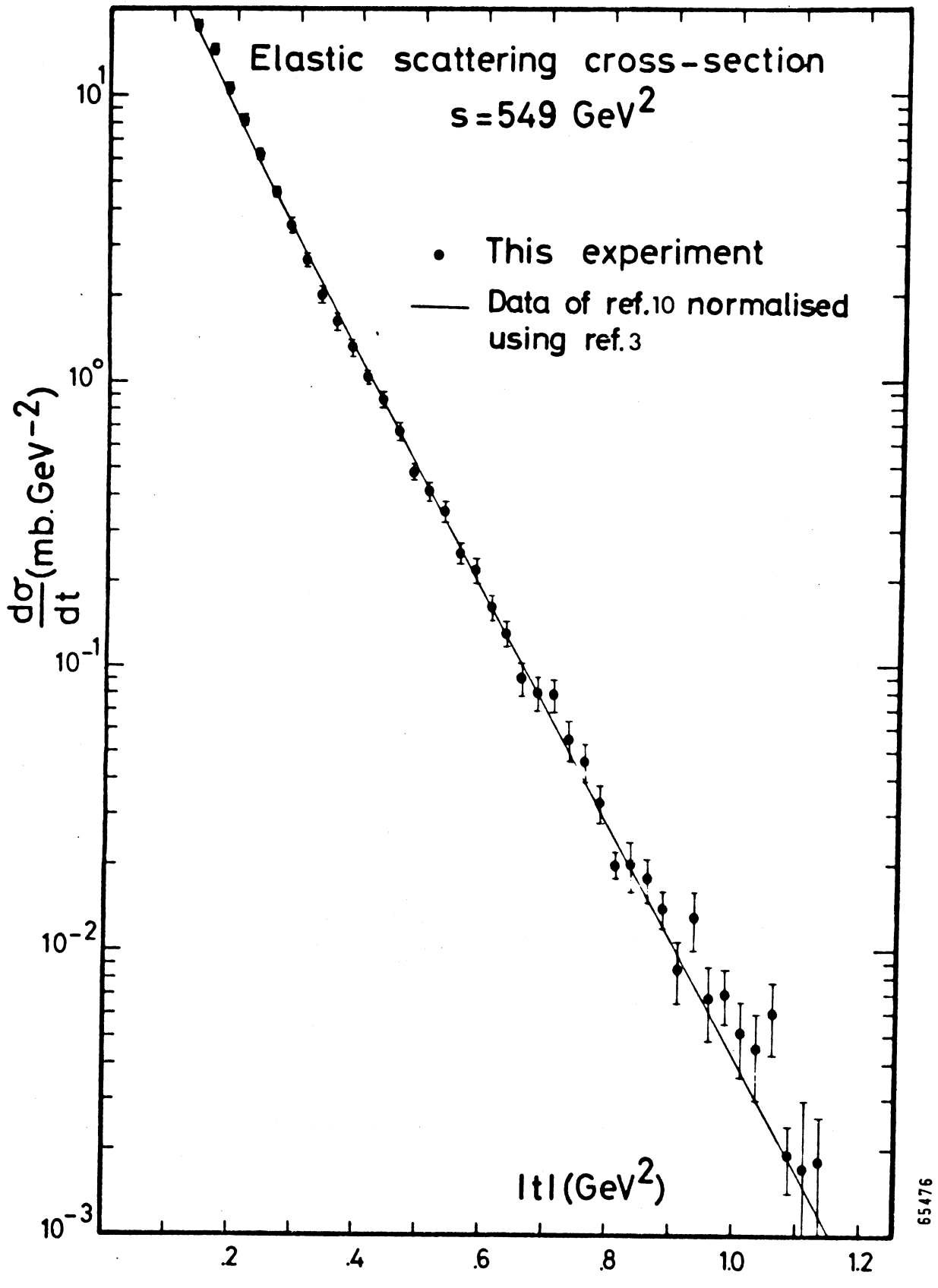
Elastic scattering cross-section
s=549 GeV2
This experiment
Data of ref.10 normalised using ref.3
dσ/dt (mb.GeV-2)
10^1
10^0
10^-1
10^-2
10^-3
.2
.4
.6
.8
1.0
1.2
|t| (GeV2)
65476

Fig. 5

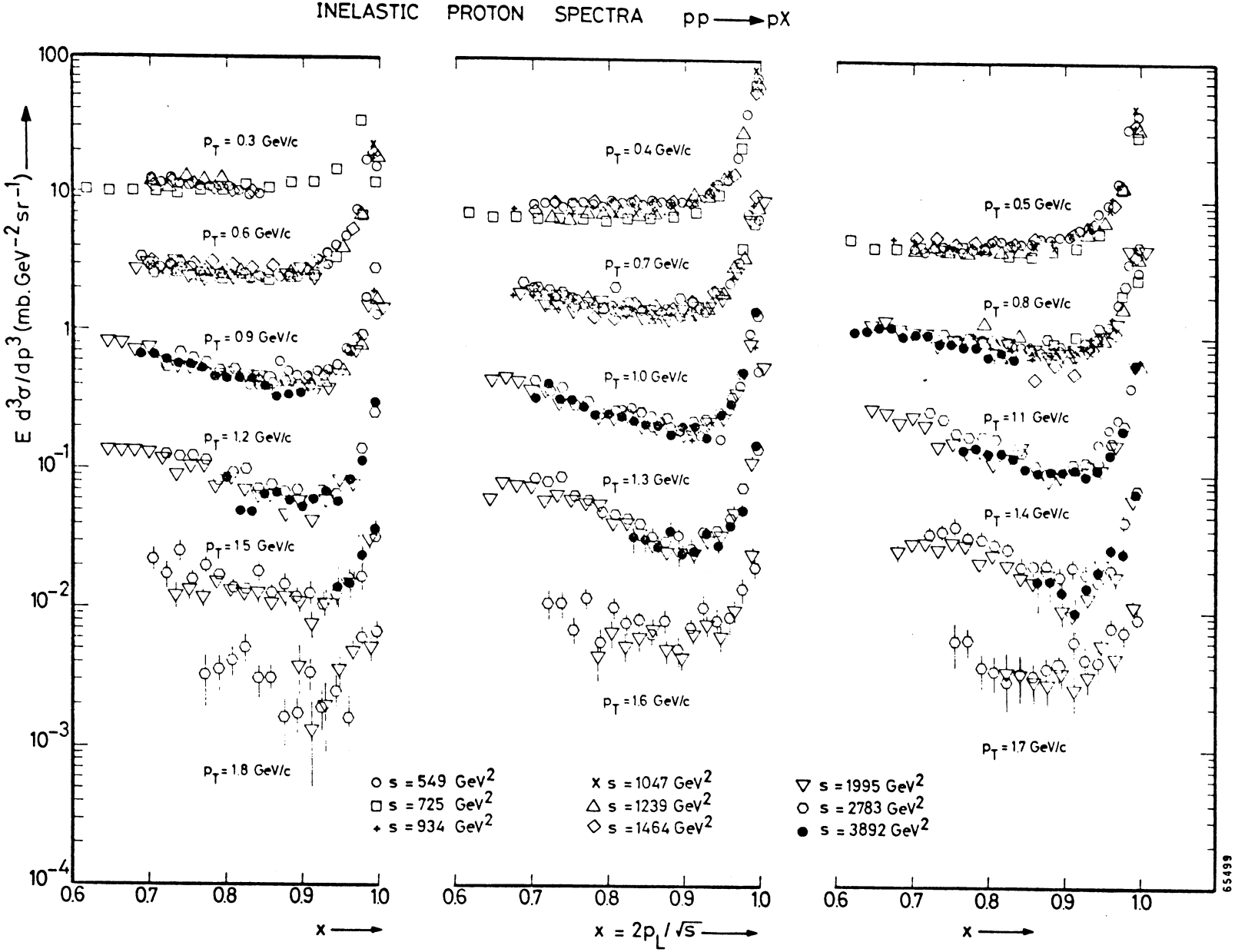
INELASTIC PROTON SPECTRA pp → pX
E d³σ/dp³ (mb. GeV⁻² sr⁻¹)
100
10
1
10⁻¹
10⁻²
10⁻³
10⁻⁴
p_T = 0.3 GeV/c
p_T = 0.6 GeV/c
p_T = 0.9 GeV/c
p_T = 1.2 GeV/c
p_T = 1.5 GeV/c
p_T = 1.8 GeV/c
p_T = 0.4 GeV/c
p_T = 0.7 GeV/c
p_T = 1.0 GeV/c
p_T = 1.3 GeV/c
p_T = 1.6 GeV/c
p_T = 0.5 GeV/c
p_T = 0.8 GeV/c
p_T = 1.1 GeV/c
p_T = 1.4 GeV/c
p_T = 1.7 GeV/c
○ s = 549 GeV²
□ s = 725 GeV²
+ s = 934 GeV²
× s = 1047 GeV²
△ s = 1239 GeV²
◇ s = 1464 GeV²
▽ s = 1995 GeV²
○ s = 2783 GeV²
● s = 3892 GeV²
0.6
0.7
0.8
0.9
1.0
x →
x = 2p_L/√s →
65499

Fig.6(a)

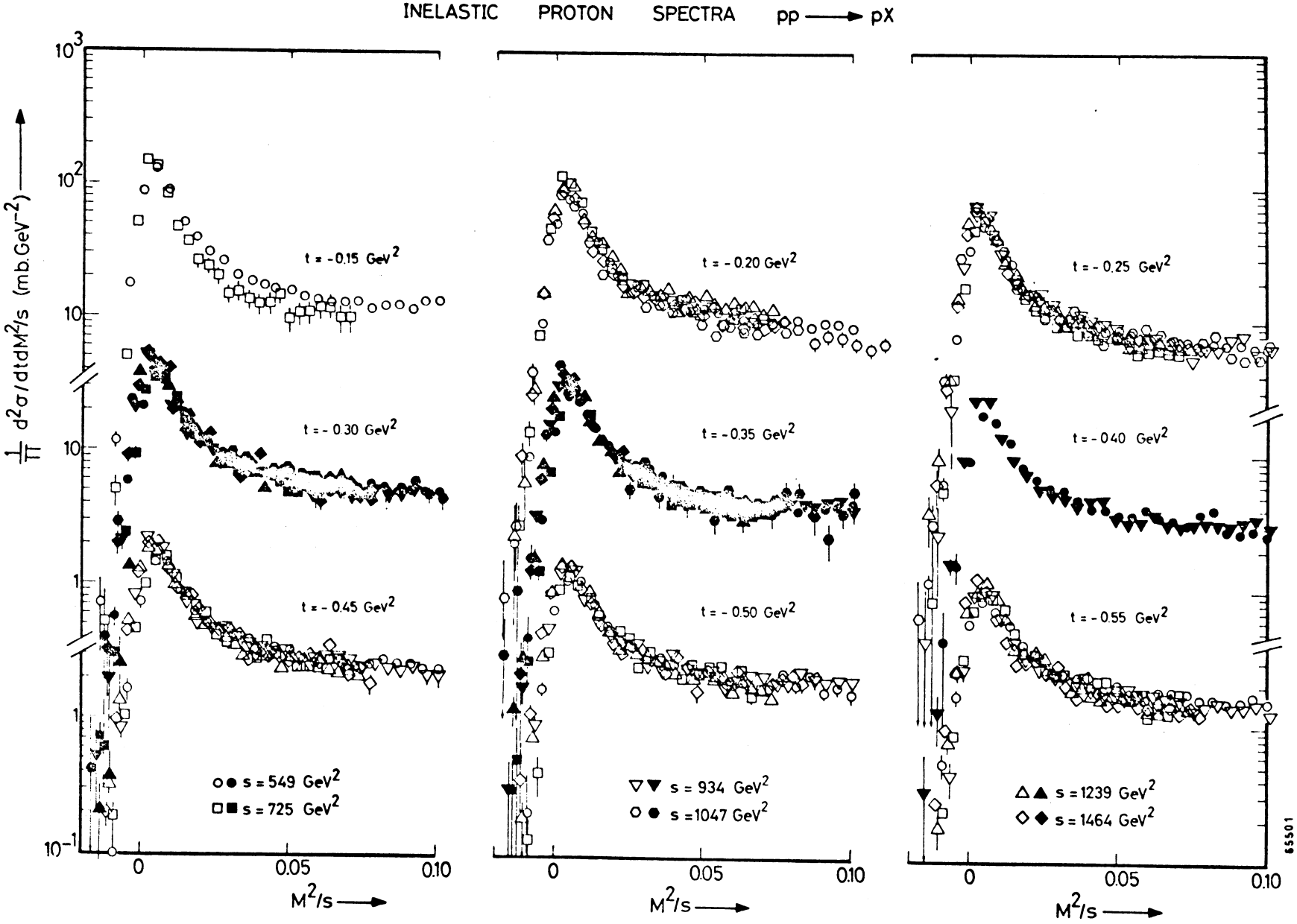
INELASTIC PROTON SPECTRA pp ⟶ pX
$\frac{1}{\pi} d^2\sigma/dtdM^2/s$ (mb.GeV^{-2})
10^3
10^2
10
1
10^{-1}
t = -0.15 GeV^2
t = -0.30 GeV^2
t = -0.45 GeV^2
t = -0.20 GeV^2
t = -0.35 GeV^2
t = -0.50 GeV^2
t = -0.25 GeV^2
t = -0.40 GeV^2
t = -0.55 GeV^2
○● s = 549 GeV^2
□■ s = 725 GeV^2
▽▼ s = 934 GeV^2
○● s = 1047 GeV^2
△▲ s = 1239 GeV^2
◇◆ s = 1464 GeV^2
0
0.05
0.10
M^2/s ⟶
65501

Fig.6(b)

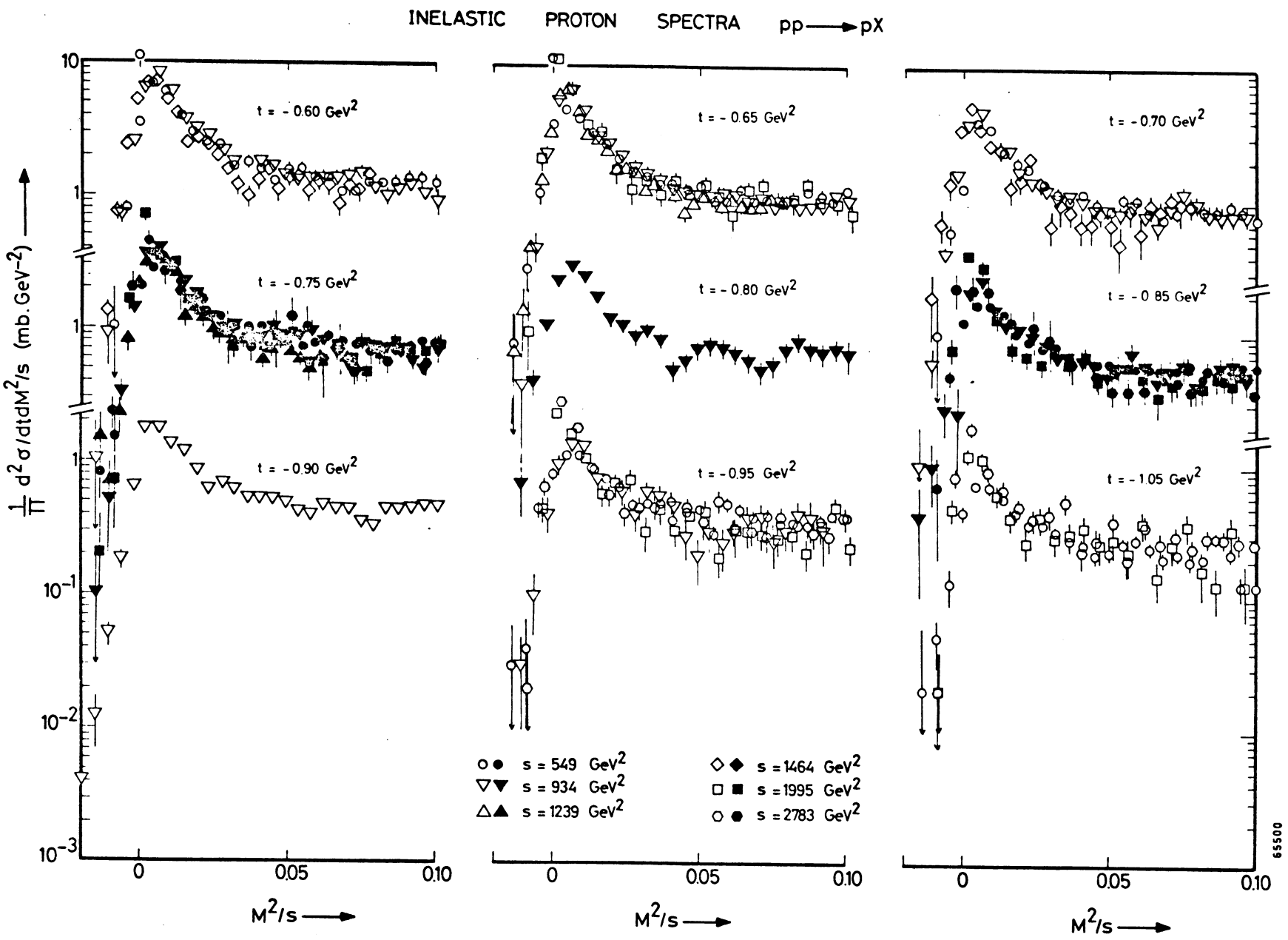
INELASTIC PROTON SPECTRA pp ⟶ pX
$\frac{1}{\pi} d^2\sigma/dtdM^2/s$ (mb.GeV^{-2}) ⟶
t = - 0.60 GeV^2
t = - 0.65 GeV^2
t = - 0.70 GeV^2
t = - 0.75 GeV^2
t = - 0.80 GeV^2
t = - 0.85 GeV^2
t = - 0.90 GeV^2
t = - 0.95 GeV^2
t = - 1.05 GeV^2
s = 549 GeV^2
s = 934 GeV^2
s = 1239 GeV^2
s = 1464 GeV^2
s = 1995 GeV^2
s = 2783 GeV^2
M^2/s ⟶
65500

Fig.6(c)

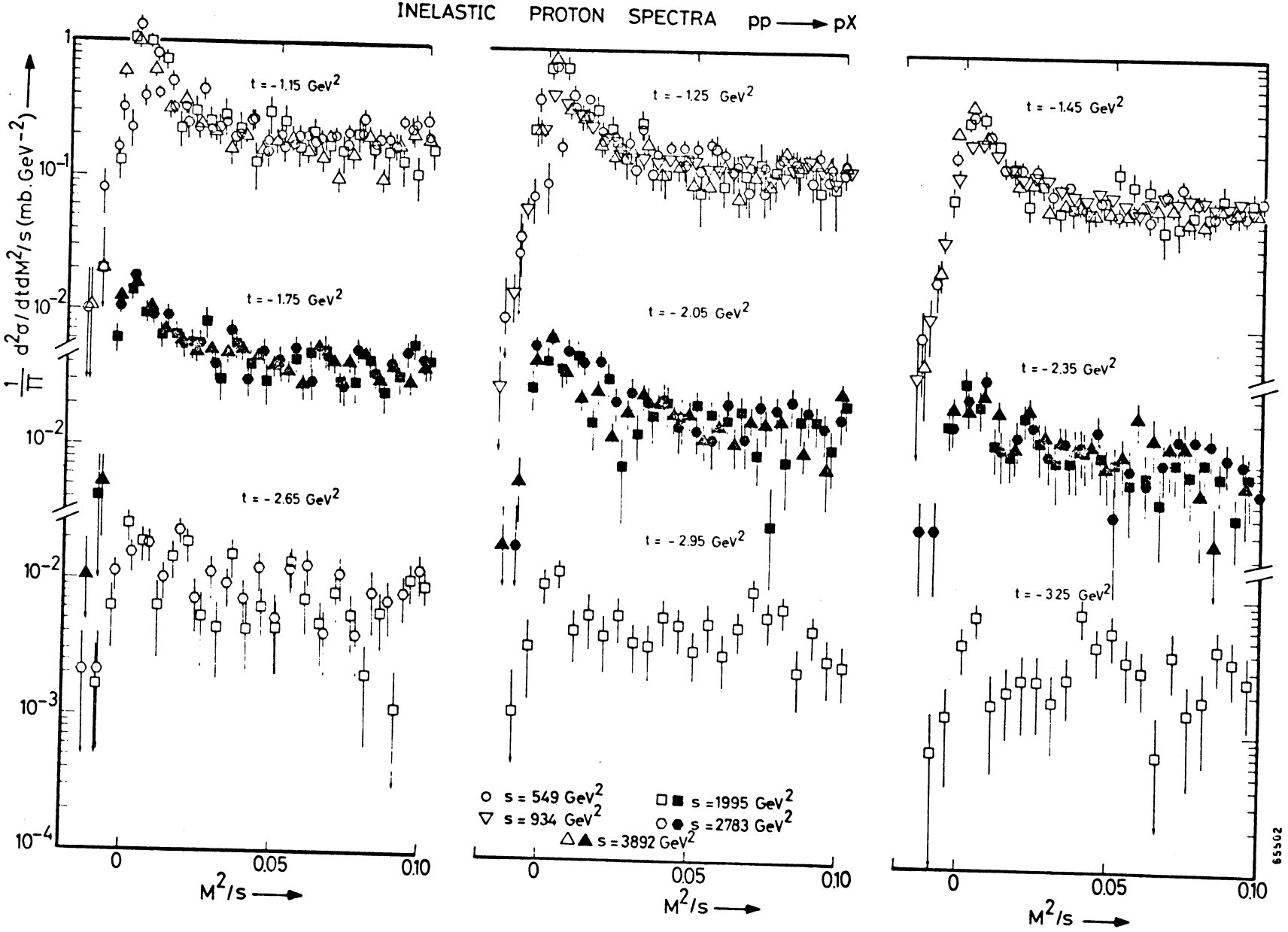
INELASTIC PROTON SPECTRA pp ⟶ pX
$\frac{1}{\pi} d^2\sigma/dtdM^2/s$ (mb.GeV^{-2})
t = -1.15 GeV^2
t = -1.75 GeV^2
t = -2.65 GeV^2
t = -1.25 GeV^2
t = -2.05 GeV^2
t = -2.95 GeV^2
t = -1.45 GeV^2
t = -2.35 GeV^2
t = -3.25 GeV^2
○ s = 549 GeV^2
▽ s = 934 GeV^2
△▲ s = 3892 GeV^2
□■ s = 1995 GeV^2
○● s = 2783 GeV^2
M^2/s ⟶
65502

Fig.6(d)

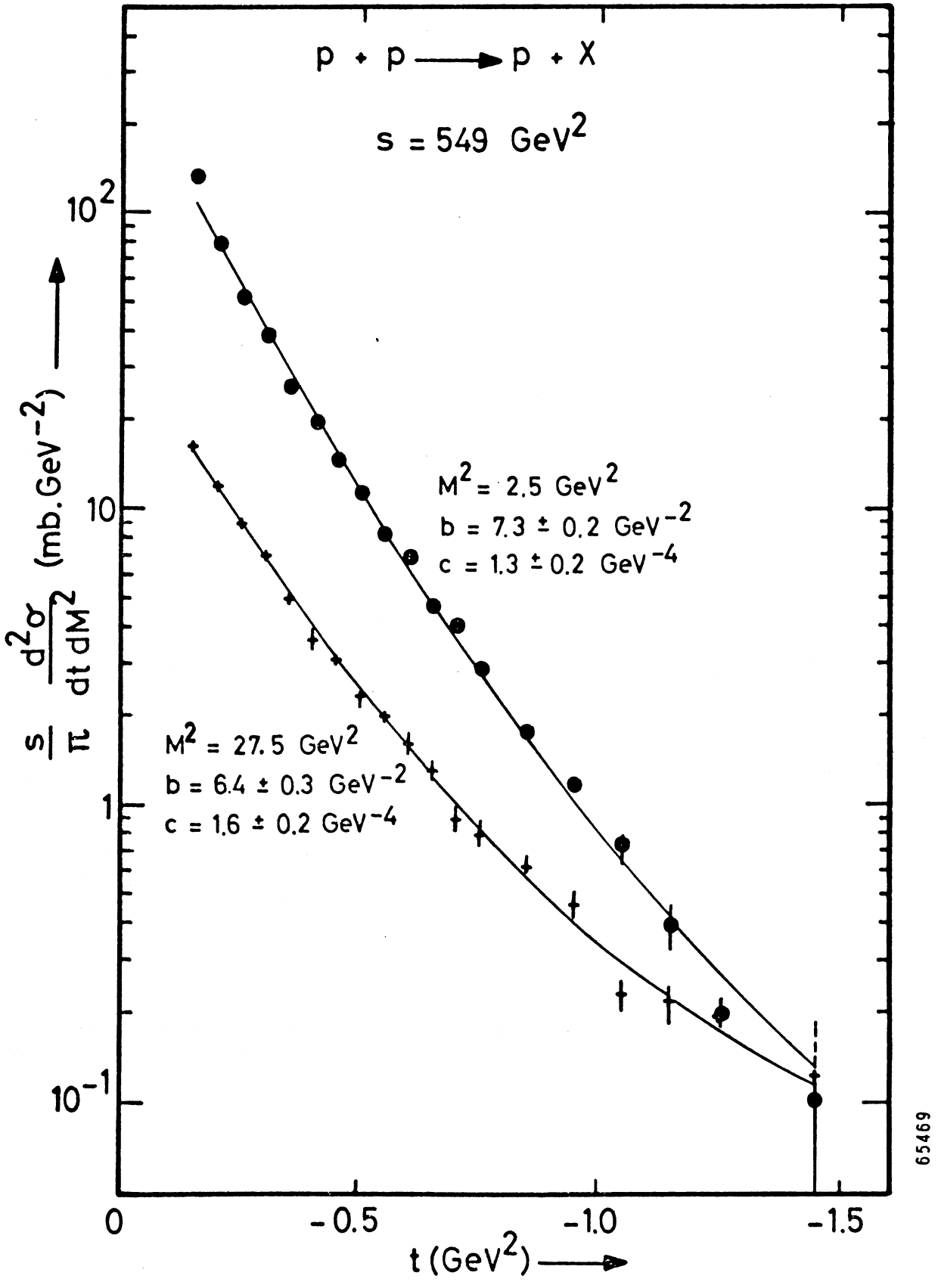
p + p ⟶ p + X
s = 549 GeV²
M² = 2.5 GeV²
b = 7.3 ± 0.2 GeV⁻²
c = 1.3 ± 0.2 GeV⁻⁴
M² = 27.5 GeV²
b = 6.4 ± 0.3 GeV⁻²
c = 1.6 ± 0.2 GeV⁻⁴
s/π d²σ/dt dM² (mb.GeV⁻²) ⟶
10²
10
1
10⁻¹
0
-0.5
-1.0
-1.5
t (GeV²) ⟶
65469

Fig. 7

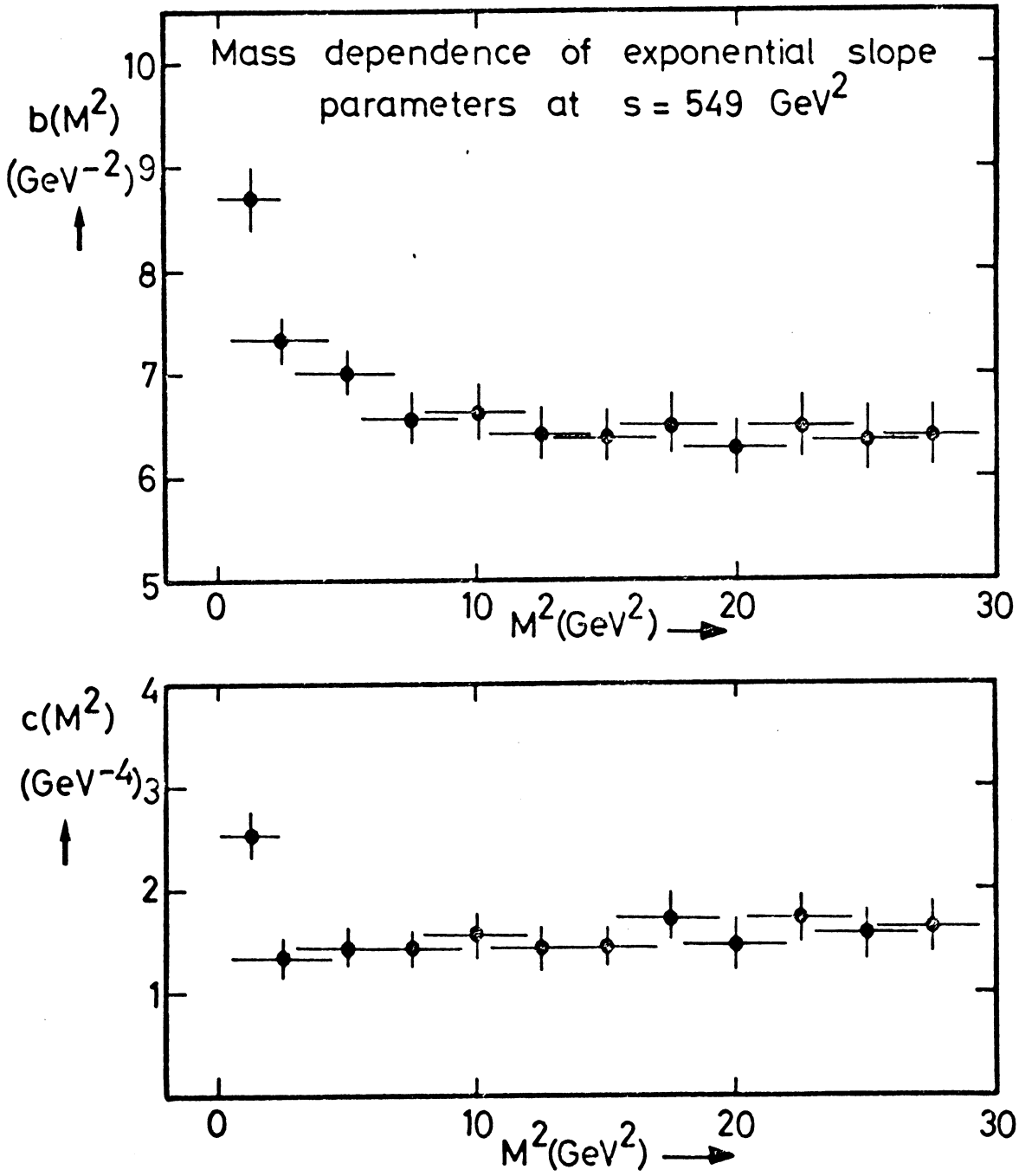
Mass dependence of exponential slope parameters at s = 549 GeV^2
$b(M^2)$ (GeV^{-2})
10
9
8
7
6
5
0
10
20
30
$M^2(GeV^2)$
$c(M^2)$ (GeV^{-4})
4
3
2
1
0
10
20
30
$M^2(GeV^2)$
65470

Fig.8

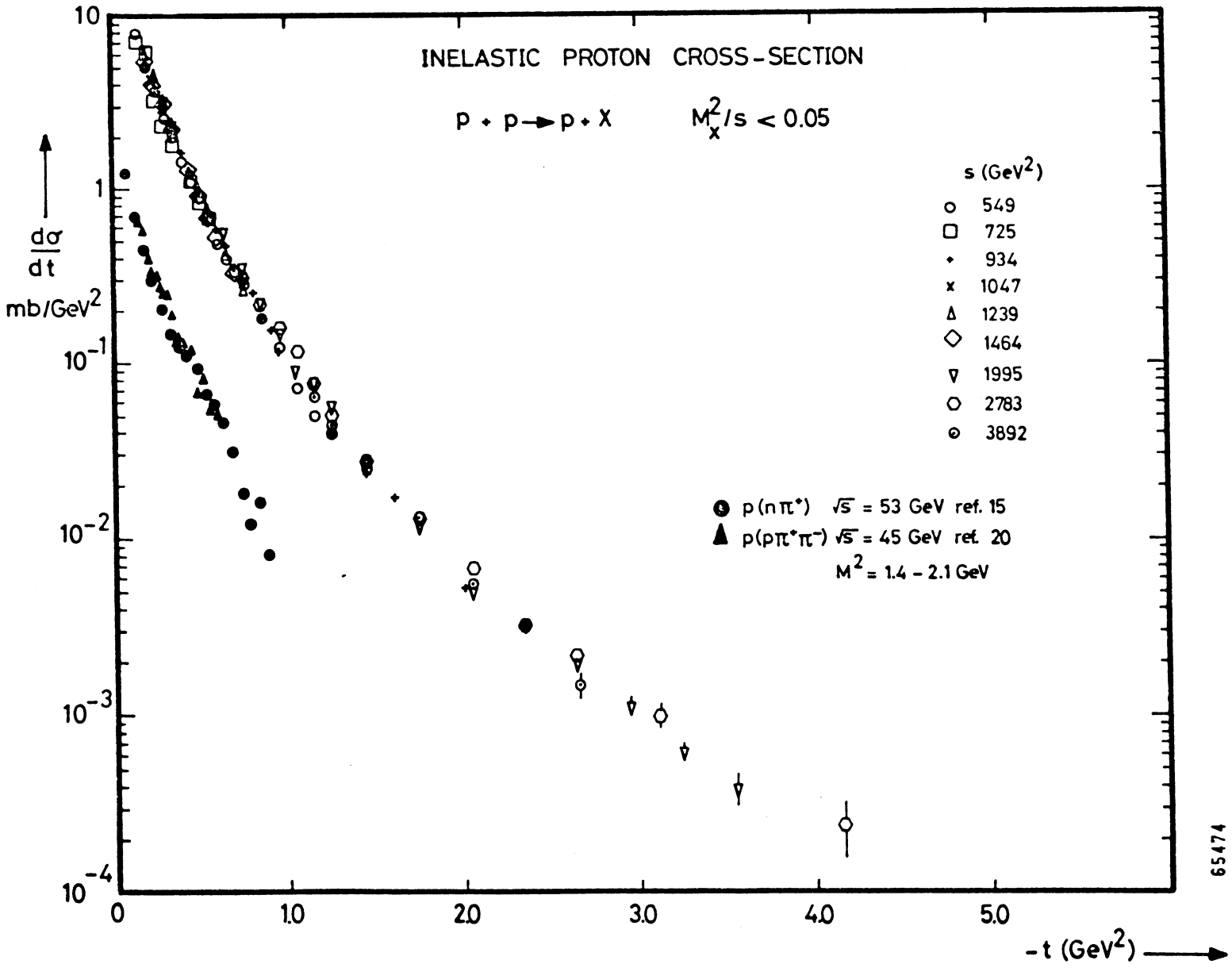
INELASTIC PROTON CROSS-SECTION
p + p → p + X
$M_x^2/s < 0.05$
s (GeV²)
549
725
934
1047
1239
1464
1995
2783
3892
p(nπ⁺) √s = 53 GeV ref. 15
p(pπ⁺π⁻) √s = 45 GeV ref. 20
M² = 1.4 - 2.1 GeV
dσ/dt
mb/GeV²
10
1
10⁻¹
10⁻²
10⁻³
10⁻⁴
0
1.0
2.0
3.0
4.0
5.0
-t (GeV²)
65474

Fig. 9

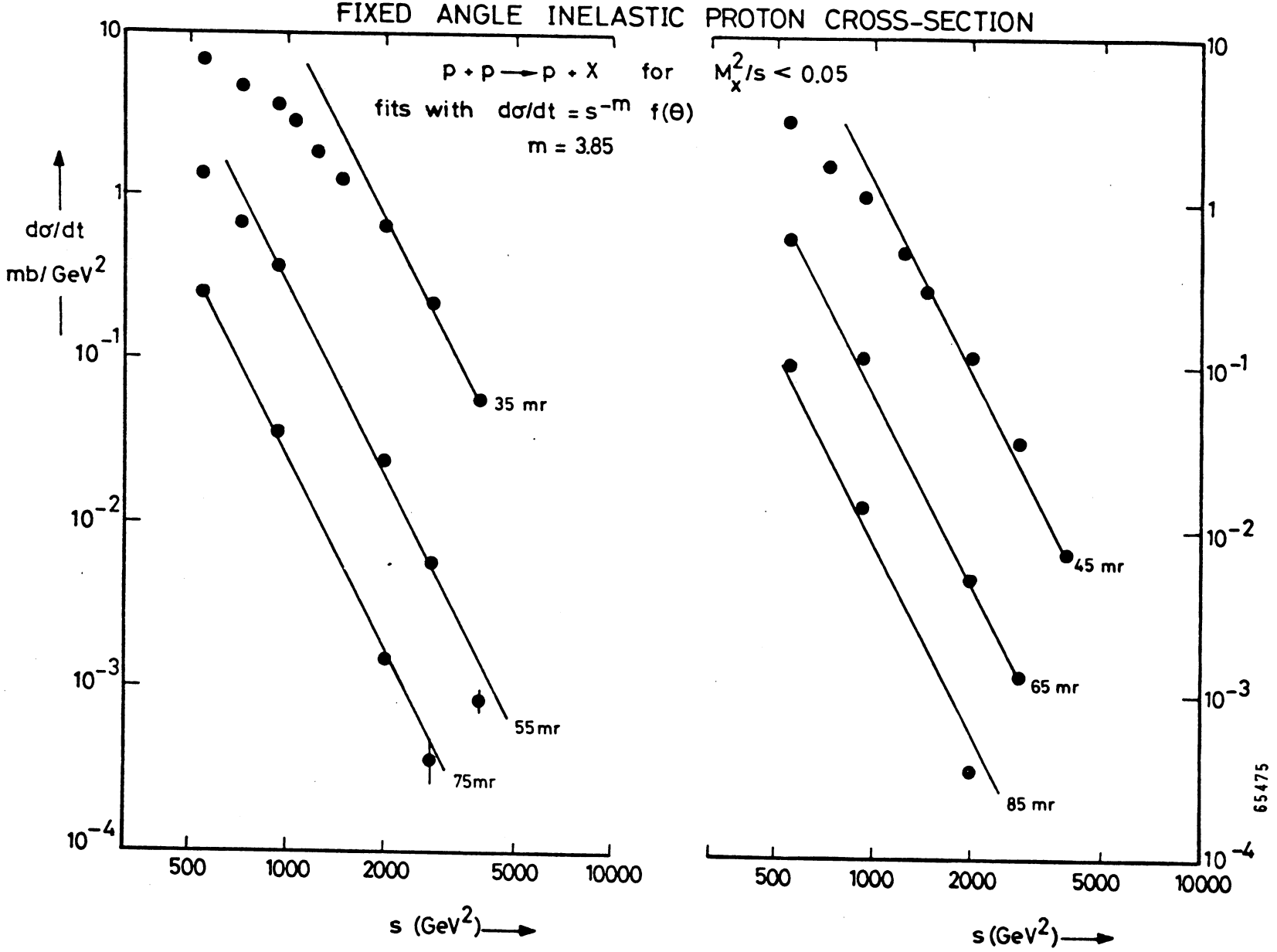
FIXED ANGLE INELASTIC PROTON CROSS-SECTION
p + p → p + X for $M_x^2/s < 0.05$
fits with $d\sigma/dt = s^{-m} f(\theta)$
m = 3.85
$d\sigma/dt$
mb/ GeV^2
35 mr
55mr
75mr
45 mr
65 mr
85 mr
s (GeV^2)
65475

Fig.10

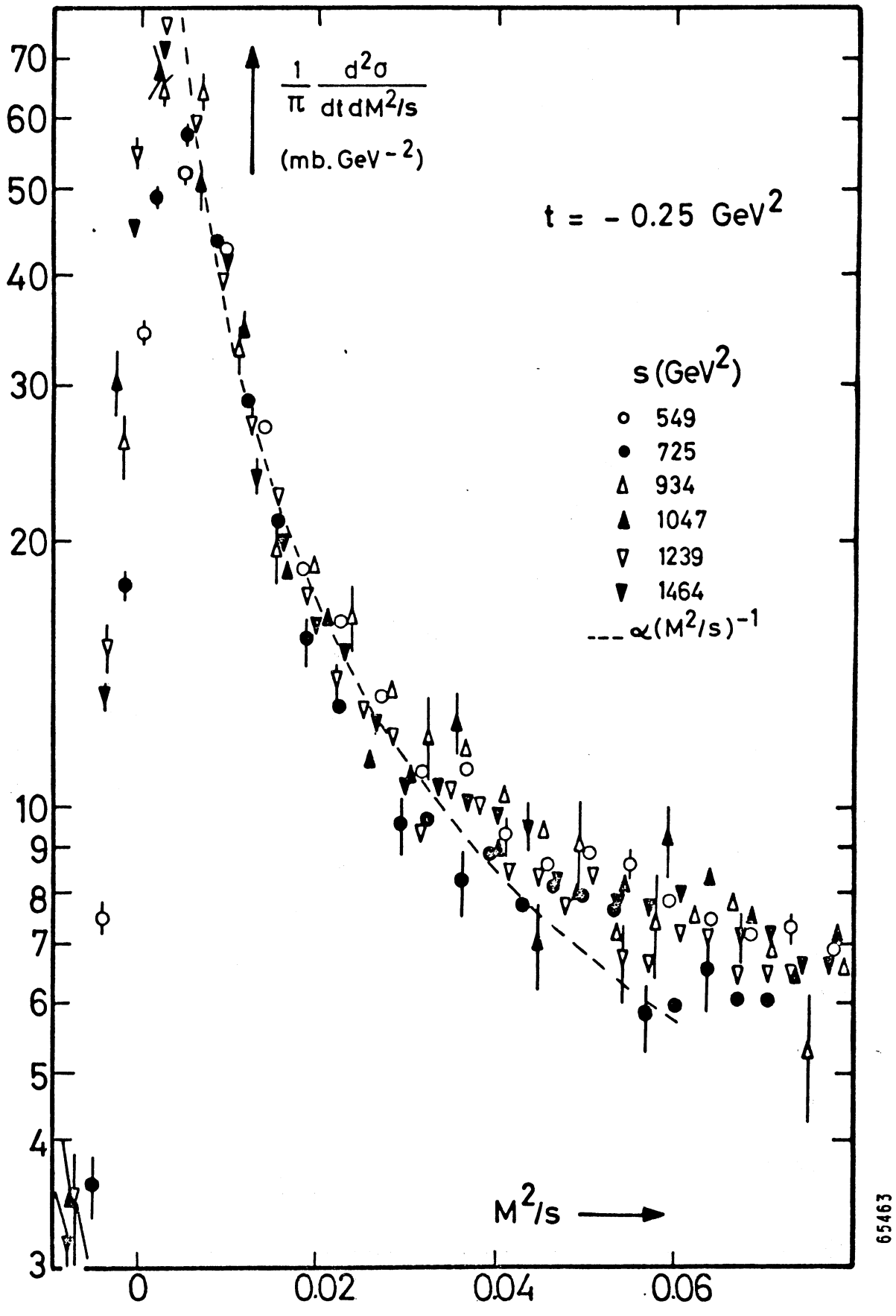
$\frac{1}{\pi}\frac{d^2\sigma}{dt\,dM^2/s}$
(mb. GeV^{-2})
t = - 0.25 GeV^2
s (GeV^2)
549
725
934
1047
1239
1464
$\propto (M^2/s)^{-1}$
M^2/s
65463

Fig.11(a)

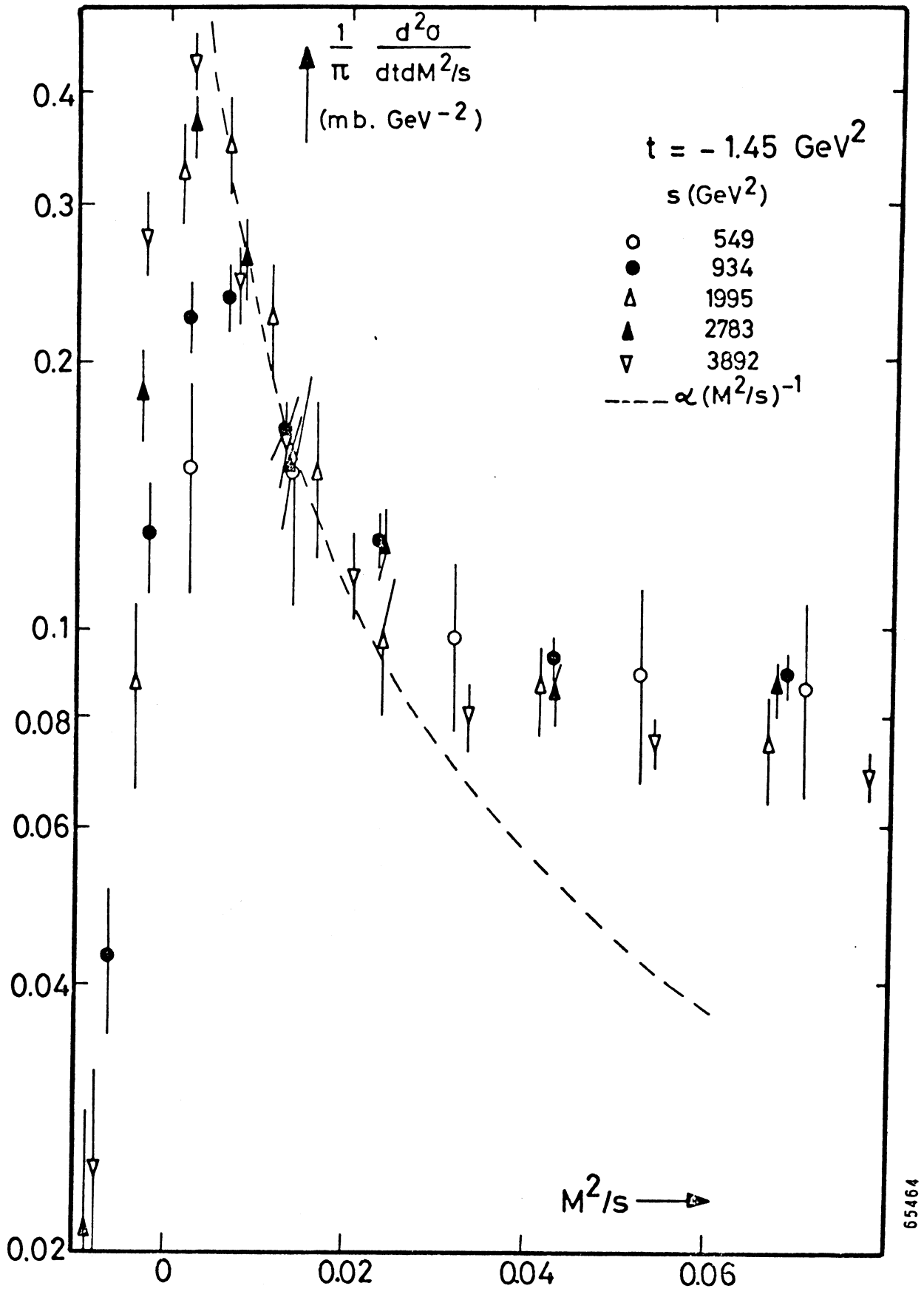
$\frac{1}{\pi}\frac{d^2\sigma}{dtdM^2/s}$
(mb. GeV^{-2})
t = - 1.45 GeV^2
s (GeV^2)
549
934
1995
2783
3892
$\propto (M^2/s)^{-1}$
0.4
0.3
0.2
0.1
0.08
0.06
0.04
0.02
0
0.02
0.04
0.06
M^2/s
65464

Fig.11(b)

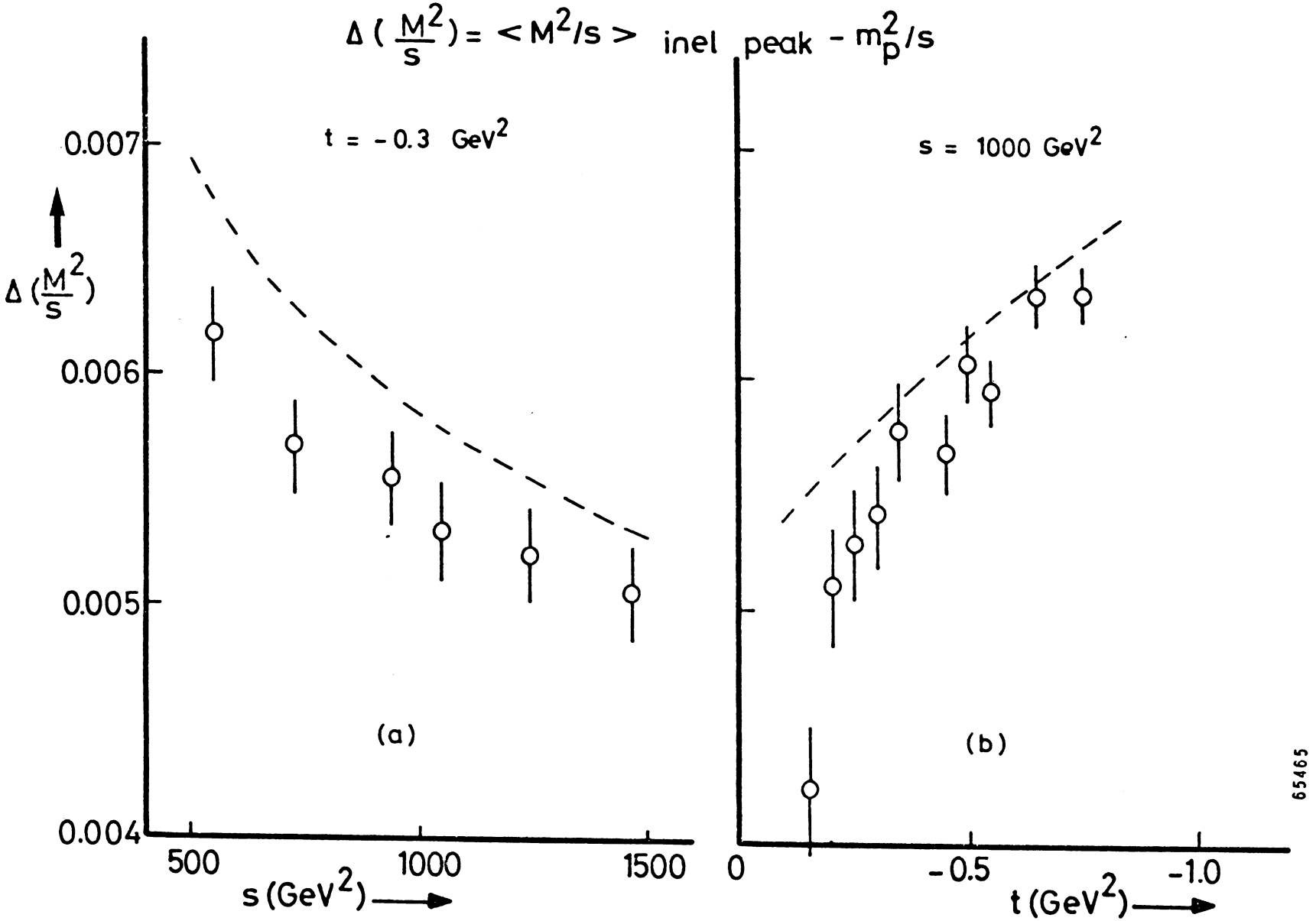
$\Delta\left(\frac{M^2}{s}\right) = \langle M^2/s \rangle$ inel peak $- m_p^2/s$
t = - 0.3 GeV^2
s = 1000 GeV^2
$\Delta\left(\frac{M^2}{s}\right)$
0.007
0.006
0.005
0.004
500
1000
1500
s (GeV^2)
(a)
0
-0.5
-1.0
t (GeV^2)
(b)
65465

Fig. 12

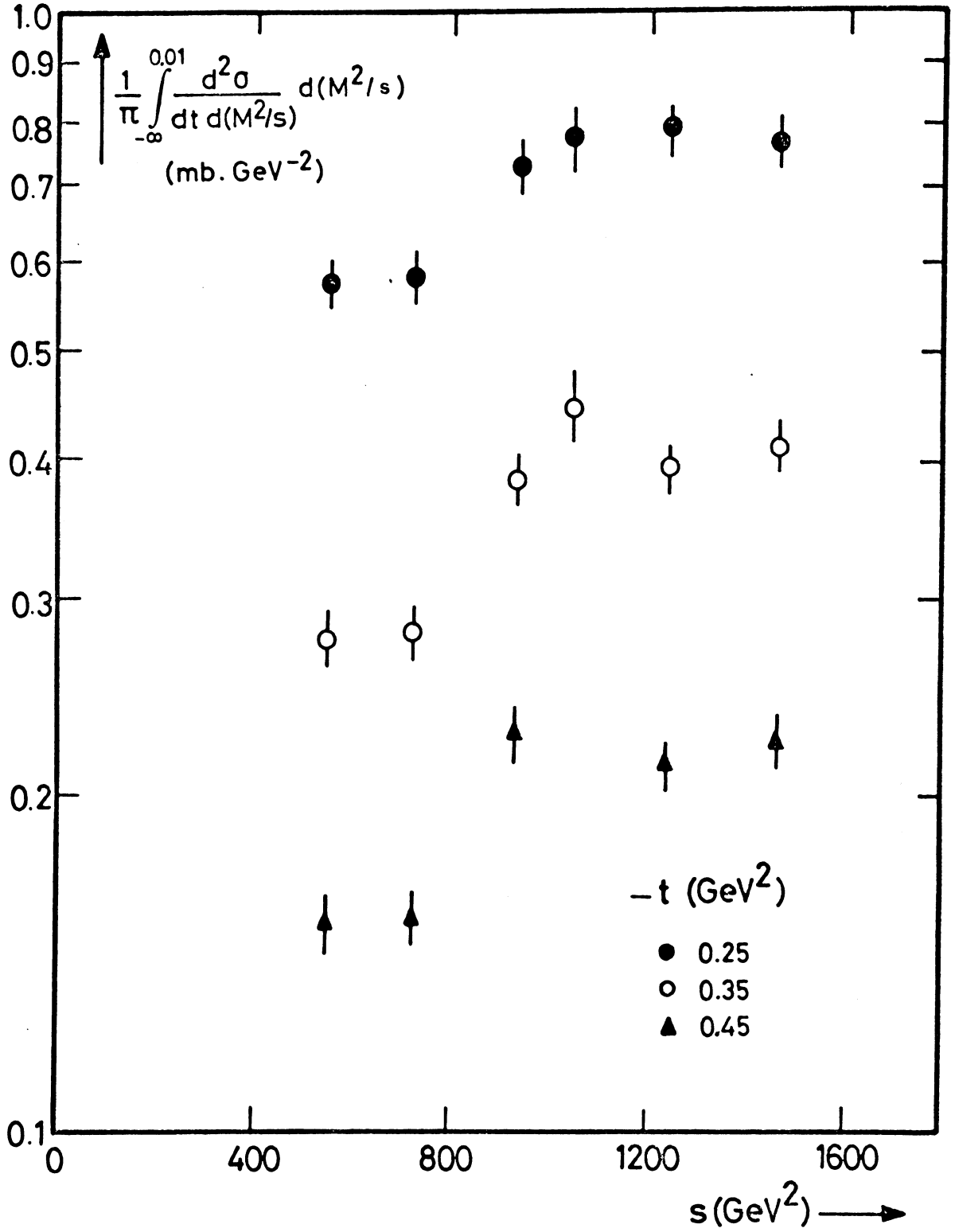
1.0
0.9
0.8
0.7
0.6
0.5
0.4
0.3
0.2
0.1
0
400
800
1200
1600
$\frac{1}{\pi}\int_{-\infty}^{0.01}\frac{d^2\sigma}{dt\,d(M^2/s)}\,d(M^2/s)$
(mb. GeV^{-2})
$-t$ (GeV^2)
0.25
0.35
0.45
s (GeV^2) ⟶
65466

Fig.13(a)

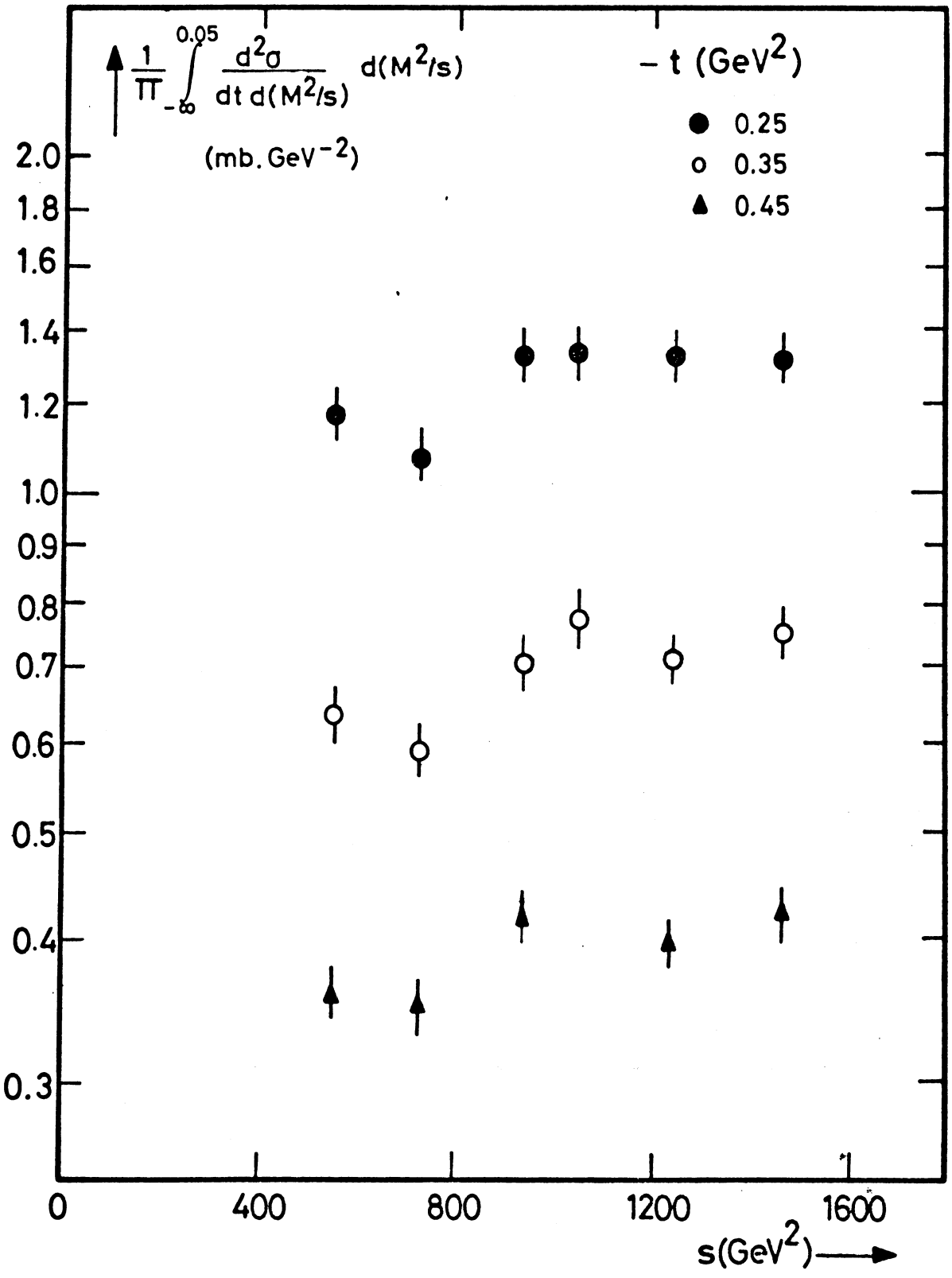
$\frac{1}{\pi}\int_{-\infty}^{0.05}\frac{d^2\sigma}{dt\,d(M^2/s)}\,d(M^2/s)$
(mb. GeV^{-2})
$-t$ (GeV^2)
0.25
0.35
0.45
2.0
1.8
1.6
1.4
1.2
1.0
0.9
0.8
0.7
0.6
0.5
0.4
0.3
0
400
800
1200
1600
s(GeV^2)
65467

Fig.13(b)

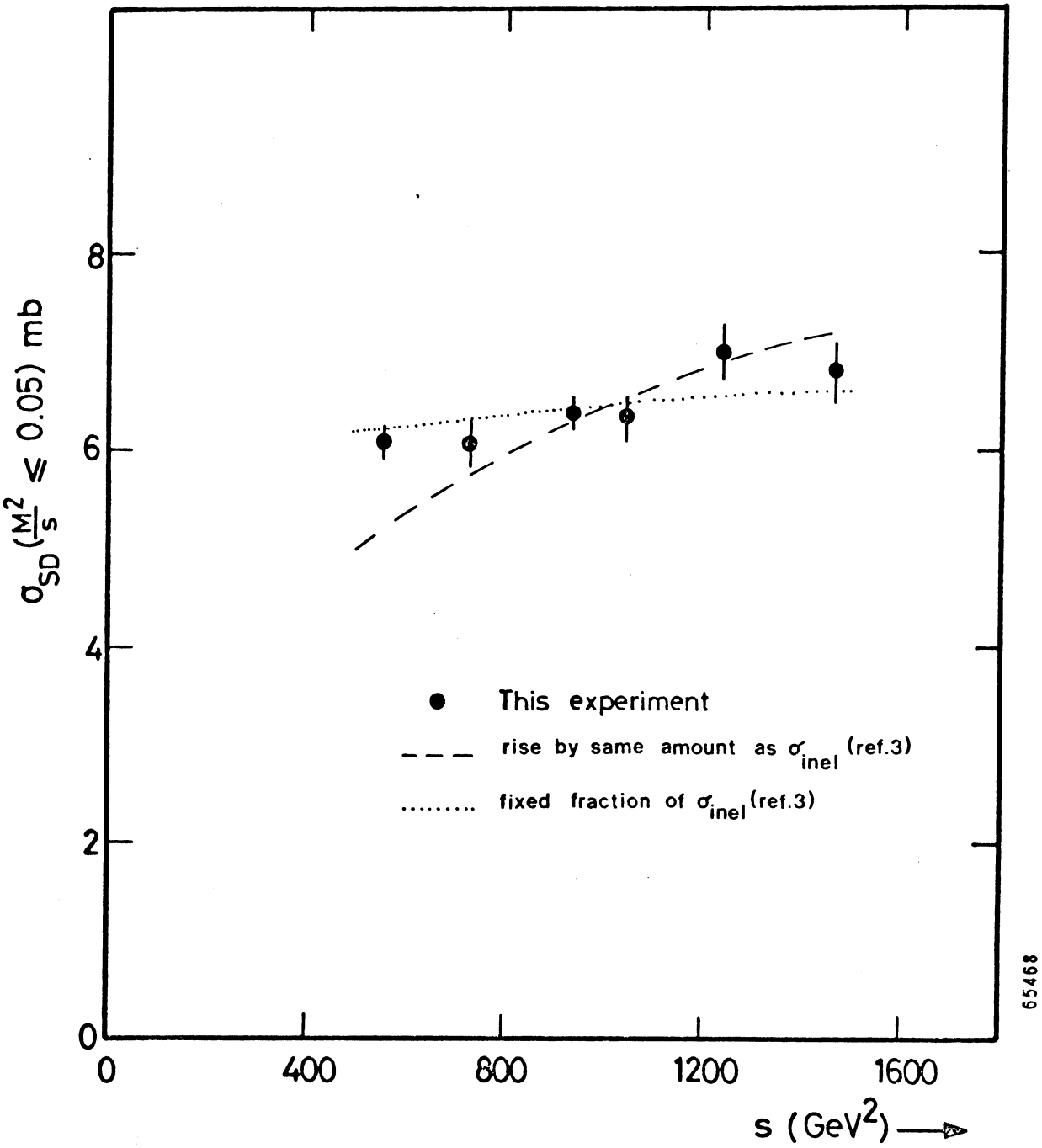
$\sigma_{SD}(\frac{M^2}{s} \leq 0.05)$ mb
0
2
4
6
8
0
400
800
1200
1600
s (GeV^2) ⟶
● This experiment
– – – rise by same amount as σ_{inel} (ref.3)
..... fixed fraction of σ_{inel} (ref.3)
65468

Fig. 14

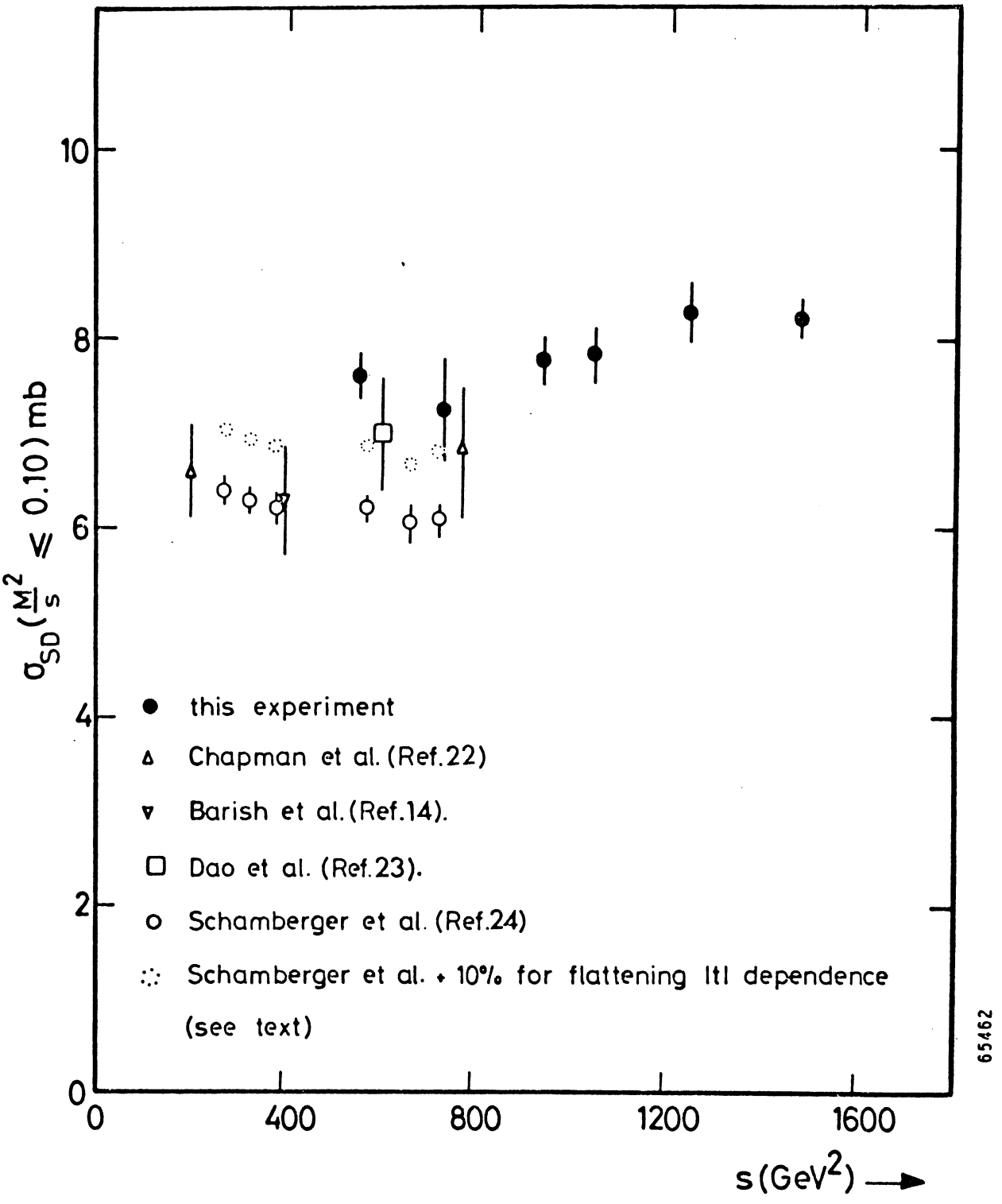
10
8
6
4
2
0
0
400
800
1200
1600
s(GeV²) ⟶
σSD(M²/s ≤ 0.10) mb
● this experiment
Δ Chapman et al. (Ref.22)
▽ Barish et al.(Ref.14).
□ Dao et al. (Ref.23).
o Schamberger et al. (Ref.24)
∴ Schamberger et al. + 10% for flattening |t| dependence (see text)
65462

Fig. 15